



This is to certify that the

dissertation entitled

ANALYSIS AND STABILITY OF LARGE-SPAN FLEXIBLE CONDUITS

presented by

Benjamin Nduchekwe Okeagu

has been accepted towards fulfillment of the requirements for

Doctor of Philosophy degree in Civil Engineering

Date //ov. //, 32

George A. Soyed



RETURNING MATERIALS:
Place in book drop to remove this checkout from your record. FINES will be charged if book is returned after the date stamped below.

ANALYSIS AND STABILITY OF LARGE-SPAN FLEXIBLE CONDUITS

Ву

Benjamin Nduchekwe Okeagu

AN ABSTRACT OF A DISSERTATION

Submitted to
Michigan State University
in partial fulfillment of the requirements
for the degree of

DOCTOR OF PHILOSOPHY

Department of Civil and Sanitary Engineering

ABSTRACT

ANALYSIS AND STABILITY OF LARGE-SPAN FLEXIBLE CONDUITS

bv

Benjamin Nduchekwe Okeagu

The objectives of the present study are twofold:

- 1) To examine the characteristics of the coefficients of soil reaction for flexible conduits, and develop simple formulas for their evaluation.
- 2) To use such formulas in the prebuckling and buckling analyses of the conduits. Both circular and elliptical conduits are examined in order to investigate the effect of the shape of the conduit on its stability.

The need for this study arises from the fact that existing studies employ physical idealizations that ignore certain salient parameters of the soil-structure interaction problem.

The findings suggest the following:

- a) The coefficients of soil reaction vary considerably around the conduit, depending on the span of the conduit, the depth of embeddment, and the direction of action.
- b) A good portion of the buckling strength of the conduit is derived from its interaction with the surrounding fill.
- c) The shape of the conduit has considerable influence on its stability.

Theoretical results from the present study show reasonable agreement with ones from relevant buckling tests.

ACKNOWLEDGEMENTS

The present work has been carried out under the patient advice and supervision of Dr. George Abdel Sayed to whom the author is most deeply indebted. Dr. Sayed's contributions to this work are truly priceless and the author wishes to hope that he will continue to be his mentor.

The writer is grateful to other members of his doctoral committee for their useful suggestions.

Thanks are due to Ms. Nancy Hunt and Ms. Vicki Switzer for their skillful typing of the manuscript.

Finally, the author is indebted to all members of his family for their support and prayers.

TABLE OF CONTENTS

	Page
ACKNOWLEDGEMENTS	ii
TABLE OF CONTENTS	lii
LIST OF TABLES	iv
LIST OF FIGURES	vii
NOTATIONS	ix
CHAPTER I. INTRODUCTION	1
CHAPTER II. REVIEW OF LITERATURE	6
CHAPTER III. DETERMINATION OF THE COEFFICIENT OF SOIL REACTION	24
CHAPTER IV. PRE-BUCKLING AND BUCKLING ANALYSIS OF ELASTICALLY SUPPORTED RING	38
CHAPTER V. DISCUSSION AND CONCLUSIONS	67
REFERENCES	76
TABLES	80
FIGURES	132
APPENDICES	167

LIST OF TABLES

TABLE		PAGE
3-1:	HYPERBOLIC PARAMETERS USED	80
3-2:	RESULTS FOR P = $33.3^{\#}$, H _C = 4 AND DIAMETER = 100 INCHES	81
3-3:	RESULTS FOR P = 33.3 $^{\text{\#}}$, H _C = 6.4 $^{\circ}$ AND DIAMETER = 100 INCHES	82
3-4:	RESULTS FOR P=300#, H _C =6.4 AND DIAMETER=200 INCHES	83
3-5:	RESULTS FOR P=300 [#] , H _C =8', AND DIAMETER=200 INCHES	84
3-6:	RESULTS FOR P=300 [#] , H _C =11.73 [*] , AND DIAMETER=200 INCHES	85
3-7:	RESULTS FOR P=300 [#] , H _C =4 ⁻ , AND DIAMETER=300 INCHES	86
3-8:	RESULTS FOR P=100 [#] , H _C =6.39', AND DIAMETER=300 INCHES	87
3-9:	RESULTS FOR P=300 [#] , H _C =6.39´ AND DIAMETER=300 INCHES	88
3-10:	RESULTS FOR P=500 [#] , H _C =6.39 [^] , AND DIAMETER=300 INCHES	89
3-11:	RESULTS FOR P=100 [#] , H _C =8', AND DIAMETER=300 INCHES	90
3-12:	RESULTS FOR P=300 [#] , H _C =8', AND DIAMETER=300 INCHES	91
3-13:	RESULTS FOR P=500 [#] , H _C =8', AND DIAMETER=300 INCHES	92
3-14:	RESULTS FOR P=300 [#] , H _C =11.73 [*] , AND DIAMETER=300 INCHES	93
3-15:	RESULTS FOR P=500 [#] , H _C =11.73 ⁻ , AND DIAMETER=300 INCHES	94
3-16:	RESULTS FOR P=100 [#] , H _C =12.64 ⁻ , AND DIAMETER=300 INCHES	95
3-17:	RESULTS FOR P=300 [#] , H _C =12.64 ⁻ , AND DIAMETER=300 INCHES	96
3-18:	RESULTS FOR P=500 [#] , H _C -12.64, AND DIAMETER=300 INCHES	97
3-19:	RESULTS FOR P-100 [#] , H _C =20.36 ⁻ , AND DIAMETER=300 INCHES	98
3-20:	RESULTS FOR P=300 [#] , H _C =20.36 ⁻ , AND DIAMETER=300 INCHES	99
3-21:	RESULTS FOR P=500 [#] , H _C =20.36 ⁻ , AND DIAMETER=300 INCHES	100
3-22-	LOADING SCUPPINE	101

TABLE		PAGE
3-23:	RECOMMENDED VALUES OF K ₁ AND n _h (AFTER TERZAGHI 1955)	101
3-24:	RESULTS FOR H = 4', DIAMETER=200 INCHES, AND P=50 LBS	102
3-25:	RESULTS FOR H _C = 4', DIAMETER = 200 INCHES AND P = 100 LBS	103
3-26:	RESULTS FOR H = 5.4, DIAMETER=200 INCHES, AND P=100 LBS	104
3-27:	RESULTS FOR H = 8, DIAMETER=200 INCHES, AND P=100 LBS	105
3-28:	RESULTS FOR H = 11.23, DIAMETER=200 INCHES, AND P=100 LBS	106
3-29:	RESULTS FOR H = 4°, DIAMETER=300 INCHES, AND P=100 LBS	107
3-30:	RESULTS FOR H = 6.4, DIAMETER=200 INCHES, AND P=50 LBS	108
3-31:	RESULTS FOR H = 8°, DIAMETER=300 INCHES, AND P=50 LBS	109
3-32:	RESULTS FOR H = 8', DIAMETER=300 INCHES, AND P=100 LBS	110
3-33:	RESULTS FOR H _C = 11.23', DIAMETER=300 INCHES, AND P=50 LBS	111
3-34:	RESULTS FOR H _C = 12.64', DIAMETER=300 INCHES, AND P=50 LBS	112
3-35:	RESULTS FOR H _C = 12.64', DIAMETER=300 INCHES, AND P=100 LBS	113
3-36:	COMPARISON OF PROPOSED AND FEM RESULTS FOR MEDIUM SOIL (CIRCULAR)	114
3-37:	COMPARISON OF PROPOSED AND FEM RESULTS FOR DENSE SOIL (CIRCULAR)	115
4-1:	THEORETICAL PRE-BUCKLING THRUSTS	116
4-2:	THEORETICAL PRE-BUCKLING DEFLECTIONS	117
4-3:	THEORETICAL PRE-BUCKLING MOMENTS	118
4-4:	VARIATION OF λ WITH SPAN	119
4-5:	COMPARISON OF PROPOSED AND FEM RESULTS FOR DENSE SOIL (ELLIPTICAL)	120
4-6:	COMPARISON WITH TEST RESULTS	121
4-7:	COMPARISON WITH TEST RESULTS	121
4-8:	COMPARISON WITH TEST RESULTS	122
4-9:	COMPARISON OF THEORETICAL FORMULATIONS OF COEFFICIENT OF SOIL REACTION (SOIL SUPPORT MODULUS)	123

TABLE		PAGE
4-10:	VALUES OF K _S IN TONS?CU. FT FOR SQUARE PLATES,	
	1 FT X 1 FT, or BEAMS 1 FT WIDE, RESTING ON SAND (AFTER TERZAGHI, 1955)	124
4-11:	COMPARISON OF THEORETICAL CRITICAL PRESSURES (CIRCULAR)	125
4-12:	VARIATION OF CRITICAL PRESSURE WITH $\frac{P_1}{P_0}$	126
4-13:	VARIATION OF CRITICAL PRESSURES WITH ASPECT RATIO (ELLIPTICAL SECTION)	127
4-14:	VARIATION OF CRITICAL PRESSURE WITH DEPTH	128
4-15:	VARIATION WITH DEPTH OF RELATIVE CROWN DEFLECTION DURING BUCKLING (CIRCULAR)	128
A-1:	DATA REDUCTION	129
A-2 •	DATA DEDILOTON	131

LIST OF FIGURES

FIGURE		PAGE
1-1:	VARIATION OF THE CROWN MOMENT AS A FUNCTION OF SUBGRADE REACTION	132
2-1:	GEOMETRY OF CORRUGATION	133
2-2:	SOIL BEDDING AND ENGINEERED BACKFILL AROUND THE CONDUIT	134
2-3a:	HYPERBOLIC STRESS-STRAIN RELATIONSHIP	135
2-3b:	TRANSFORMED HYPERBOLIC STRESS-STRAIN RELATIONSHIP	135
2-4:	PRESSURE DISTRIBUTION ASSUMED IN THE MARSTON- SPANGLER THEORY	136
2-5:	SOIL PRESSURE DISTRIBUTION ACCORDING TO THE RING COMPRESSION THEORY: (a) CIRCULAR SECTION: (b) ELLIPTICAL SECTION; (c) PIPE-ARCH	137
2-6:	IDEALISATION OF THE STRUCTURE FOR ANALYSIS BY FRAME-ON- ELASTIC SUPPORTS METHOD	138
2-7:	DISPERSION OF LIVE LOAD THROUGH THE SOIL-FILL	139
3-1:	LINEAR STRAIN TRIANGULAR ELEMENT	
3-2a:	9-NODE QUADRILATERAL ELEMENT	141
3-2b:	8-NODE QUADRILATERAL ELEMENT	141
3-3:	FINITE ELEMENT MESH	142
3-4:	FINITE ELEMENTS AROUND THE CONDUIT	143
3-5:	INTERFACE ELEMENT	144
3-6:	LOADING SCHEME	145
3-7:	VARIATION OF COEFFICIENT OF SOIL REACTION WITH DEPTH (300 INCH SPAN)	146
3-8:	VARIATION OF COEFFICIENT OF SOIL REACTION WITH DEPTH (200 INCH SPAN)	147

FIGURE		PAGE
3-9:	LOAD-DEFLECTION CURVE	148
3-10:	VARIATION OF $\beta *$ WITH $\frac{H}{D}$	149
3-11a:	VARIATION OF β * WITH θ FOR 300 INCH SPAN	150
3-11b:	VARIATION OF β * WITH θ FOR 200 INCH SPAN	151
4-1:	SHEAR INTERACTION MODEL (AFTER KLOPPEL AND BLOCK, 1970)	152
4-2:	VARIATION OF THEORETICAL PRE-BUCKLING DEFLECTION WITH $\boldsymbol{\theta}$	153
4-3:	VARIATION OF MOMENTS AROUND CONDUIT (TYPICAL)	154
4-4:	VARIATION OF λ WITH SPAN	155
4-5:	VARIATION OF COEFFICIENT OF SOIL REACTION AROUND CONDUIT (CIRCULAR, DENSE)	156
4-6a:	COMPARISON OF THEORETICAL CRITICAL PRESSURES (CIRCULAR)	157
4-6b:	ELLIPTICAL CONDUITS	158
4-7:	VARIATION OF CRITICAL PRESSURE WITH P1/P0	159
4-8:	VARIATION OF CRITICAL PRESSURE WITH DEPTH	160
4-9:	VARIATION OF CRITICAL PRESSURE WITH ASPECT RATIO (ELLIPTICAL SECTION)	161
4-10a:	VARIATION OF RELATIVE CROWN DEFLECTION AT INITIATION OF BUCKLING WITH DEPTH	162
4-10b:	APPROXIMATE BUCKLING CONFIGURATION (TYPICAL)	163a
4-11:	MEYERHOFF AND BAIKE'S LOADING TESTS	163b
A-1:	LOG π_1 VERSUS LOG π_2	164
A-2:	π_1 VERSUS π_2	165
A-3:	VARIATION OF C _D WITH SPAN	166

NOTATIONS

= Semi-major axis Parameters governing the virtual displacement components in the radial and tangential directions, respectively = Semi-minor axis b в* = Load-dependent stability matrix Вф = Boussinesque coefficient = Cohesion С = Pressure transfer coefficient D = Span of conduit = The smaller of the span of conduit or width of load Dh distribution = Axial rigidity in θ -direction D = Modulus of elasticity of conduit material E = Initial tangent modulus E, E_t = Tangent modulus E^ = Modulus of soil reaction F = Poisson's ratio number = Buckling stress fh H = Depth of cover HC = Depth to the crown = Coefficient of horizontal soil reaction k_h

= Coefficient of normal soil reaction

= Coefficient of tangential soil reaction

k_n

ks

K = Modulus parameter

K₁ = Modulus parameter

 $K_{\theta\theta}$ = Change of curvature of the centerline in the θ -direction

 M_{θ} = Bending moment per unit length in the θ -direction

 N_A = Axial force per unit length acting in the θ -direction

P = Atmospheric pressure R = Radius of curvature

r = Radius of gyration

U_h = Bending strain energy

U_k = Strain energy of elastic supports

V = Total potential energy

v = Tangential component of deflections

w = Normal component of deflections

X = Load-independent stability matrix

 $\alpha = \frac{H_{C}}{D}$

 β = Reduction factor to account for the depth of cover

 $\beta^* = \frac{k_s}{k_n}$

 ϵ_{α} = Axial strains at the centerline in the θ -direction

 $\lambda = \frac{k_s}{k_{ni}}$

 μ_{s} , ν_{s} = Poisson's ratio of soil

 Ω = Potential energy of external load

 ζ , η = Virtual displacement components during buckling in the normal and tangential directions, respectively

 σ_{θ} = Axial stresses in the θ -direction

CHAPTER 1

INTRODUCTION

Underground conduits are built using corrugated steel sheets and constructed to induce beneficial interaction between the conduit walls and the surrounding soil. The soil acts as an integral part of the structural system and the structure is referred to as a composite soil-steel structure. The benefits of such interaction have long been recognized by many researchers. As shown by Szechy (1), ascribing even a minimum amount of lateral support to the soil medium reduces the moments and stresses in the structure by a significant amount (Figure 1-1). This reduction is enhanced (or in certain cases hindered) at an appropriate depth of filling by the arching effects of the soil (reference 1)).

For a long time, underground conduits were limited to spans of less than 25 feet. Only in the last 15 years have soil-steel structures been built up through 54 feet spans and come to be regarded as economical alternatives to conventional short span bridges. Construction of conventional bridges is labor intensive and much of this labor is highly skilled. Major capital plant equipments, such as cranes and the like, are required and the conventional bridge components are usually made of high grade material. In contrast, the major component in soil-steel structures is soil which is widely available and one of the cheapest building materials. Further, the high performance of earth moving equipments make the construction of soil-steel structures highly productive and economical (2).

Low costs and high productivity are the main incentives for using soil-steel bridge structures. A report by the United States Federal

Highway Administration estimates that using these low cost bridges results in savings of 30% over other conventional short span bridges. Similar savings are reported in Canada (3), while the Australian experience found the cost of soil-steel bridges to be typically one-third that of the conventional bridges (4). Value analysis by a product designer (2) concludes that most conventional overpass structures do not represent optimum design. Alternative design using flexible metal arches and culverts was favored when considering all governing parameters.

The design of flexible conduits is usually governed by the circumferential thrust in the conduit walls (5). If the depth of cover is equal to or more than a minimum specified depth of one-sixth of the span, moments in the wall are not required to be calculated. The justification for the neglect of moment lies in the manner in which the interface pressure between steel conduit wall and the surrounding soil mass changes with the movement of the wall. Even if bending moment occurs locally to cause partial yielding, the resulting movement of the wall would cause an increase in the interface pressure provided by the adjacent soil mass, and this increase in pressure tends to inhibit any further movement.

In general, flexible conduits are designed to guard against the following primary modes of failure:

- Wall crushing which occurs when the compressive stresses due only to the circumferential thrust exceed the axial strength of the wall.
- 2) Separation of seams when the thrust exceeds the seam strength.
- 3) Excessive deformation due to plastic yielding under combined compressive and bending stresses.

- 4) Bearing failure of soil (typically for small and shallow conduits subjected to heavy live loads).
- 5) Soil failure above the conduit (stability of soil cover).
- 6) Buckling in the conduit walls both in the elastic and the elastic-plastic levels of stresses.

Simplified procedures are developed for the analysis and design of soil-steel structures. These procedures proved to be adequate for the design of short and medium span conduits (up to span of 25 ft) and with covers of not less than 1/6 the span (6,7,8). Herein, the first four modes of failure are the dominant consideration for design.

However, with the new trend in building conduits with larger spans and shallower covers, the latter two modes of failure tend to control the design.

The behavior and design of long-span metal conduits under shallow cover have been examined by Duncan (9) who recommended that moments in conduits should be calculated when the height to span ratio, H/S, is less than one-fourth. Duncan did not include buckling as part of the design criteria but stated that "additional research is needed to define precisely the range of conditions for which buckling failure may occur."

The stability of soil-steel structures has been examined by many investigators. Leonards and Stetkar (10) presented a summary of the information and formulas available. Almost all stability studies deal with uniformly applied boundary pressure on circular cross-sections. The only stability study that is general in nature and accomodates sections other than circular was presented by Kloppel and Glock (11). However, this study neglects the bending deformations in the determination of the critical load or pressure. Also, Kloppel and Glock considered the conduit to be supported by continuous elastic springs

(similar to Winkler approach) with the assumption that the coefficient of soil reaction is constant with no variation with the depth or direction of action.

Recently, Hafez (12) examined the problem of soil failure above

the conduit (failure mode number 5) and the author feels that attention

should be paid to proper evaluation of the buckling criteria (failure

mode number 6).

The thrust of the present research is to develop a methodology

Which can deal with everyday analysis and stability problems of soil
Steel structures under shallow or deep covers. Furthermore, the pro
posed methodology is applied to study the stability problems of soil
Steel structures. The problem is approached by employing a mathematical idealization of the soil response. This approach is similar to the analytical method proposed by Desai and Christian (13) for the design of footings, and the Spring method applied by Kloppel and Glock (1970) for the analysis and stability problems in soil-steel structures.

However, unlike Kloppel's approach, it is recognized here that a large number of parameters influence the performance of soil-steel structures.

1) A study is conducted in Chapter 3 to examine the parameters

90 Verning the coefficient of soil reaction, k_n , normal to the surface

of the conduit wall as well as the coefficient, k_s , tangential to the

wall surface, and to develop a simple formula for their evaluation.

Therefore,

2) The energy principles of mechanics and the associated variational methods are used in Chapter 4 in the pre-buckling and buckling analyses of the conduit. The geometric non-linearity of the structure is incorporated in the formulation by using non-linear straindisplacement relations. Equilibrium is then based on the deformed

geometry of the structure and thus general instability is detected.

3) Both circular and elliptical cross-sections are examined in order to study the effect of the conduit shape on its stability.

CHAPTER 2

REVIEW OF LITERATURE

In order to provide some appreciation of the complexity of the interaction problem, and a motivation for the technique adopted in the present
study, a review of current literature is presented in this chapter.

2-1 CONDUIT WALLS

The conduit walls are usually made of cold formed corrugated steel

plates. A typical corrugation profile is shown in Figure (2-1). The

plates are usually shipped unassembled and bolted together at the site.

2-2 SOIL MATERIAL

much on the selection of adequate steel walls as it is on the soil
materials used for bedding and backfill (Figure 2-2). The bedding
usually has a minimum thickness of 12 inches (30 cm) and is preshaped
in the transverse direction to accommodate the conduit invert curvature.
The backfill is placed and compacted in layers of not more than 12
inches (30 cm). At no time does the difference in levels of backfill
on the two sides of the conduit exceed twice the thickness of a compacted layer.

Granular materials are generally recommended for bedding and backfill. Such materials do not exhibit much change in their physical and engineering properties once they are constructed. Environmental changes such as moisture do not affect these properties to the same degree as they affect those of cohesive soils.

After placement of the bedding and backfill envelope, secondary material can be used to achieve the desired grade above the conduit.

However, the behavior of such material should be taken into account especially with regard to the possible effects of arching above the conduit.

2-3 CONSTITUTIVE LAWS FOR SOIL MEDIA

A major difficulty in the analysis of soil-structure interaction is an accurate description of the relations between stresses and strains in the soil media. In order to represent the interaction problem realistically, some form of non-linear relation must be used. Numerous constitutive relations have been proposed over the years and are well documented. Typical among these are the Hardin model (14) and the hyperbolic model. The later is proposed by Duncan and Chang (15) who related the tangent modulus E_t to the principal stresses σ_1 and σ_3 by the equation

$$E_{t} = E_{i}$$
 $1 - \frac{R_{f}(1-\sin\phi)(\sigma_{-\sigma_{i}})}{2C\cos\phi + 2\sigma_{s}\sin\phi}^{2}$ (2.1)

where E_i is the tangent modulus, R_f the failure ratio (that is the ratio between the measured compressive strength $(\sigma_1 - \sigma_3)_f$ and the asymptotic value of the stress difference for the hyperbolic stress-strain curve (Figure 2-3a), C the cohesion, and ϕ the angle of internal friction.

As suggested by Janbu (16), the initial tangent modulus E_i is related the confining pressure by

$$E_{i} = kP_{a} \left(\frac{\sigma_{3}}{P_{a}}\right)^{n} \tag{2.2}$$

where P is the atmospheric pressure, and k, n, constants to be determined experimentally.

Substituting this into equation (2.1) gives the final expression for the

$$E_{t} = kP_{a} \left(\frac{\sigma_{3}}{P_{a}}\right)^{n} \left[1 - \frac{R_{f}(\sigma_{1} - \sigma_{3}) (1 - \sin\phi)}{2C \cos\phi + 2 \sigma_{3} \sin\phi}\right]^{2}$$
 (2.3)

In a similar manner, the expression for the tangent values of Poisson's ratio v_t , and the shear modulus G_t at any stress level may be written as

$$v_{t} = \frac{\frac{G - F \log \left(\frac{\sigma_{3}}{P_{a}}\right)^{n}}{\frac{d(\sigma_{1} - \sigma_{3})}{kP_{a} \left(\frac{\sigma_{3}}{P_{a}}\right)^{n} \left[1 - \frac{R_{f}(\sigma_{1} - \sigma_{3})(1 - \sin\phi)}{2C \cos\phi + 2 \sigma_{3} \sin\phi}\right]}}$$
(2.4)

and

$$G_{t} = G_{i} \left[1 - \frac{R (\sigma_{1} - \sigma_{3}) (1 - \sin \phi)}{2 \sigma_{3} \sin \phi + 2C \cos \phi} \right]^{2}$$
 (2.5)

where G, F, and d are parameters to be determined experimentally, and G; is the initial value of the shear modulus.

2-4 FORCE ANALYSIS

In this section, some of the existing techniques for calculating the force effects in the conduit walls of soil-steel structures are discussed.

2-4-1 Marston-Spangler Theory

The theory of loads on buried conduits developed by Marston (17)

and later modified by Spangler (18) represents one of the earliest

formal investigations conducted on this subject. Marston based his

theory on an assumed column of soil transferring load directly on the conduit and derived the following expression

$$W = C \gamma B^2 \tag{2.6}$$

where

C = a calculation coefficient

B = span of the conduit

 γ = unit weight of soil

W = load on the conduit.

Marston considered only a single concentrated load, Spangler assumed the pressure distribution shown in Figure (2-4). Soil pressures at the top and bottom of the conduit are assumed uniform while a parabolic lateral pressure is assumed at the sides with a maximum at the springline. The vertical pressures are assumed to extend over the span of the conduit while the lateral pressures subtend an angle of 100° at the center of the conduit. The uniform pressure is taken as the sum of the over-burden pressure and any distributed live load, P_L, at the top of the conduit

$$P_{c} = \gamma_{s}h + P_{L} \tag{2.7}$$

where P_c = the uniform vertical pressure, h = the depth of cover above the crown of the conduit, P_L = the equivalent live load pressure including impact.

For a conduit uniformly supported by a well compacted soil, the maximum horizontal pressures at the sides are taken to be 1.35 the vertical pressure on the top of the structure. Based on the assumed

pressure distribution, the thrust in the wall of the conduit is found to be 0.7 P_CR at the top and bottom of the wall and P_CR at the sides, with a maximum of about 1.1 P_CR at the haunches. Similarly the moment in the wall is taken as 0.02 P_CR^2 at the top, sides and bottom, and $-0.02 P_CR^2$ at the haunches.

Based on the model shown in Figure (2-4), Spangler derived what has now come to be known as the IOWA FORMULA for calculating the crown deflection

$$\Delta x = \frac{D_1 K_1 W r^3}{EI + 0.061 E^4 r^3}$$
 (2.8)

where

D₁ = Deflection lag factor of compensate for the volume change of the soil with time.

 K_1 = Bedding constant which varies with the angle of bedding.

W = Load on the conduit per unit length.

r = Radius of the conduit.

EI = Conduit wall stiffness per inch.

E' = Modulus of soil reaction.

The Iowa formula had been used extensively in culvert design with a 5% decrease in the vertical diameter of the culvert generally considered the safe limiting value for the control of deflection. The conduit was considered to be in a state of incipient failure if the decrease in the vertical diameter reached 20%, prompting the use of a factor of safety of 4.0 against instability.

In view of its empirical nature, Spangler's theory applies with

limited success only to small-span conduits under deep fillings. With

recent trends toward larger spans, the theory is grossly inadequate for

the following reasons:

- 1) The 5% limit for control of deflection is too generous since for large spans -- culverts spanning as much as 54 feet -- a 5% decrease in the vertical diameter can be quite excessive.
- 2) Watkins (1960) has found that under certain conditions, the conduit wall can fail by ring buckling long before the 20% limit on the vertical crown deflection is attained.
- 3) For culverts under shallow cover, subjected to live loads, the assumption of a pressure distribution extending over the full span of the conduit can be over-conservative (Bakt, 1980).
- 4) The assumed pressure distribution is arbitrary and so is the parameter defined as the modulus of soil reaction.

2-4.2 Ring Compression Theory

White and Layer (1960) assume a uniform pressure around a circular conduit buried to a depth of at least one-eight its span in a well-compacted fill. The uniform pressure, P, consists of the overburden pressure, γh , and a uniform live and impact load pressure, P_L .

That is,

$$P = \gamma h + P_{L} \tag{2.9}$$

where γ is the unit weight of soil, h the depth of cover, and P_L the equivalent live and impact load pressure. The circumferential thrust, T, is expressed as

$$T = PD/2 \tag{2.10}$$

Where D is the span of the conduit.

The ring compression theory is also extended to non-circular conduits

and thus implies that the soil pressure is greatest at the point of minimum radius as illustrated in Figure (2-5).

2-4.3 Method of Watkins

Watkins (19) gives the following expression for the thrust, \mathbf{T}_{L} , in the conduit wall due to live loads

$$T_{L} = 0.5 C_{p} \sigma_{L} (I+1) D_{h}$$
 (2.11)

where

C_p = a pressure transfer coefficient

 σ_L = the equivalent uniformly distributed pressure at the level of the crown

I = the impact factor.

The pressure transfer coefficient, c_p , accounts for the arching action of dead loads. σ_L is computed from Boussinesq's theory of force effects on an elastic half space, and is expressed as

$$\sigma_{L} = \frac{P C_{b}}{H_{c}^{2}} \tag{2.12}$$

where P is the concentrated load applied at the level of the embankment, H the depth of cover to the crown, and C the Boussinesque

In using Boussinesq's theory, it is assumed that it applies even to large cavities in the elastic half space. This assumption is found to be invalid and the load dispersion differs in the longitudinal and transverse directions of the conduit (20). The use of c_p presumes that the phenomenon of arching applies to live and dead loads in like manner. There is no evidence to support these assumptions.

2-4.4 Kaiser Aluminum Method

This method is based on finite element analysis and provides expressions for the thrusts and bending moments due to live loads. Hence,

$$T_{L} = k_{D}LL \tag{2.13}$$

where

 T_{T} = thrust due to live load

$$k_p = 1.0 \text{ for } \frac{H}{D_h} \le 0.25$$

$$= 1.23 - \frac{H}{D_h} \text{ for } 0.25 \le \frac{H}{D_h} \le 0.75$$

$$= 0.5 \text{ for } \frac{H}{D_h} \ge 0.75$$
(2.14, a-c)

D_b = Span of the conduit

LL = the equivalent line load corresponding to applied concentrated
forces.

The bending moments in the metal arch, due to live load is given as

$$M_{L} = R_{L} M_{h} D_{L} L$$
 (2.15)

wh ere

$$k_{\rm m} = 0.018 - 0.004 \log_{10} N_{\rm f} \text{ for } N_{\rm f} \le 5000$$

$$= 0.0032 \text{ for } N_{\rm f} \ge 5000$$

$$R_{\rm L} = \frac{0.265 - 0.053 \log_{10} N_{\rm f}}{(\frac{\rm H}{\rm F})} \le 1.0 \qquad (2.15, a,b)$$

$$N_{f} = \frac{E_{s}(D_{h})^{3}}{EI}$$
 (2.16, c)

EI = fluxural rigidity per unit length of conduit

 E_s = secant modulus of the fill material.

The equivalent line loads in equations (2.13) and (2.15) are obtained from Boussinesq's theory in much the same way as Watkin's method.

The Kaiser Aluminum method leads to conclusions that do not agree with test data. For example, it predicts that for depths of cover between 0.3 and 0.5 meters (1.0 and 17.0 feet), live load effects remain constant. In contrast, tests by Bakt (20) show that live load effects decrease quite rapidly with the depth of cover.

2-4.5 Frame on Elastic Supports

This procedure employs the Winkler model, replacing a unit length of the culvert wall by a two-dimensional frame and the supporting soil by discreet elastic springs (Figure 2-6). Two interacting zones of earth pressure are identified — a zone of active and a zone of passive earth pressure. The active pressure is due to the movement of the soil toward the conduit and consists of a radial and a tangential component. The tangential component is the result of frictional forces developed between the soil and the conduit as the conduit deflects downwards.

It is considered negligible in the upper portion of the culvert oppel and Glock (1970). The radial active pressure is taken in the

$$P = P_{S} \cos \left(\frac{\pi}{2\phi^{0}}\right) \tag{2.17}$$

where P_s is the vertical compression at the crown and ϕ^0 the spreading

angle (Figure 2-6).

The spreading angle ϕ^0 depends on the ratio, λ , of the horizontal active pressure to the vertical compression in the soil, and is expressed as:

$$\lambda = \cos \left(\frac{\pi^2}{4\phi^0}\right) \tag{2.18}$$

where:

 λ = 0.5 for depths of cover exceeding the span

= 0.0 for depths of cover less than the span.

The high value of λ for deep filling accounts for the reduction of the vertical compression of the soil by arching. For shallow culverts, λ is taken to be zero to reflect the fact that the vertical compression at the level of the crown, P_s (due mainly to live loads), is much larger than the horizontal active pressure. The vertical compression at the level of the crown, P_s , is given as

$$P_S = \gamma H + P_O$$
 for $P_O < \gamma H$ (deep cover) (2.19, a-b)
= 1.1 ($\gamma H + P_O$) for $P_O > \gamma H$ (shallow cover)

where P_0 is the live load pressure, H the depth of cover, and γ the weight of the soil.

10% increase in the case of shallow fillings accounts for concentration of live loads on top of the crown.

In the zone of passive pressure, the walls of the culvert move

ards against the supporting fill. The passive pressure is assumed

act in the form of spring supports, each having a tangential reaction,

and a normal reaction, F. For a typical location, n, on the culvert

wall, these components are given as:

$$\mathbf{F}_{\mathbf{n}} = \mathbf{P}_{\mathbf{n}} + \mathbf{S}_{\mathbf{n}} \mathbf{W}_{\mathbf{n}} \tag{2.20}$$

where P_n is the active part of applied loading, S_n the spring constant, and W_n the radial displacement. Similarly,

$$T_{n} = \mu F_{n} \tag{2.21}$$

where µ is the coefficient of friction.

2-4.6 The Finite Element Method

The geometric and material non-linearities encountered in soilsteel structures render a complete analytical solution intractable

The finite element method (21) is clearly the only technique that is able
to simulate most of the aspects of the interaction problem with a minimum of over-simplifying assumptions. It is capable of modelling the

Presence or lack of friction between the soil and the conduit walls

well as the non-linear behavior of the soil and conduit walls.

First a finite element mesh is drawn to simulate the soil mass and culvert wall. A two-dimensional analysis is then performed to culvert the nodal stresses, displacements and other quantities of terest. Clearly the complexity, accuracy and therefore degree of correct of the finite element method depend on the type of elements and refinement of the discretization.

2-4.7 Theory of Elasticity

A circular soil-steel structure has been analyzed as an elastic Cylindrical shell embedded in an isotropic elastic medium of infinite extent (22). The problem is considerably simplified by introducing

some physical idealizations. The complete solution process, as might be expected, is very rigorous in detail and the final expressions are equally involved.

Burns' solution (22) has received a lot of attention in spite of being quite restrictive. The culvert is considered to be embedded to a depth of at least 1½ times its diameter in a weightless, homogenous, isotropic and linearly elastic medium of infinite extent. Stresses and deformations are determined for two limiting cases: (i) full slip (that is zero shear stress between the soil and the conduit wall), and (ii) no slip.

Assumptions such as the ones mentioned above over-simplify the problem, severly limiting the range of applications of elasticity solutions.

2-4.8 Practical Code Provisions on Force Analysis

The Ontario Highway Bridge Design Code gives live load thrusts,

T_L, as

$$T_{L} = 0.5 \sigma_{L} D_{H}^{m} m_{f} (I+1)$$
 (2.22)

where

 σ_{L} = the equivalent uniformly distributed load at the level of the crown.

 $m_f^{}$ = modification factor for multi-lane loading.

I = dynamic load factor.

 $\mathbf{D}_{\mathbf{H}}$ = the smaller of the span of the conduit or width of load distribution.

The equivalent distributed load σ_L is calculated on the basis of a 2:1 dispersion (Figure 2-7a) -- that is, the lines of dispersion slope down

to the crown at the ratio of 2 vertically to 1 horizontally. The modification factor m_f is taken as 1 for a single vehicle, and 0.95 for two vehicles. The impact factor, I, for a single lane is given as

$$I = 0.4$$
 for $H = 0$

= 2.0 for $H \ge 2$ meters (80 inches).

For depths of filling, H, between 0.16 D and 2 meters, a linear interpolation is permitted.

The OHBDC method avoids the assumption of a load dispersion extending over the full span of the conduit which may be conservative for shallow conduits.

The method of the American Iron and Steel Institute (AISI) is similar to Watkin's method except that the arching effects (of both live and dead loads) are completely ignored. The thrust, T_L, due to live loads is given simply as

$$T_{L} = 0.5 \sigma_{L} (I+1)D_{h}$$
 (2.23)

with identical notations as in equation (2.11).

The American Association of State Highway and Transportation

Officials' method (AASHTO) is virtually identical to AISI method. The

same expression is used for the thrusts due to live loads, with identi
notations. That is,

$$T_{T_{i}} = 0.5 \sigma_{T_{i}} (I+1) D_{h}$$
 (2.24)

only difference is that for a depth of cover, H, exceeding 0.61

meters (about 2 feet), the live load is assumed dispersed in such a way

to be uniformly distributed over a square of sides 1.75 H. In the

case of multiple concentrated loads with over-lapping square areas,

the effective area is defined by the outside limits of the over-lapping

squares. The total width of dispersion in this case is confined to

the span of the conduit (Figure 2-7b).

2-5 STRENGTH ANALYSIS

The existing techniques for calculating the distribution of force effects on soil-steel structures were the subjects of the preceding sections on force analysis. The present section examines the ability of the structures to sustain the force effects.

Rather detailed study of the literature on this subject is given in the report by Leonards and Stetkar (1977). With the exception of Kloppel and Glock (1970), all theories deal with uniform radial boundary pressures.

2-5.1 Practical Code Provisions on Strength Analysis

For strength analysis, the OHBDC considers the conduit wall to be divided into two zones — an upper zone in which the radial displacements are directed toward the inside of the conduit, and a lower zone with radial displacements outward towards the soil.

The elastic buckling stress, f_b , of the wall in both zones is \mathbf{Siven} by

$$f_{b} = \frac{3 E \beta}{(12 \text{KR/r})^2}$$
 (2.25)

B a reduction factor to account for the depth of cover. For depths cover exceeding twice the radius of curvature at the crown, β is taken as 1.0, and for other cases as:

$$\beta = (\frac{H}{2R})^{0.5} \tag{2.26}$$

The factor K is a function of the relative stiffness of the conduit wall with respect to the adjacent soil, and is expressed as

$$K = \lambda \left(\frac{EI}{ER^3}\right)^{0.25} \le 0.5$$
 (2.27)

where EI is the flexural rigidity of the conduit wall. The demarcation between the two buckling zones (that is the upper and lower zones) is accounted for through the factor λ . For buckling in the lower zone, λ is taken as 1.22, and for the upper zone as

$$\lambda = 1.22 \left[1.0 + 2\left(\frac{EI}{ER}\right)^{0.25}\right]$$
 (2.28)

where

$$\overline{E} = E' \left[1 - \left(\frac{R}{P+H} \right)^2 \right] \tag{2.29}$$

H = depth of cover above the crown of the conduit

E' = modulus of soil reaction.

Both the AASHTO specifications (American Association of State

Highway and Transportation Officials, 1973) and the AISI (American

and Steel Institute, 1971) use equation (2.25) to calculate the

astic buckling stress in the wall of the conduit. The latter assumes

Value of K of 0.27 for corrugated steel pipes with backfill compacted

85% standard density.

2-6 COEFFICIENT OF SOIL REACTION

The concept of coefficient of soil reaction, K, was first introduced by Winkler (1867) and has since been applied by a number of investigators. It had previously been erroneously thought that this coefficient was an exclusive soil parameter which could be expressed purely in terms of the elastic constants of the soil medium. This misconception was first pointed out by Terzaghi (23). Attempts to incorporate other salient properties of the soil-structure system have since been made by Mayerhof and Baike (24), Kloppel and Block (1970), and Luscher (25).

For culverts embedded in sand backfill, Meyerhoff and Baike gave
the following expression for the coefficient of soil reaction

$$k = \frac{E_{S}}{1.5 R}$$
 (2.30)

where E is the modulus of soil, R the conduit radius, and K the coefficient of soil reaction.

The authors offer no rationale for their expression other than that "the resistance of fills in the horizontal direction will usually govern in case of sands and gravels."

Kloppel and Glock derived their expression by considering a plane

Lete of strain of an elastic plate with a circular opening (representing the conduit). The plate (representing the soil medium medium)

Considered to have a constant modulus of elasticity E_s, and the

Pening a radius R. The opening is subjected to a radial compressive

Ce P_o and the authors show through plate theory that K is given by:

$$k = \frac{E_s}{R(1+v_s)}$$
 (2.31)

where v_s is the Poisson's ratio of soil.

Herein it should be noted that the plane strain analysis of isotropic media resulted in the existence of tensile stresses of equal magnitude and perpendicular to the radial stresses.

The expression for the coefficient of soil reaction due to Luscher is:

$$k = \frac{E_{s} \left[1 - \left(\frac{R_{i}}{R_{o}}\right)^{2}\right]}{(1 + v_{s}) \left\{1 + \left(\frac{R_{i}}{R_{o}}\right)^{2} (1 - 2v_{s})\right\} R}$$
 (2.32)

where:

 E_g = the soil modulus

 $v_{\rm g}$ = the poisson's ratio of soil

R, = inside radius of elastic ring of soil support

R = outside radius of elastic ring of soil support

R = conduit radius.

The expression was based on empirical results derived from small scale model tests and includes the effects of the depth of filling.

For a fairly deep cover, the ratio $(\frac{1}{R})^2$ in equation (2.32) is nearly zero, and if the poisson's ratio, v_s , of the soil medium is taken as 0.5, both expressions (Luscher, Kloppel and Block) simplify to that given in equation (2.30). In all the above expressions, the coefficient of soil reaction is assumed to be constant all around a given

conduit, and the surrounding soil medium is represented by an isotropic, homogenous, linear continuum.

CHAPTER 3

DETERMINATION OF THE COEFFICIENT OF SOIL REACTION

INTRODUCTION

Many investigators have attempted to examine the behavior of soilsteel structure systems by employing diverse empirical and analytical
techniques. These range from empirical estimation of the ring compression stresses to highly sophisticated finite element analyses incorporating non-linear and stress-dependent properties of the soil media. In
between these two approaches, exist the idealized models of soil-structure
interaction analysis (26,27) which attempt to strike a balance between
them. This approach utilizes the physical idealization or
analog modelling of the soil-structure interaction problems in terms of
Winkler element (Kloppel and Glock (1970)). Herein it should be noted
that the above range of interaction analyses and the idealized models
are not unique to soil-steel structures but also exist in the analysis
of soil-supported footings and rafts.

Analytically, the problems in soil-steel structures are considerably simplified by the introduction of a physical idealization of the soil-structure interaction. By using such idealization, a number of problems can be examined relatively conveniently, such as analyses of live load effects, stability problems and three dimensional behavior of the structures. Admittedly, the difficulty in this approach is that the spring constants and shear stiffness are not unique soil properties independent of the problem under consideration. They are related to the soil properties, as well as the geometric and stiffness parameters of the structure. However, despite the complexity and the approximate nature of the analog modelling schemes, they present very

useful tools to analysts and designers. They provide the facility to readily investigate the influence of soil support as well as the conduit geometry and stiffness properties on the failure characteristics of the structure.

The objective of this chapter is to improve this approach and make it more attractive to engineers. Herein explicit results are obtained incorporating the different parameters governing the soil effects, and more accurate idealization is achieved for the coefficient of soil reaction. They are obtained by relating the results of internal force components and deformations calculated with rigorous finite element analysis (12) to equivalent results obtained from the system modelling of the problem. The finite element analysis developed in (12) also forms the basis for verifying the results of the system modelling.

3-1 FINITE ELEMENT FORMULATION

The composite system of the conduit walls and the supporting fill is discretized by a number of finite elements (Figures (3-1) - (3-4)). Higher order elements are used around the culvert walls to reflect the steeper variations in soil stresses. Further away from the conduit walls, constant strain triangular elements are used to model the soil mass, while the conduit wall itself is discretized into twenty beam elements. The constitutive relations for the soil media are based on the stress-dependent hyperbolic model as shown in Chapter 2. The development of the finite element model and computer program is presented in detail in reference (12) and briefly outlined here.

An analytical model is used to reflect the normal and shear stresses resulting from the interaction between the conduit and the surrounding soil. Such interaction results from the relative movement of the soil with respect to the conduit wall at the soil-conduit interface, and the

relative movement of the soil particles with respect to each other. The interface element is a two-node spring type element (Figure (3-5)) possessing no physical dimensions, enabling it to be placed between the conduit and the soil without distorting the conduit geometry. Each interface element is assigned a normal and a tangential stiffness, k_n and k_s , respectively. Both are taken as zero in case of tension between the soil and the conduit wall. In order to minimize the overlap between nodes on either side of the interface in compression, k_n is assigned a very large number, while a non-linear relationship is used for the shear stiffness

$$\tau_{s} = K_{I} \gamma_{w} \left(\frac{\sigma_{n}}{P_{a}}\right)^{n} \left[1 - \frac{R_{fs} T_{s}}{\sigma_{n} tan \Delta}\right]^{2}$$
(3.1)

where

 $\tau_{\mathbf{s}}$ is the applied shear stress, $R_{\mathbf{f}\mathbf{s}}$ the failure ratio, $\sigma_{\mathbf{n}}$ the normal stress, $\gamma_{\mathbf{w}}$ the unit weight of water, Δ the angle of friction between the soil and the conduit wall, $K_{\mathbf{I}}$ a dimensionless stiffness number, and $n_{\mathbf{g}}$ the stiffness exponent.

An analytical incremental procedure is used to simulate construction processes. The filling is applied in ten successive increments and a sequence of linear analyses are carried out using the stress-strain relationships of the form

$$\{\Delta\sigma\} = [c]\{\Delta\epsilon\} \tag{3.2}$$

where $\{\Delta\sigma\}$ is the incremental stress vector, $\{\Delta\epsilon\}$ the incremental strain vector, and [c] the constitutive matrix.

The effect of soil compaction is included in the form of equivalent

nodal loads applied on top of each construction layer. Before proceeding to the next layer, these are removed by applying equal and opposite forces.

3-2 FACTORS AFFECTING THE COEFFICIENT OF SOIL REACTION

The coefficient of soil reaction, k, is the unit pressure developed as the sides of the conduit move outward a unit distance against the fill. As noted earlier, this coefficient is not a unique soil property, depending instead on a variety of parameters pertaining to the soil-conduit system. The parameters selected for investigation in this study are

- 1) The degree of compaction, Ω ;
- 2) the depth of cover, H (ft, in);
- 3) the span of the culvert, D (ft, in);
- 4) the flexural rigidity of the culvert wall, EI (in²/in);
- 5) soil modulus, E (psi);
- 6) Poisson's ratio of soil, v_{g} ;
- 7) magnitude and direction of soil displacement Δ_{g} , θ respectively;
- 8) the unit weight of soil, γ (pcf);
- 9) the relative density of soil (defined as dense and medium).

Mathematically these are expressed as

$$K = f(\Omega, H, D, EI, E_{g}, v_{g}, \Delta_{g}, \theta, \gamma)$$
 (3.3)

modulus, E, and the Poisson's ratio, V, are very complicated in general, as well as non-linear and stress-dependent. Consequently, the development of an analytical model incorporating the wide variability of these parameters is virtually impossible. For purposes of computational

convenience, this study is restricted to two particular class of soils, namely a well-compacted dense, and a medium dense granular backfill. This limitation is valid since it is required in practice to use only well-compacted, granular soil. For such type of soils, the hyperbolic parameters, on the basis of studies by Duncan et al (1977) may be taken equal, or as close as possible to those in Table (3-1). Therefore E and $\nu_{\mathbf{g}}$ are considered to be prescribed quantities and their effects on the coefficient of soil reaction are accounted for. A stronger case for the elimination of $\mathbf{E}_{\mathbf{c}}$ and $\boldsymbol{\nu}_{\mathbf{c}}$ from extensive consideration comes from the fact that the subsequent analysis utilizes the theory of dimensional analysis which requires that the significant parameters be dimensionless as well as independent of each other. It was noted previously that E and $\nu_{\mathbf{q}}$ are dependent upon stress levels, which in turn vary with the depths of cover, H. Therefore to satisfy the limitation of independence as required by the theory of dimensional analysis, $E_{\rm g}$, $v_{\rm g}$ and H cannot be considered separately. It has been found convenient to eliminate $\mathbf{E}_{\mathbf{g}}$ and $\mathbf{V}_{\mathbf{g}}$ in favor of the more readily amenable parameter, H.

With E and v_s eliminated from further consideration, the theory of dimensional analysis (28) is applied to furnish the following non-dimensional form of equation (3.3)

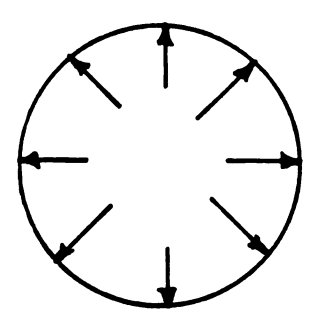
$$\frac{k}{\gamma} = f \left(\frac{H}{D}, \frac{EI}{\gamma D^4}, \frac{\Delta}{D}, \theta, \Omega\right)$$
 (3.4)

(A brief discussion of the theory of dimensional analysis is presented in the appendix.)

The advantage of equation (3.4) lies in the reduction of the number of independent terms. Rather than conduct a parametric study involving nine separate terms as required by equation (3.3), the number of terms

is reduced to only five in equation (3.4). This represents substantial savings in time and expense in the present study. Furthermore, each non-dimensional term is considered varied if at least one of the parameters it consists of is varied. Therefore the choice of which parameters to vary is often dictated by convenience and economy.

The method of Kloppel and Glock presented in Chapter 2 identifies two interacting zones of earth pressure — a zone of active and a zone of passive pressure. In order to compute the coefficient of soil reaction, it is desirable to devise a technique for separating the effects of one from the other. (Throughout the rest of this chapter, emphasis is placed on the normal component, k_n , of the coefficient of soil reaction. In the following chapter, shear interaction is examined.) To achieve the desired separation, equal normal concentrated forces are applied at the nodes of the beam elements to induce outward displacements all around the conduit as shown below.



With such a device, the influence of active pressure is eliminated and the coefficient of soil reaction normal to the conduit wall is given simply as:

$$k_{ni} = \frac{\sigma_i}{\Delta_i} \tag{3.5}$$

where Δ_i is the normal displacement at the ith interface node, σ_i the normal stress at i in the direction of Δ_i , and k_{ni} the desired coefficient of soil reaction.

3-3.1 The Effects of Compaction and Flexural Rigidity, EI

Soil stabilization is probably the single most important factor in most culvert installations. Rather than compute the response to a range of values of the degree of compaction, this study accounts for compaction by specifying a dense, granular backfill compacted to the recommended AASHTO standards. (Later, the case of medium dense soil is examined.) In this way, the degree of compaction is eliminated from further consideration as a separate, independent entity. Furthermore, the primary effect of compaction is usually to improve the quality of the soil, notably the unit weight. Since the unit weight, Y, is retained in equation (3.4), the influence of compaction is in effect reflected.

There is evidence in the literature (29) that the effect of the flexural rigidity, EI, of the conduit wall on the coefficient of soil reaction is quite negligible. This conclusion is presumed accurate and the term $EI/\gamma D^4$ therefore dropped from equation (3.4). Hence no separate examination of this term is conducted herein.

3-3.2 The Effects of the Depth of Cover, and the Span of the Conduit

The effects of the depth of cover, H, and the span of the conduit,

D, are examined in this study by computing values of the coefficient of

SOil reaction corresponding to a range of values of H and D. Results

for H of 4.0, 6.4, 8.0, 11.73, 12.64, and 20.36 feet and for D of 300, 200 and 100 inches are presented in Tables (3-2) - (3-21). They are also presented in a non-dimensional form by plotting k/γ versus H/D in Figures (3-7) and (3-8). The plots are nonlinear, and can be described with sufficient accuracy as suggested by Bowles (30), by the following relationship

$$\frac{k}{\gamma} = A_s + C_d \left(\frac{H}{D}\right)^n \tag{3.6}$$

with $A_g = 0$ for sand filling.

Equation (3.6) is developed in detail later.

3-3.3 The Effects of Magnitude and Direction of Soil Displacement ($\Delta_{_{\mathbf{S}}}$, θ)

To study the effects of the magnitude of soil displacements, a range of uniform normal forces are applied according to the loading schedule summarized in Table (3-22). Corresponding values of the coefficient of soil reaction are shown in Tables (3-2) - (3-21) for diameters of 100, 200 and 300 inches. These clearly show that the coefficient of soil reaction is practically independent of the magnitude of soil displacements, for displacements not exceeding 0.1 inches. Furthermore, the load-displacement relationship (Figure 3-9) is linear in the practical range of displacements.

Evidence that subgrade reaction may be related to the direction of soil displacement comes from Terzaghi (1955) and Vesic (31). Terzaghi proposed expressions for the coefficients of vertical and horizontal subgrade reaction, $k_{_{\rm V}}$ and $k_{_{\rm h}}$ respectively, based on the results of plate load tests. According to him, the coefficient of vertical subgrade reaction, $k_{_{\rm V}}$, for beams on elastic foundation may be expressed as:

$$k_v = K_1 \left(\frac{B+1}{B}\right)^2 \left(1 + \frac{2D}{B}\right)$$
 (3.7a)

For piles under lateral loads, a similar expression is given for the coefficient of horizontal subgrade reaction

$$k_{h} = n_{h} \frac{D}{B} \tag{3.7b}$$

where in equations (3.7),

B = the width of the beam or pile

D = the depth of embeddment

 n_h and K_1 = constants based on results of plate load tests. Recommended values of K_1 and n_h for sand filling are given in Table (3-23).

By extending the results of laboratory triaxial tests to footings, $\mbox{Vesic (31) proposed that the coefficient of vertical subgrade reaction,} \\ \mbox{$k_{\rm w}$, may be expressed as}$

$$k_{v} = \frac{0.65}{B} \sqrt{\frac{E_{s}B^{4}}{E_{b}I}} \frac{E_{s}}{1-v^{2}}$$
 (3.8)

where:

B = width of footing

I_b = moment of inertia of footing

E_b = modulus of elasticity of footing

 $E_{g} = modulus of elasticity of soil$

v = Poisson's ratio.

Though empirical in nature, equations (3.7) and (3.8) clearly show that $k_{_{\mbox{$V$}}}$ and $k_{_{\mbox{$h$}}}$ are significantly different for identical sets of soil

parameters and beam, footing or pile dimensions. Since the results of the present study indicate that the coefficient of soil reaction is independent of the magnitude of soil displacements, the only variable responsible for this difference must be the direction of soil displacements, θ . The effects of variations in θ is accounted for in the subsequent discussion.

3-4 DEVELOPMENT OF THE EXPRESSION FOR THE NORMAL COMPONENT OF COEFFICIENT OF SOIL REACTION

In the preceeding sections, the effects of a number of parameters on the coefficient of soil reaction were discussed and after deleting those factors considered negligible, the coefficient of soil reaction was shown to be given by the following equation

$$\pi_1 = f(\pi_2, \pi_3)$$
 (3.9)

where

 $\pi_1 = k/\gamma$

 $\pi_2 = H/D$

 $\pi_3 = \theta$

Equation (3.9) is referred to as a prediction equation, and represents an unknown function which must be established by a suitable analytical procedure. A rational procedure for achieving this is discussed by Murphy (Reference (28)) and adopted here without proof. The method involves plotting the dependent variable as successive functions of each of the independent variables with all but one of the later held constant each time. As an illustration, consider the case described in equation (3.9). First π_1 is plotted as a function of π_2 , with π_3 held constant at π_3 , say. From such a graph, a suitable curve-fitting technique is employed to develop a relationship between π_1 and π_2 (for the constant

value of π_3). Suppose this function is designated as

$$\pi_1 = f(\pi_2, \overline{\pi}_3)$$
 (3.10a)

Next, the procedure is repeated for π_3 with π_2 held constant (at $\overline{\pi}_2$ say) resulting in a similar expression in π_2 . Suppose this is written as

$$\pi_1 = f(\overline{\pi}_2, \, \pi_3)$$
 (3.10b)

An equation of the form of (3.10a) or (3.10b) is called a component equation and the choice of the constant values π_2 and π_3 are completely arbitrary. It is shown in (28) that the component equations may be combined into a prediction equation as

$$\pi_1(\pi_2, \pi_3) = \frac{f(\pi_2, \overline{\pi}_3) * f(\overline{\pi}_2, \pi_3)}{F(\overline{\pi}_2, \overline{\pi}_3)} S^{-2}$$
(3.11)

where:

S = the number of dimensionless, independent parameters (three
in the present case).

 $F(\overline{\pi}_2, \overline{\pi}_3) = \text{equation (3.10a)}$ evaluated at $\overline{\pi}_2$, or equation (3.10b) evaluated at $\overline{\pi}_3$

Hence, the prediction equation can be expressed as a product of its component equations combined in some appropriate manner. Obviously, since this technique is semi-empirical, the chances of error increase with the number of variables involved.

The technique is now applied to the present study. The sign convention for this purpose is that θ is positive in the clockwise direction, increasing from zero at the crown. Furthermore, only one-half of the conduit $(0 \le \theta \le 180^{\circ})$ is considered since the coefficient of soil reaction is virtually symmetrical about the vertical axis of the conduit (Tables 3-2 to 3-35). Hence, any expressions developed

for one half of the conduit, automatically satisfy the other.

Figures (3.7) and (3.8) show plots of k/γ versus H/D with θ held constant at suitable values. From these graphs and using the method described herein, in conjunction with the method of least squares, the expression for the coefficient of soil reaction for the dense soil is found to be

$$\frac{k}{\gamma} = C_{d} C_{\theta} \sqrt{\frac{H}{D}}$$
 (3.12)

where

$$C_d = 4.25 - \frac{0.75D}{100}$$

$$C_{\theta} = \frac{1+5.4 \ \theta/\pi}{4}$$

Finally, if H in equation (3.12) is replaced by

$$H = H_c + \frac{D}{2} (1 - \cos \theta)$$

the expression can finally be written as

$$\frac{k}{\gamma} = C_{d} C_{\theta} \sqrt{\alpha + \frac{1}{2} (1 - \cos \theta)}$$
 (3.13)

where, α = the depth ratio , $\frac{H_c}{D}$, and H_c = depth to the crown of the conduit, D = the span of the conduit in inches.

3-5 THE EFFECT OF THE RELATIVE DENSITY OF SOIL

So far the discussion has centered on granular soils with high relative density. What follows is a parametric numerical study of the effects of relative density on the coefficient of soil reaction. For

the purposes of this study, relative density is defined simply as dense or medium dense. A variation in relative density is accomplished by changing the hyperbolic parameters as summarized in Table (3-1). For example, while a modulus factor, k, of 3100 is assigned to the dense soil, a value of 1200 is ascribed to the medium soil. The loading schedule and all pertinent discussions given previously for the dense soil still apply.

The results are presented in Tables (3-24) to (3-35). In order to integrate these results into a mathematical expression for the coefficient of soil reaction, it is found convenient to calculate the ratio β^* of the coefficient of soil reaction for the medium soil to that of the dense soil at corresponding points around the conduit. β^* is plotted as a function of H/D and of θ in Figures (3-10) and (3-11). From these plots and also from Tables (3-24) to (3-35) it is seen that β^* can be represented with sufficient accuracy by the following equation

$$\beta^* = C_1 + C_2 (\theta) \tag{3.14}$$

where C_1 , C_2 are functions of the span of the conduit. Using the least squares curve-fitting technique, equation (3.14) is found to simplify to

$$\beta^* = 0.45 + \frac{D}{200} \left(\frac{\theta}{\pi} - 0.5 \right)^2 \tag{3.15}$$

Therefore it is proposed herein that the coefficient of soil reaction, k_{n} , in the normal direction to the wall of the conduit may in general be given as:

$$k_{n} = \gamma \beta * C_{d} C_{\theta} \sqrt{\frac{H}{D}}$$
 (3.16)

where

$$C_d = 4.25 - \frac{0.75D}{100}$$

$$C_{\theta} = \frac{1 + 5.4 \, \theta/\pi}{4}$$

 β * = 1.0 for dense soils

= 0.45 +
$$\frac{D}{200}$$
 ($\frac{\theta}{\pi}$ - 0.5)² for medium dense soils.

H = depth to the point on the conduit where k_n is desired.

D = span of the conduit.

 γ = unit weight of soil.

Equation (3.16) is compared with results from the finite element method (12) in Tables (3-36) and (3-37) and agreement with these is seen to be quite good.

CHAPTER 4

PRE-BUCKLING AND BUCKLING ANALYSES OF ELASTICALLY SUPPORTED RING

INTRODUCTION

The soil-steel structure can be analyzed as an orthotropic shell supported by the soil for which the coefficients of soil reaction are determined in Chapter 3. However, such analysis could be simplified by considering a plane slice of unit width of the conduit and surrounding soil. This approach is considered adequate since:

- 1) Dead load is usually uniform along the axis of the conduit.
- 2) Effect of live load is simulated by equivalent pressure after considering its dispersion in the longitudinal direction.
- 3) Bending and axial rigidity of the shell in the longitudinal direction is considerably small when compared with those in the curved direction.

Therefore the analysis and stability of the conduit are examined considering the conduit as a frame elastically supported by the soil, using an energy approach.

4-1 ENERGY THEORIES

The principle of stationary potential energy states that of all displacements satisfying given boundary conditions, those which satisfy the equilibrium conditions make the potential energy a stationary value — maximum, minimum or neutral. This can be expressed by the condition

$$\delta V = 0 \tag{4.1}$$

For stable equilibrium, the potential energy is a minimum (maximum for unstable and unchanged for neutral equilibrium).

4-2.1 Potential Energy Expressions in Pre-Buckling Analysis

Pre-buckling displacements and stress-resultants are assumed, for the purposes of this study, to be determined with sufficient accuracy by linear theory. This assumption is seen to be adequate (33), hence second and higher-order terms are excluded from the energy equations.

The potential energy, V, of an elastic system is the sum of the strain energy, U, and the potential energy, Ω , of external forces. Hence the total potential energy can be expressed as

$$V = U + \Omega \tag{4.2}$$

For an elastically supported ring, the strain energy consists of the bending strain energy, \mathbf{U}_{b} , the membrane strain energy, \mathbf{U}_{m} , and the strain energy of the elastic supports, \mathbf{U}_{k} . Hence,

$$U = U_{\mathbf{b}} + U_{\mathbf{m}} + U_{\mathbf{k}} \tag{4.3}$$

where,

$$U_{b} = \frac{R}{2} \int_{0}^{2\pi} \frac{M_{\theta}^{2} d\theta}{EI}$$

$$U_{m} = \frac{EA}{2} \int_{0}^{2\pi} \epsilon_{\theta}^{2} ds$$

$$U_{k} = \frac{1}{2} \int_{0}^{2\pi} k_{n} w^{2} ds + \frac{1}{2} \int_{0}^{2\pi} k_{s} v^{2} ds$$

$$(4.4, a-c)$$

Furthermore, the bending moment $\mathbf{M}_{\boldsymbol{\theta}}$ is given by

$$M_{\theta} = \frac{EI}{R^2} (\ddot{w} + w) \tag{4.5a}$$

and the strain, $\epsilon_{\textrm{A}}\text{, of the centerline in the }\theta\text{-direction by,}$

$$\varepsilon_{\theta} = \frac{1}{R} \left(\frac{dv}{d\theta} - w \right)$$
 (4.5b)

where in equations (4.4) and (4.5),

the dot denotes differentiation with respect to θ .

R = radius of the ring

A = area of cross-section

k = coefficient of soil reaction (normal or tangential as the case
 may be)

w, v = displacement components in the normal and tangential directions, respectively.

A choice of suitable displacement functions $w(\theta)$ and $v(\theta)$ is made consistent with the boundary conditions. For the complete ring, the boundary requirement is that w and v be periodic in θ . The tangential displacement, v, may further be taken in such a form as to make the extension of the centerline of the ring zero. This simplification is equivalent to replacing the actual ring by a hypothetical ideal ring with negligible extension of the centerline.

Hence,

$$\varepsilon_{A} = 0 = \frac{1}{R} \left(\frac{dv}{dA} - w \right) \tag{4.6}$$

The condition of inextensional deformation of the ring therefore is

$$\frac{\mathrm{d}\mathbf{v}}{\mathrm{d}\theta} - \mathbf{w} = 0 \tag{4.7a}$$

or
$$v = \int w d\theta$$
 (4.7b)

The following displacement functions are chosen:

$$\mathbf{w}(\theta) = \sum_{n=1}^{\infty} \mathbf{w}_{n} \cos n\theta$$

$$\mathbf{v}(\theta) = \sum_{n=1}^{\infty} \frac{1}{n} \mathbf{w}_{n} \sin n\theta$$
(4.8a,b)

Substitution of these into equations (4.4) gives

$$U_{b} = \frac{EI\pi}{2R^{3}} \sum_{n=2}^{\infty} (1-n^{2})^{2} W_{n}^{2}$$
 (4.9)

$$U_{k} = \frac{R}{2} \int_{\theta_{0}}^{2\pi} k_{n} \sum_{n=m}^{\infty} \sum_{m}^{\infty} W_{n}W_{m} \cos n\theta \cos m\theta d\theta + \frac{k_{s}R}{2} \int_{\theta_{0}}^{2\pi} \sum_{n=0}^{\infty} \frac{W_{n}^{2}}{n^{2}} \sin n\theta d\theta \quad (4.10)$$

Finally, using the expression developed in Chapter 3 for k_n , and also employing the trapezoid (as discussed in the Appendix) rule of numerical integration, equation (4.10) becomes

$$U_{k} = \frac{\pi R k_{s}}{2} \sum_{n=1}^{\infty} \frac{w_{n}^{2}}{n^{2}} - k_{s} R \sum_{n=1}^{\infty} (\frac{\theta}{2} - \frac{\sin 2n\theta}{4n}) \frac{w_{n}^{2}}{n^{2}}$$

$$+ \frac{\gamma C_{d} R}{8} (\frac{\pi}{3} - \theta_{o}) (2.8\sqrt{\alpha + .25} \sum_{n=1}^{\infty} \sum_{m=1}^{\infty} w_{n} w_{m}^{\cos n\pi} \frac{\cos m\pi}{3})$$

$$+ \frac{\pi \gamma C_{d} R}{48} [2.8\sqrt{\alpha + .25} \sum_{n=1}^{\infty} \sum_{m=1}^{\infty} w_{n} w_{m}^{\cos n\pi} \frac{\cos m\pi}{3} \cos m\pi + 6.4\sqrt{\alpha + 1} \sum_{n=1}^{\infty} \sum_{m=1}^{\infty} w_{n} w_{m}^{\cos n\pi} (-1)^{m+n}$$

$$+ 7.4\sqrt{\alpha + .5} \sum_{n=1}^{\infty} \sum_{m=1}^{\infty} w_{n} w_{m}^{\cos n\pi} \frac{\cos m\pi}{2}$$

$$+ 9.2\sqrt{\alpha + .75} \sum_{n=1}^{\infty} \sum_{m=1}^{\infty} w_{n} w_{m}^{\cos n\pi} \frac{\cos 2\pi m}{3}$$

$$+ 11.0\sqrt{\alpha + .933} \sum_{n=1}^{\infty} \sum_{m=1}^{\infty} w_{n} w_{m}^{\cos 5\pi m} \frac{\cos 5\pi m}{6} \frac{\cos 5\pi m}{6} \frac{\cos 5\pi m}{6}$$

$$(4.11)$$

In the above expression, θ_0 is the point of inflection. It is given approximately, as suggested by Sayed (32), by the following equation

$$\theta_{0} = 1.6 + 0.2 \log \frac{EI}{E^{1}R^{3}} \text{ radians}$$
 (4.12)

where:

EI = flexural rigidity of ring

E' = modulus of soil reaction

R = radius of the ring.

An iterative procedure for determining θ_{0} is described subsequently.

4-2.2 Potential Energy of External Load

The potential energy, Ω , of the external radial forces is given by

$$\Omega = R \int_{\Omega}^{2\pi} q(\theta) w d\theta$$
 (4.13)

The load dispersion criterion proposed by Kloppel and Glock (Chapter 2) is adopted here. Hence the loading function for a shallow conduit is taken as

$$q(\theta) = P_{S}\cos\theta, \frac{-\pi}{2} \le \theta \le \frac{\pi}{2}$$

$$= 0 \text{ elsewhere}$$
(4.14)

where p_s is the maximum pressure intensity at the level of the crown. Introducing equation (4.14) into (4.13) and integrating yields

$$\Omega = 2R \int_{0}^{\pi/2} P_{s} \cos \theta \sum_{n=1}^{\infty} W_{n} \cos \theta d\theta$$

$$= \frac{\pi R P_{s} W_{1}}{2} + P_{s} R \sum_{n=2}^{\infty} W_{n} \frac{\sin (\frac{n\pi}{2} - \frac{\pi}{2})}{(n-1)} + \frac{\sin (\frac{n\pi}{2} + \frac{\pi}{2})}{(n+1)}$$
(4.15)

Finally, equations (4.9), (4.11), and (4.15) are introduced into equation (4.1) to give

$$\begin{split} \frac{\partial v}{\partial w_1} &= 0 = k_s R w_1 \left[\pi - (\frac{\theta}{2} - \frac{\sin 2\theta}{4}) \right] \\ &+ \frac{\gamma C_d R}{4} (\frac{\pi}{3} - \theta) (2.8 \sqrt{\alpha + .25} \sum_{m=1}^{\infty} w_m \frac{\cos m\pi}{3} \cos \frac{\pi}{3}) \\ &+ \frac{\gamma C_d R}{24} \left[2.8 \sqrt{\alpha + .25} \sum_{m=1}^{\infty} w_m \frac{\cos m\pi}{3} \cos \frac{\pi}{3} + 6.4 \sqrt{\alpha + 1} \sum_{m=1}^{\infty} w_m (-1)^{m+1} \right] \\ &+ 9.2 \sqrt{\alpha + .75} \sum_{m=1}^{\infty} w_m \frac{\cos 2m\pi \cos 2\pi}{3} \\ &+ 11.0 \sqrt{\alpha + .933} \sum_{m=1}^{\infty} w_m \frac{\cos \frac{5m\pi}{6} \cos 5\pi}{6} - \frac{\pi P_s R}{2} \\ &+ 11.0 \sqrt{\alpha + .933} \sum_{m=1}^{\infty} w_m \frac{\cos \frac{5m\pi}{6} \cos 5\pi}{6} - \frac{\sin 2n\theta}{4} \right] \\ &+ \frac{\gamma C_d R}{4} (\frac{\pi}{3} - \theta_o) (2.8 \sqrt{\alpha + .25} \sum_{m=1}^{\infty} w_m \frac{\cos m\pi}{3} \cos \frac{\pi}{3}) \\ &+ \frac{\gamma C_d R\pi}{24} \left[2.8 \sqrt{\alpha + .25} \sum_{m=1}^{\infty} w_m \frac{\cos m\pi}{3} \cos \frac{\pi}{3} + 6.4 \sqrt{\alpha + 1} \sum_{m=1}^{\infty} w_m (-1)^{m+n} \right] \\ &+ 7.4 \sqrt{\alpha + .5} \sum_{m=1}^{\infty} w_m \frac{\cos 2\pi n}{2} \cos \frac{\pi}{3} \\ &+ 11.0 \sqrt{\alpha + .933} \sum_{m=1}^{\infty} w_m \frac{\cos 2\pi n}{6} \cos \frac{2\pi n}{6} \\ &- P_s R \left[\frac{\sin (\frac{n\pi}{2} - \frac{\pi}{2})}{(n-1)} + \frac{\sin (\frac{n\pi}{2} + \frac{\pi}{2})}{(n+1)} \right], n > 1 \end{split}$$

4-3 SOME OBSERVATIONS ON THE SOLUTION SCHEME

A computer program is written to solve equations (4-16) for various soil-conduit parameters. In addition to the unknown displacement coefficients, W_n , the point of inflection, θ_0 , and the constant coefficient of soil reaction, k_s , in the tangential direction to the wall of the conduit are also unknown. The program is designed to iterate over both of the later quantities (that is θ_0 and k_s) until an acceptable convergence is achieved. In the absence of experimental data, solutions from the finite element method (12) are used as the sole basis for verifying the pre-buckling displacements and stress-resultants.

Literature on the coefficient of soil reaction, k_s, in the tangential direction to the wall of the conduit, is very scarce. Kloppel and Glock (1970) have proposed a model of shear interaction that argues for a total exclusion of the tangential component of the coefficient of soil reaction. According to this model, a set of shear stresses is induced around the upper section of the conduit as a result of the direct influence of live load as shown in Figure (4-la). Subsequent deformation of the conduit induces a similar set of shear stresses acting in an opposite sense to those due to loading (Figure 4-lb). Both sets of stresses counteract each other to an extent that is not precisely determinate. However, it seems reasonable, according to this model, to ignore any resultant shear stresses since they are adjudged too small to make a significant contribution to the overall soil-structure interaction.

The provision in this computer solution, of a tangential (in addition to a normal) component of the coefficient of soil reaction is believed to be a more realistic modelling of the interaction phenomenon. The results of the computer solution indicate that for any set of conduit dimensions and live loads, the soil-structure interaction is

modelled with sufficient accuracy by taking the coefficient of tangential reaction, $k_{\rm S}$, to be constant. In particular, it has been found convenient for the purposes of developing an appropriate expression for $k_{\rm S}$, to take this constant coefficient as some multiple of the normal component, $k_{\rm S}$, at the invert, expressed by the following equation

$$k_{s} = \lambda k_{n_{i}} \tag{4.17}$$

where,

 λ = a constant less than 1.0

= 0 for
$$0 \le \theta \le \theta_0$$

The computer program, as noted earlier, performs an iterative routine. Starting with very small values of k_s and θ_o , subsequent solutions are sought with small increments of these till a reasonable convergence is achieved. The displacement at the crown of the conduit is negative (inwards). Between the crown and the springline, the displacement reverses and becomes positive (outwards) just beyond the point of inflection, θ . In other words, the test for convergence is the angle θ_{0} (incremented from zero) beyond which $w(\theta_{0})$ just reverses directions. A typical set of results is presented in Table (4-1) -(4-3) and results from finite element analysis are also presented for comparison. These results are also plotted in Figures (4-2) and (4-3). In addition, values of the constant coefficient, λ , corresponding to these are presented in Table (4-4) and Figure (4-4). Of interest is the indication that λ is practically independent of the span, D, of the conduit. Using the method of least squares, λ is found to be approximately equal to 0.2. If this value is substituted into Equation (4-17) the expression for k_s may finally be written as

$$k_s = 0.32 (4.25 - \frac{0.75D}{100})\sqrt{\alpha + 1}$$
 (4.18)

4-4 BUCKLING ANALYSIS

The ring compression theory of White and Layer (1960) suggests that the flexural rigidity of underground flexible conduits governs mainly in the installation stages while the compressive strength of the conduit material and joints governs the behavior under load, provided there is an adequate backfill. The theory, however, disregards the actual properties of soils. Furthermore, buckling may in fact govern the behavior, under load, of flexible conduits whose spans are much larger than those considered in the ring compression theory. Therefore an adequate examination of the buckling limits of large-span flexible conduits is necessary.

The second variation of potential energy is used to establish the criterion of elastic stability. The theory was developed with specific reference to elastic stability by E. Trefftz and has since been employed extensively (33, 34). It is based on the concept that a stationary mechanical system is in stable equilibrium if, and only if, the potential energy, V, of the system attains a relative minimum; hence the change, ΔV , of potential energy is such that $\Delta V > 0$ for any small virtual displacement of the system that is consistent with the constraints. The potential energy for an elastic system, is given in Equation (4-2). Consequently, the change, ΔV , in potential energy due to an infinitesimal (virtual) displacement from an equilibrium configuration is

$$\Delta V = \Delta U + \Delta \Omega \tag{4.19}$$

For an elastic system, ΔU may be written as

$$\Delta U = \delta U + \frac{1}{2!} \delta^2 U + \frac{1}{3!} \delta^3 U + \dots + \frac{1}{n!} \delta^n U$$
 (4.20)

in which $\delta^n U$ (the n^{th} variation of U) is the volume integral of a homogenous polynomial of n^{th} degree in the components of the virtual displacement vector and its first derivatives (35).

Similarly, the change, $\Delta\Omega$, in the potential energy of the external load is

$$\Delta\Omega = \delta\Omega + \frac{1}{2!} \delta^2 \Omega + \frac{1}{3!} \delta^3 \Omega + \dots + \frac{1}{n!} \delta^n \Omega$$
 (4.21)

The principle of virtual work requires that the first variation $(\delta U + \delta \Omega)$ of the potential energy vanish for any equilibrium configuration. Thus if the virtual displacements are small, the sign of ΔV is controlled by the sign of $\delta^2 U + \delta^2 \Omega$. Therefore the equilibrium is stable if, and only if, $\delta^2 U + \delta^2 \Omega > 0$ for all virtual displacements, and the criterion of stability, is that the second variation of potential energy be positive-definite. The critical load for a structure is the limiting load at which the structure first loses its stability -that is, the load at which $\delta^2 V$ ceases to be positive-definite as the load is increased from zero. Accordingly, the question of stability resolves into a mathematical study of the nature of the second variation of the potential energy. More importantly, the theory is readily generalized for multiple-degree-of-freedom systems. For a structure whose potential energy is a function of say, two variables A and B, and for arbitrary small virtual displacements A1 and B1 from some equilibrium configuration (A_0 , B_0), the change, ΔV in potential energy may be written in a Taylor's series expansion as

$$\Delta V = \frac{\partial V}{\partial A} (A_0, B_0) A_1 + \frac{\partial V}{\partial B} (A_0, B_0) B_1$$

$$+ \frac{1}{2!} \frac{\partial^2 V}{\partial A^2} (A_0, B_0) A_1^2 + 2 \frac{\partial^2 V}{\partial A \partial B} (A_0, B_0) A_1 B_1$$

$$+ \frac{\partial^2 V}{\partial B^2} (A_0, B_0) B_1^2$$
(4.22)

Hence,

$$\Delta V = \delta V + \frac{1}{2!} \delta^2 V + \frac{1}{3!} \delta^2 V + \dots$$
 (4.23a)

where:

$$\delta V = \frac{\partial V}{\partial A} (A_0, B_0) A_1 + \frac{\partial V}{\partial B} (A_0, B_0) B_1 \qquad (4.23b)$$

and

$$\delta^{2}V = \frac{\partial^{2}V}{\partial A^{2}} (A_{0}, B_{0}) A_{1}^{2} + \frac{2\partial^{2}V}{\partial A\partial B} (A_{0}, B_{0}) A_{1}B_{1} + \frac{\partial^{2}V}{\partial B^{2}} (A_{0}, B_{0}) B_{1}^{2} (4.23c)$$

The appropriate condition for the limit of positive-definiteness of a quadratic form is that the determinant of the coefficients equal zero. Hence, in the present example, the condition for the initial loss of stability may be written as

$$\begin{vmatrix} \frac{\partial^2 V}{\partial A^2} & (A_0, B_0) & \frac{\partial^2 V}{\partial A \partial B} & (A_0, B_0) \\ \frac{\partial^2 V}{\partial A \partial B} & (A_0, B_0) & \frac{\partial^2 V}{\partial B^2} & (A_0, B_0) \end{vmatrix} = 0 \qquad (4.24)$$

The use of the vanishing of the second variation of potential energy as a criterion of stability raises the question whether the equilibrium is stable at the critical load itself — that is, whether the equilibrium is stable for $P \leq P_{Cr}$, or merely for $P \leq P_{Cr}$.

Fortunately, this distinction is of little consequence in the determination of the critical load (34) and the use of the vanishing of the second variation of potential energy is a sufficient criterion.

4-5 ENERGY EXPRESSIONS IN BUCKLING ANALYSIS

In the pre-buckling analysis, it was assumed that linear theory was sufficient to ensure an accurate determination of the deflections and stress-resultants. In contrast, the development of expressions for the second variation of potential energy requires consideration of non-linearity (33), and equilibrium is based on the deformed geometry of the conduit. Recognizing this necessity, non-linear terms are retained in the geometric relationships. It is realized however, that retention of all non-linear terms is not practical and certain simplifying assumptions therefore become imperative. For example, the ring is assumed to buckle without any incremental membrane strains, and it is further assumed that the prebuckling membrane strains may be neglected without any loss of accuracy (36).

The expressions for the strains and changes of curvature may be written as

$$\overline{\varepsilon}_{\theta} = \frac{1}{R} \left\{ (\overline{v}_{\theta} - \overline{w}) + \frac{1}{2} (\overline{v} + \overline{w}_{\theta})^2 \right\}$$
 (4.25a)

and,

$$\overline{K}_{\theta\theta} = \frac{1}{R^2} (\overline{W}_{\theta\theta} + \overline{W}) \tag{4.25b}$$

where $K_{\theta\theta}$ = change in curvature of the centerline in the θ -direction, $\overline{\epsilon}_{\theta}$ = axial strain of the centerline in the θ -direction, the bar denotes the sum of the pre-buckling equilibrium configuration and the corresponding virtual component. If w and v represent the displacement vector defining an equilibrium configuration, and ζ , η the respective components of the incremental virtual displacement vector during buckling,

then, neglecting the pre-buckling rotation of the ring element, $v+w_{\theta}$, which is very small, equations (4.25) may be rewritten as

$$\overline{\varepsilon}_{\theta} = \frac{1}{R} \left\{ v_{\theta} - w + \eta_{\theta} - \zeta + \frac{1}{2} (\eta + \zeta_{\theta})^2 \right\}$$
 (4.26a)

and,

$$\overline{K}_{\theta\theta} = \frac{1}{R^2} (w_{\theta\theta} + w + \zeta_{\theta\theta} + \zeta)$$
 (4.26b)

The bending and membrane strain energy \mathbf{U}_{b} and \mathbf{U}_{m} respectively, are given by

$$U_{b} = R \int_{\Omega}^{2\pi} \frac{1}{2} \left(M_{\theta} \overline{K}_{\theta \theta} \right) d\theta$$
 (4.27a)

and

$$U_{m} = \frac{R}{2} \int_{0}^{2\pi} N_{\dot{\theta}} \overline{\epsilon}_{\dot{\theta}} d\theta \qquad (4.27b)$$

where N_{θ} = the axial force per unit length acting at the centerline in the θ -direction.

It is shown in reference (35) that ${\rm N}_{\rm H}$ and ${\rm M}_{\rm H}$ are given by

$$N_{\theta} = \frac{Et}{R} \left(\frac{\dot{v}}{v} - \overline{w} \right) - \frac{EI}{R^2} (\overline{w} + \frac{\dot{w}}{w})$$
 (4.28a)

and,

$$M_{\theta} = \frac{EI}{R^2} \left(\frac{..}{W} + \overline{W} \right) \tag{4.28b}$$

Therefore using equations (4.26) and (4.28) in equation (4.27), the strain energy components may finally be written as:

$$U_{b} = \frac{1}{2R} \int_{0}^{2\pi} \frac{EI}{R^{2}} (w + w_{\theta\theta} + \zeta + \zeta_{\theta\theta})^{2} d\theta$$
 (4.29a)

and,

$$U_{m} = \frac{R}{2} \int_{0}^{2\pi} \frac{Et}{R^{2}} \left[(\mathbf{v}_{\theta} - \mathbf{w} + \eta_{\theta} - \zeta) - \frac{EI}{R^{2}} (\mathbf{w} + \zeta_{\theta\theta} + \zeta + \mathbf{w}_{\theta\theta})^{T} \left\{ \frac{1}{R} \left[\mathbf{v}_{\theta} - \mathbf{w} + \eta_{\theta} - \zeta + \frac{1}{2} (\eta + \zeta_{\theta})^{2} \right] \right\} d\theta$$

$$(4.29b)$$

At this juncture, the strain energy, $\mathbf{U}_{\mathbf{k}}$, of the elastic supports is included. Then by expanding what is left of the total strain energy $(\mathbf{U}_{\mathbf{b}} + \mathbf{U}_{\mathbf{m}} + \mathbf{U}_{\mathbf{k}})$ and applying the fundamental definition of the second variation stated earlier, the second variation of the strain energy may be written, retaining no higher than quadratic terms, as

$$\delta^{2}U = R \left[\int_{\Omega}^{2\pi} k_{n} \zeta^{2} + \frac{EI}{R^{4}} (\zeta_{\theta\theta} + \zeta)^{2} \right] d\theta$$
 (4.30)

The problem of buckling of rings subjected to nonuniform pressures is much more involved than that of uniform pressure. The first attempt to consider nonuniform loads was apparently due to Almroth (37) who considered a pressure load of the form $P = P_0(1+\cos\theta)$. If the load remains normal to the conduit wall as the conduit deforms, the second variation of potential energy of external forces is shown in reference (35) to be given by:

$$\delta^{2}\Omega = \int_{0}^{2\pi} P (\zeta^{2} + 2\zeta_{\theta} \eta + \eta^{2}) d\theta$$
 (4.31)

It is of interest to note that $\delta^2\Omega$, unlike the first variation, depends only on the loading function and the virtual displacement components.

The problem of determining the limits of elastic stability is now reduced to one of seeking the appropriate expressions for the second variation, $\delta^2 V$, of the total potential energy. In this particular case, equations (4.30) and (4.31) combine to give:

$$\delta^{2}V = \int_{0}^{2\pi} \left[\frac{EI}{R^{3}} (\zeta_{\theta\theta} + \zeta)^{2} + RK_{n}\zeta^{2} + P(\zeta^{2} + 2\zeta_{\theta}\eta + \eta^{2}) \right] d\theta$$
 (4.32)

Equation (4.32) may be solved by any number of suitable methods. In one such method, the appropriate Euler equations of variational calculus (see appendix) are found and together with the associated boundary condition, these yield a boundary value problem. The Euler equations for an integral of the form of equation (4.32) are

$$\frac{\partial \mathbf{F}}{\partial \eta} - \frac{\mathbf{d}}{\mathbf{d}\theta} \frac{\partial \mathbf{F}}{\partial \eta_{\theta}} = 0$$

$$\frac{\partial \mathbf{F}}{\partial \zeta} - \frac{\mathbf{d}}{\mathbf{d}\theta} \frac{\partial \mathbf{F}}{\partial \zeta_{\theta}} + \frac{\mathbf{d}^{2}}{\mathbf{d}\theta^{2}} \frac{\partial \mathbf{F}}{\partial \zeta_{\theta\theta}} = 0$$
(4.33, a-b)

where F is the integrand in equation (4.32)

Solving the final set of differential equations can sometimes, as in the present case, present difficulties.

A simpler approach is the "direct-energy" method, so-called because the second variation of potential energy is minimized directly without resort to Euler equations. This is done by evaluating

the integrals in equation (4.32) term-by-term (after assuming suitable admissible displacement functions), and then applying the criterion for the limit of positive-definiteness of quadratic form discussed earlier. Because of the assumption of admissible displacement functions, this gives an upper-bound solution.

4-6 SYMMETRIC BUCKLING

If the buckling waves occur in a symmetric mode, the virtual displacement components ζ and η may be taken in the form of infinite Fourier series

$$\zeta(\theta) = \sum_{n=2}^{\infty} \mathbf{A}_n \cos n\theta$$

$$\eta(\theta) = \sum_{n=2}^{\infty} \mathbf{B}_n \sin n\theta$$
(4.34, a-b)

where rigid body displacements have been neglected by deleting terms corresponding to n = 1.

Equations (4.34) automatically satisfy the boundary requirements that the admissible displacement functions be periodic in θ . Further, the coefficient of soil reaction, k_n , may be conveniently expressed as an infinite series

$$k_{n} = \frac{k_{o}}{2} + \sum_{j=1}^{\infty} k_{j} \cos j\theta + \sum_{b=1}^{\infty} k_{b} \sin b\theta$$
 (4.35)

where,

$$k_{o} = \frac{2}{\pi} \int_{0}^{\pi} k_{n}(\theta) d\theta$$

$$k_{j} = \frac{2}{\pi} \int_{0}^{\pi} k_{n}(\theta) \cos_{j}\theta d\theta$$
(4.36, a-c)

 $k_b = 0$ (k is symmetric about the vertical axis of the ring)

Using equations (4.34) and (4.36) in (4.32), we get:

$$\delta^{2}V = \int_{0}^{2\pi} \left[\frac{EI}{R^{3}} \sum_{n=2}^{\infty} \sum_{m=2}^{\infty} (1-nm)^{2} A_{n} A_{m} \cos n\theta \cos m\theta + R \left(\frac{k_{0}}{2} + \sum_{j=1}^{\infty} k_{j} \cos_{j}\theta\right) \sum_{n=2}^{\infty} \sum_{m=2}^{\infty} A_{n} A_{m} \cos n\theta \cos m\theta + P(\theta) \left\{\sum_{n=2}^{\infty} \sum_{m=2}^{\infty} A_{n} A_{m} \cos n\theta \cos m\theta - 2 \sum_{n=2}^{\infty} \sum_{m=2}^{\infty} nA_{n} B_{m} \sin n\theta \sin m\theta + \sum_{n=2}^{\infty} \sum_{m=2}^{\infty} B_{n} B_{m} \sin n\theta \sin m\theta\right\} d\theta$$

$$(4.37)$$

where, $P(\theta) = P_0 + P_1 \cos \theta$

It is seen (Figure (4-5)) that a good approximation is obtained by taking only two terms of the soil coefficient function — that is, $k_n(\theta) = \frac{k}{2} + k_1 \cos\theta - \text{and also by taking } P_1 = P_0, \text{ so that } P(\theta) = P_0(1+\cos\theta).$

Now,

$$\int_{0}^{\pi} \cos \theta \cos \theta d\theta = \int_{0}^{\pi} \sin \theta \sin \theta d\theta = \frac{\pi}{2}, n = m$$

$$= 0, n \neq m$$

$$\int_{0}^{2\pi} \cos \theta \cos \theta \cos \theta d\theta = 0, n \neq j + m \text{ or } j \neq m + n \text{ or } m \neq j + n$$

$$= \frac{\pi}{2}, n = j + m \text{ or } j = m + n \text{ or } m = j + n$$

$$\int_{0}^{2\pi} \cos \theta \sin \theta \sin \theta d\theta = 0, n \neq j + m \text{ or } j \neq n + m \text{ or } m \neq j + n$$

$$= \frac{\pi}{2}, n = j + m \text{ or } j = n + m \text{ or } m = j + n$$

$$\int_{0}^{2\pi} \sin j\theta \cos n\theta \cos m\theta = 0$$

Using the above relations in equation (4.37) and performing the integration, the second variation of potential energy becomes

$$\delta^{2}V = \frac{\pi E I}{R^{3}} \sum_{n=2}^{\infty} (1-n^{2})^{2} A_{n}^{2} + \frac{\pi k_{o}R}{2} \sum_{n=2}^{\infty} A_{n}^{2}$$

$$+ P_{o}\pi \left[\sum_{n=2}^{\infty} B_{n}^{2} - 2 \sum_{n=2}^{\infty} nA_{n}B_{n} + \sum_{n=2}^{\infty} A_{n}^{2}\right], n=m$$

$$+ \frac{\pi R k_{1}}{2} \sum_{n=2}^{\infty} \sum_{m=2}^{\infty} A_{n}A_{m} + \frac{P_{o}\pi}{2} \left[\sum_{n=2}^{\infty} \sum_{m=2}^{\infty} A_{n}A_{m} + \frac{P_{o}\pi}{2} \left[\sum_{n=2}^{\infty$$

Equation (4.38) represents a quadratic form in the displacement parameters. Differentiating this quadratic form with respect to each of the parameters, a set of homogenous linear equations in the parameters is obtained. The matrix containing these parameters is called the stability matrix. Clearly, the stability matrix contains two sets of terms, namely a submatrix of load-independent terms X_{nm} , and one of load-dependent berms B_{nm}^* . The critical pressure is represented by the value of P_0 for which the determinant of the stability matrix vanishes. Because of the coupling of terms in A_n , B_n and A_m , B_m ($m \neq n$), the indicated differentiation is accomplished in two parts — first with n=m, and then with $n \neq m$. With F as defined earlier, differentiation for n = m gives

$$\frac{\partial F}{\partial A_n} = \frac{2\pi EI}{R^3} (1-n^2)^2 A_n + \pi K_0 RA_n - P_0 \pi (2nB_n - 2A_n) = 0 \qquad (4.39a)$$

$$\frac{\partial F}{\partial B_n} = 2P_0 \pi B_n - 2n\pi A_n P_0 \tag{4.39b}$$

Solving for B_n in equation (4-39b) and substituting in equation (4.39a) gives

$$\left[\frac{2EI}{R^3} (1-n^2)^2 + k_0 R + 2P_0(n^2-1)\right] A_n = 0$$
 (4.39c)

Equation (4.39c) constitutes the diagonal elements, x and B_{nn}^{*} of the stability matrix.

That is,

$$x_{nn} = \frac{2EI}{R^3} (1-n^2)^2 + K_0 R$$
 (4.40a)

$$B_{nn}^{\star} = 2(n^2 - 1) \tag{4.40b}$$

Similarly for $n \neq m$, differentiation yields:

$$\frac{\partial F}{\partial A_{n}} = \pi k_{1} R(A_{n+1} + A_{n-1}) + P_{0} \pi [A_{n+1} + A_{n-1} + n(B_{n+1} + B_{n-1})] = 0$$

$$\frac{\partial F}{\partial B_{n}} = P_{0} \pi [-\{B_{n+1} - (n+1) A_{n+1}\} - \{B_{n-1} - (n-1) A_{n-1}\}] = 0$$

$$(4.41, a-b)$$

A special class of problems is obtained by letting the off-diagonal elements $(A_{n+1}, B_{n+1}, A_{n-1}, B_{n-1})$ of the stability matrix vanish. In this case, equations (4.41) are identically zero, and equation (4.39c) then simplifies to

$$P_{CT} = \frac{EI(n^2-1)}{R^3} + \frac{K_0R}{2(n^2-1)}$$
 (4.42)

which is the classical solution for a uniformly supported circular ring under uniform boundary pressure.

For the non-uniformly supported and non-uniformly loaded ring, equation (4.4lb) is satisfiedd in one of two ways:

(i)
$$B_{n+1} = (n+1) A_{n+1} \text{ and } B_{n-1} = (n-1) A_{n-1}$$

(ii)
$$B_{n+1} = (n-1) A_{n-1} \text{ and } B_{n-1} = (n+1) A_{n+1}$$

In either case, substitution into equation (4.4la) yields

$$\frac{\partial F}{\partial A_{n}} = 0 = \pi k_{1} R \left(A_{n+1} + A_{n-1} \right) + P_{0} \pi \left[\left\{ n (n-1) + 1 \right\} A_{n-1} + \left\{ n (n+1) + 1 \right\} \right] A_{n+1}$$
(4.43)

Equation (4.43) constitutes the off-diagonal elements of the stability matrix. (The fact that cases (ii) and (iii) give identical results is due to the symmetry of the stability matrix.)

Hence,

$$X(n,n+1) = X(n,n-1) = k_1R$$
 $B*(n,n-1) = n(n-1) + 1$
 $B*(n,n+1) = n(n+1) + 1$

(4.44, a-c)

As stated earlier, the stability condition is

$$\left|X + P_{O}B^{\star}\right| = 0 \tag{4.45}$$

This is the standard eigenvalue problem, and the lowest eigenvalue represents the buckling load. Several techniques are available for solving matrix eigenvalue problems. This study employs the iterative Jacobi method, as outlined in the appendix, because of its ability to furnish the eigenvectors along with the eigenvalues without requiring a separate set of procedures as in most other method. This is particularly useful if an approximate geometric configuration of the ring during buckling, is desired.

4-7 NONSYMMETRIC BUCKLING

For this case, the boundary requirements are still that the virtual displacement components be periodic in θ . Hence the following displacement functions are admissible

$$\zeta = \sum_{n=2}^{\infty} (A_n \cos n\theta + B_n \sin n\theta)$$

$$\eta = \sum_{n=2}^{\infty} (C_n \sin n\theta + D_n \cos n\theta)$$
(4.46, a-b)

Using these equations in equation (4.32) and carrying out the integration yields

$$\delta^{2}V = 0 = \frac{EI\pi}{R^{3}} \sum_{n=2}^{\infty} (1-n^{2})^{2} (A_{n}^{2} + B_{n}^{2}) + \frac{k_{o}\pi R}{2} \sum_{n=2}^{\infty} (A_{n}^{2} + B_{n}^{2})$$

$$+ P_{o}\pi (\sum_{n=2}^{\infty} A_{n}^{2} + \sum_{n=2}^{\infty} B_{n}^{2} + \sum_{n=2}^{\infty} C_{n}^{2} + \sum_{n=2}^{\infty} D_{n}^{2}$$

$$- 2 \sum_{n=2}^{\infty} nA_{n}C_{n} + 2 \sum_{n=2}^{\infty} nB_{n}D_{n}), n=m$$

$$+ \frac{k_{1}\pi R}{2} (\sum_{n=2}^{\infty} \sum_{n=2}^{\infty} A_{n}A_{m} - \sum_{n=2}^{\infty} \sum_{n=2}^{\infty} B_{n}B_{m}) + \frac{P_{o}\pi}{2} (\sum_{n=2}^{\infty} \sum_{n=2}^{\infty} A_{n}A_{m} - \sum_{n=2}^{\infty} \sum_{n=2}^{\infty} B_{n}B_{m}$$

$$- \sum_{n=2}^{\infty} \sum_{n=2}^{\infty} C_{n}C_{m} + \sum_{n=2}^{\infty} \sum_{n=2}^{\infty} D_{n}D_{m} + 2 \sum_{n=2}^{\infty} \sum_{n=2}^{\infty} nA_{n}C_{m} + 2 \sum_{n=2}^{\infty} \sum_{n=2}^{\infty} nB_{n}D_{m}), n=m+1$$

$$+ \sum_{n=2}^{\infty} \sum_{n=2}^{\infty} C_{n}C_{m} + \sum_{n=2}^{\infty} \sum_{n=2}^{\infty} D_{n}D_{m} + 2 \sum_{n=2}^{\infty} \sum_{n=2}^{\infty} nA_{n}C_{m} + 2 \sum_{n=2}^{\infty} \sum_{n=2}^{\infty} nB_{n}D_{m}), n=m+1$$

$$+ \sum_{n=2}^{\infty} \sum_{n=2}^{\infty} C_{n}C_{m} + \sum_{n=2}^{\infty} \sum_{n=2}^{\infty} D_{n}D_{n} + 2 \sum_{n=2}^{\infty} \sum_{n=2}^{\infty} \sum_{n=2}^{\infty} nA_{n}C_{m} + 2 \sum_{n=2}^{\infty} \sum_{n=2}^{\infty} \sum_{n=2}^{\infty} nB_{n}D_{n}), n=m+1$$

$$+ \sum_{n=2}^{\infty} \sum_{n=2}^{\infty} C_{n}C_{m} + \sum_{n=2}^{\infty} \sum_{n=2}^{\infty} D_{n}D_{n} + 2 \sum_{n=2}^{\infty} \sum_{n=2}^{\infty} \sum_{n=2}^{\infty} nA_{n}C_{m} + 2 \sum_{n=2}^{\infty} \sum_{n=2}^{\infty} \sum_{n=2}^{\infty} nB_{n}D_{n}), n=m+1$$

$$+ \sum_{n=2}^{\infty} \sum_{n=2}^{\infty} C_{n}C_{n} + \sum_{n=2}^{\infty} \sum_{n=2}^{\infty} D_{n}D_{n} + 2 \sum_{n=2}^{\infty} \sum_{n=2}^{\infty} \sum_{n=2}^{\infty} nA_{n}C_{n} + 2 \sum_{n=2}^{\infty} \sum_{n=2}^{\infty} \sum_{n=2}^{\infty} \sum_{n=2}^{\infty} \sum_{n=2}^{\infty} nA_{n}C_{n} + 2 \sum_{n=2}^{\infty} \sum_{n=2}^{\infty}$$

Proceeding in a manner similar to the symmetric case, the quadratic form is differentiated with respect to the displacement parameters to obtain the elements of the stability matrix.

Hence, for n=m, differentiation gives:

$$\frac{\partial F}{\partial A_{n}} = 0 = \frac{2\pi EI}{R^{3}} (1-n^{2})^{2} A_{n} + \pi R k_{o} A_{n} + 2\pi P_{o} (A_{n}-nC_{n})$$

$$\frac{\partial F}{\partial B_{n}} = 0 = \frac{2\pi EI}{R^{3}} (1-n^{2})^{2} B_{n} + \pi R k_{o} B_{n} + 2\pi P_{o} (B_{n}-nD_{n})$$

$$\frac{\partial F}{\partial C_{n}} = 0 = 2\pi P_{o} (C_{n}-nA_{n})$$

$$\frac{\partial F}{\partial D_{n}} = 0 = 2\pi P_{o} (D_{n}-nB_{n})$$
(4.48, a-d)

Solving for C_n and D_n in the last two equations and substituting in the first two gives

$$\frac{\partial F}{\partial A_{n}} = 0 = \frac{2\pi EI}{R^{3}} (1-n^{2})^{2} A_{n} + \pi k_{o} RA_{n} + 2\pi P_{o} (n^{2}-1) A_{n}$$

$$\frac{\partial F}{\partial B_{n}} = 0 = \frac{2\pi EI}{R^{3}} (1-n^{2})^{2} B_{n} + \pi k_{o} RB_{n} + 2\pi P_{o} (n^{2}-1) B_{n}$$
(4.49, a-b)

Each of equations (4.49) is a function of only one type of displacement parameters. Therefore only one set of these equations is necessary to generate the elements of the stability matrix.

Hence

$$X(n,n) = \frac{2EI}{R^3} (1-n^2)^2 + k_0 R$$
 (4.50a)

$$B*(n,n) = 2(n^2-1)$$
 (4.50b)

Similarly for $n \neq m$, differentiation gives

$$\frac{\partial F}{\partial A_{n}} = 0 = \pi R k_{1} (A_{n+1} + A_{n-1}) + P_{0} \pi (nC_{n+1} + A_{n+1} + nC_{n-1} + A_{n-1})$$

$$(4.51, a-b)$$

$$\frac{\partial F}{\partial C_{n}} = 0 = P_{0} \pi [(n+1)A_{n+1} + (n-1)A_{n-1} - C_{n+1} - C_{n-1}]$$

Equations (4.51) are seen to be identical to equation (4.41) obtained for the symmetric case. Therefore the elements of the stability matrix can be written directly as

$$x(n,n+1) = K(n,n-1) = k_1R$$

$$B^*(n,n-1) = n(n-1) + 1$$

$$B^*(n,n+1) = n(n+1) + 1$$
(4.52, a-c)

4-8.1 Elliptical Cross-Section

So far, the discussion has centered exclusively on circular cross-section, resulting in the simplest possible solution, but lacking generality. In what follows, the theory is extended to rings of elliptical cross-section. As suggested by Brush and Almroth (33), shells of a general shape subjected to axisymmetric load can be expected to fail through the passing of a limit point. Therefore the same criterion is used to define the limit of elastic stability of the elliptical ring as for the circular ring — that is the load at which $\delta^2 V$ ceases to be positive-definite as the load is increased from zero.

In the previous chapter, the coefficient of soil reaction in the normal direction to the wall of the conduit, was shown to be related to the span, D, of the conduit, the depth of cover, H, and the direction of action, θ , by equation (3.16). In order to show that this expression applies equally well to general shapes, it is necessary to extend it to an elliptical section. For this purpose the following expression for the depth, H, to any point on the elliptical conduit is quite useful (Figure (4-6a)):

$$H = H_C + Z \tag{4.53a}$$

where:

 $H_c = depth to the crown$

$$Z = b \left\{ 1 - \frac{b\cos\theta}{\left[a^2\sin^2\theta + b^2\cos^2\theta\right]^{1/2}} \right\}$$
 (4.53b)

Like the circular ring, the results are compared to the corresponding solutions from finite element analysis. The properties of the ellipse chosen for this purpose are

Span, D = 286 inches

Semi-minor axis, b = 80.5 inches

Semi-major axis, a = 143 inches

The results for depths of cover to the crown of 4, 6 and 8 feet are shown in Table (4-5) and agreement with results from finite element analyses is seen to be reasonable. Therefore the expressions for the coefficients of soil reaction proposed herein are believed to apply reasonably well to conduits of arbitrary geometry. (In practice of course, geometry is prescribed.)

The pre-buckling analysis for the elliptical conduit is identical in outline to that of the circular section. Hence, a separate elaborate presentation is not considered necessary here.

4-8.2 Stability Analysis

The radius of curvature of the elliptical section varies around the conduit, and the expressions for the second variation of potential energy (equation (4.32)) must be modified to reflect this. The radius of curvature, R, at any point on the conduit is given by (39)

$$R(\theta) = a^{2}b^{2} \frac{1}{\left[a^{2}\sin^{2}\theta + b^{2}\cos^{2}\theta\right]^{3/2}}$$

$$= \frac{b^{2}}{a} \frac{1}{\left[1 - s^{2}\cos^{2}\theta\right]^{3/2}}$$
(37)

where

$$\varepsilon^2 = 1 - \left(\frac{b}{a}\right)^2$$

a = semi-major axis

b = semi-minor axis

R = radius of curvature.

Hence, the second variation of potential energy for the elliptical ring may be written as

$$\delta^{2} v = \int_{0}^{2\pi} \left\{ \frac{EIa^{3}}{b^{6}} \left(1 - \epsilon^{2} \cos^{2}\theta \right)^{9/2} \left(\zeta_{\theta \theta} + \zeta \right)^{2} + \frac{b^{2} k_{n} \zeta^{2}}{a \left[1 - \epsilon^{2} \cos^{2}\theta \right]^{3/2}} + P \left(\zeta^{2} + 2\zeta_{\theta} \eta + \eta^{2} \right) \right\} d\theta$$
(4.55)

(As a check, it is seen that for a = b = R, equation (4.55) reduces to equation (4.32) obtained for the circular conduit of radius, R.)

As in the circular cross-section, the only boundary requirement for the elliptical ring is still that the virtual displacement functions be periodic in θ . Therefore the same set of functions are admissible for the elliptical ring as for the circular.

Hence,

$$\zeta(\theta) = \sum_{n=2}^{\infty} A_n \cos n\theta$$

$$\eta(\theta) = \sum_{n=2}^{\infty} B_n \sin n\theta$$
(4.56, a-b)

where rigid body displacements have been automatically deleted as explained for the circular section.

Introducing these into equation (4.55) gives

$$\delta^{2}V = \int_{0}^{2\pi} \left\{ \frac{\text{EIa}^{3}}{b^{6}} \left(1 - \epsilon^{2} \cos^{2}\theta \right)^{9/2} \sum_{n}^{\infty} \left[A_{n} \cos n\theta - n^{2} A_{n} \cos n\theta \right]^{2} \right.$$

$$+ \frac{b^{2}k_{n}}{a \left[1 - \epsilon^{2} \cos^{2}\theta \right]^{3/2}} \sum_{n}^{\infty} \sum_{m}^{\infty} A_{n} A_{m} \cos n\theta \cos m\theta$$

$$+ P\left[\sum_{n}^{\infty} \sum_{m}^{\infty} A_{n} A_{m} \cos n\theta \cos m\theta - 2 \sum_{n}^{\infty} \sum_{m}^{\infty} A_{n} B_{m} \sin n\theta \sin m\theta \right] \right\} d\theta$$

$$+ \sum_{n}^{\infty} \sum_{m}^{\infty} B_{n} B_{m} \sin n\theta \sin m\theta \right] d\theta \qquad (4.57)$$

Evidently, equation (4.57) is difficult to integrate in terms of elementary functions, hence recourse is sought to numerical integration schemes. In particular, the trapezoid rule (38) is used. Briefly, for a function $f(\theta)$ defined on some interval $0-\pi$ say, integration by trapezoid rule furnishes the following

$$\int_{0}^{\pi} f(\theta) d\theta \simeq \frac{\Delta \theta}{2} \left[f(0) + f(\pi) + 2 \sum_{i=1}^{n-1} f_{i} \right] + \text{Error terms} \qquad (4.58)$$

If the uniform interval $\Delta\theta$ is kept sufficiently small, the error terms are relatively negligible. (The trapezoid rule is developed in detail in the appendix.)

Then using equations (4.53) and (3.16) in (4.57) numerical integration yields the following expression for the elliptical conduit embedded in dense fill:

$$\begin{split} \delta^{2}v &= \frac{\text{ETa}^{2}}{6b^{4}} \left[\left(1 - \epsilon^{2} \right)^{9/2} \sum_{n=m}^{\infty} \sum_{m=1}^{\infty} \left(1 - n^{2} - m^{2} + n^{2} m^{2} \right) \lambda_{n} \lambda_{m} \right. \\ &+ \left(1 - \epsilon^{2} \right)^{9/2} \sum_{n=m}^{\infty} \sum_{m=1}^{\infty} \left(1 - n^{2} - m^{2} + n^{2} m^{2} \right) \lambda_{n} \lambda_{m} \left(-1 \right)^{m+n} \\ &+ \left(1 - 0 \cdot 75\epsilon^{2} \right)^{9/2} \sum_{n=m}^{\infty} \sum_{m=1}^{\infty} \left(1 - n^{2} - m^{2} + n^{2} m^{2} \right) \lambda_{n} \lambda_{m} \left. \begin{array}{c} \cos m \pi \\ 6 \end{array} \\ &+ \left(1 - 0 \cdot 25\epsilon^{2} \right)^{9/2} \sum_{n=m}^{\infty} \sum_{m=1}^{\infty} \left(1 - n^{2} - m^{2} + n^{2} m^{2} \right) \lambda_{n} \lambda_{m} \left. \begin{array}{c} \cos m \pi \\ 3 \end{array} \right. \\ &+ \sum_{n=1}^{\infty} \sum_{m=1}^{\infty} \left(1 - n^{2} - m^{2} + n^{2} m^{2} \right) \lambda_{n} \lambda_{m} \left. \begin{array}{c} \cos m \pi \\ 3 \end{array} \right. \\ &+ \sum_{n=1}^{\infty} \sum_{m=1}^{\infty} \left(1 - n^{2} - m^{2} + n^{2} m^{2} \right) \lambda_{n} \lambda_{m} \left. \begin{array}{c} \cos \frac{\pi \pi}{3} \end{array} \right. \\ &+ \sum_{n=1}^{\infty} \sum_{m=1}^{\infty} \left(1 - n^{2} - m^{2} + n^{2} m^{2} \right) \lambda_{n} \lambda_{m} \left. \begin{array}{c} \cos \frac{\pi \pi}{3} \end{array} \right. \\ &+ \left(1 - \cdot 75\epsilon^{2} \right)^{9/2} \sum_{n=1}^{\infty} \sum_{m=1}^{\infty} \left(1 - n^{2} - m^{2} + n^{2} m^{2} \right) \lambda_{n} \lambda_{m} \left. \begin{array}{c} \cos \frac{\pi \pi}{3} \end{array} \right. \\ &+ \left(1 - \cdot 75\epsilon^{2} \right)^{9/2} \sum_{n=1}^{\infty} \sum_{m=1}^{\infty} \left(1 - n^{2} - m^{2} + n^{2} m^{2} \right) \lambda_{n} \lambda_{m} \right. \\ &+ \left(1 - \cdot 75\epsilon^{2} \right)^{9/2} \sum_{n=1}^{\infty} \sum_{m=1}^{\infty} \lambda_{n} \lambda_{m} + \frac{3 \cdot 2a^{2}}{2b} \left(-1 \right)^{m+n} \sqrt{\alpha + \frac{2b}{b}} \sum_{n=1}^{\infty} \sum_{n=1}^{\infty} \lambda_{n} \lambda_{m} \\ &+ \left(1 - \cdot 75\epsilon^{2} \right)^{9/2} \sqrt{\alpha} + \frac{b}{D} \left(1 - \frac{.866b}{\left[\cdot 75a^{2} + \cdot 25b^{2} \right]^{3/2}} \right) \sum_{n=1}^{\infty} \sum_{m=1}^{\infty} \lambda_{n} \lambda_{m} \\ &+ \left(1 - \cdot 75\epsilon^{2} \right) \sqrt{\alpha} + \frac{b}{D} \left(1 - \frac{.5b}{\left[\cdot 75a^{2} + \cdot 25b^{2} \right]^{3/2}} \right) \sum_{n=1}^{\infty} \sum_{n=1}^{\infty} \lambda_{n} \lambda_{m} \\ &+ \left(1 - \cdot 75\epsilon^{2} \right) \sqrt{\alpha} + \frac{b}{D} \left(1 - \frac{.5b}{\left[\cdot 75a^{2} + \cdot 25b^{2} \right]^{3/2}} \right) \sum_{n=1}^{\infty} \sum_{n=1}^{\infty} \lambda_{n} \lambda_{m} \\ &+ \left(1 - \cdot 75\epsilon^{2} \right) \sqrt{\alpha} + \frac{b}{D} \left(1 - \frac{.5b}{\left[\cdot 75a^{2} + \cdot 25b^{2} \right]^{3/2}} \right) \sum_{n=1}^{\infty} \sum_{n=1}^{\infty} \lambda_{n} \lambda_{m} \\ &+ \left(1 - \cdot 75\epsilon^{2} \right) \sqrt{\alpha} + \frac{b}{D} \left(1 - \frac{.5b}{\left[\cdot 75a^{2} + \cdot 25b^{2} \right]^{3/2}} \right) \sum_{n=1}^{\infty} \sum_{n=1}^{\infty} \lambda_{n} \lambda_{m} \\ &+ \left(1 - \cdot 75\epsilon^{2} \right) \sqrt{\alpha} + \frac{b}{D} \left(1 - \frac{.5b}{\left[\cdot 75a^{2} + \cdot 25b^{2} \right]^{3/2}} \right) \sum_{n=1}^{\infty} \sum_{n=1}^{\infty} \lambda_{n} \lambda_{m} \\ &+ \left(1 - \cdot 75\epsilon^{2} \right) \sqrt{\alpha} + \frac{b}{D} \left(1 - \frac{.5b}{\left[$$

$$+ P_{O}\pi \left[\sum_{n=1}^{\infty} B_{n}^{2} - 2\sum_{n=1}^{\infty} nA_{n}B_{n} + \sum_{n=1}^{\infty} A_{n}^{2}\right], \quad n=m$$

$$+ \frac{P_{O}\pi}{2} \left[\sum_{n=1}^{\infty} \sum_{m=1}^{\infty} A_{n}A_{m} + 2\sum_{n=1}^{\infty} \sum_{m=1}^{\infty} nA_{n}B_{m} - \sum_{n=1}^{\infty} \sum_{m=1}^{\infty} B_{n}B_{m}\right], \quad n=m+1 \quad \text{or} \quad m=n+1 \quad n, m\neq 1 \quad (4.59)$$

The quadratic form is reduced to a stability matrix and the resulting eigenvalue problem solved in much the same manner as the circular cross-section.

4-9 COMPARISON WITH TEST RESULTS

The present study is compared in Tables (4-6) to (4-8) with results of buckling tests by Meyerhof and Baike (1963), Watkins and Moser (40), and Luscher (1963). While agreements with the results of Watkins and Moser is quite good, there is considerable discrepancy with Luscher's results. This is the special case of uniform boundary pressures and uniform elastic support (coefficient of soil reaction) discussed in the preceding chapter. The discrepancy may be due in part to the fact that Luscher's results in themselves exhibit a great deal of scatter due probably to the rather small dimensions of the test parameters (0.815 inch for the radius of the conduit and less than 0.75 inch for the depth of cover). For such small scale tests, the effects of imperfections may be considerable.

Meyerhof and Baike's tests do not really belong to the standard class of buried conduits. Quarter sections of a circular conduit resting on compacted sand backfill, were loaded to failure by loads applied directly to the ends of the sheets (figure 4-11). This is a more severe condition of loading than the case encountered in practice in which the load is applied on the buried conduit through the fill.

(The present study falls in the later category.) Consequently, the later case should yield higher buckling pressures than the former.

Table (4-7) shows that this is the case, with results from the present study (based on a minimum cover of 3 inches, and medium soil) giving consistently higher critical pressures than those of Meyerhof and Baike. However, in all but one case, the two results agree to within 20%.

CHAPTER 5

DISCUSSION

The present study may be broadly divided into two parts:

- An examination of the characteristics of the coefficient of soil reaction.
- 2) Pre-buckling analysis and the determination of the limits of elastic stability.

5-1 COEFFICIENT OF SOIL REACTION

The concept of coefficient of soil reaction is used to describe the restraint offered against the outward movement of the conduit by the supporting fill. The significant work in this area belongs to Meyerhof and Baike (1963), Kloppel and Glock (1970), and Luscher (1963) as reviewed in Chapter 2. A comparison of the theoretical formulation is presented in Table (4-9). As noted earlier, the above studies considered the soil medium to be represented by an isotropic, homogeneous, linear continuum. Further, for a Poisson's ratio of soil, v_s , of 0.5 the expressions simplify to a constant value of coefficient of soil reaction given by

$$k = \frac{E_S}{1.5R} \tag{5.1}$$

where E is the soil modulus considered to be constant, and R the conduit radius.

This author believes that the assumptions inherent in equation (5.1) are quite conservative and suggests the expressions developed in Chapter

3. These expressions result from a numerical modelling of the interaction

process by means of non-linear finite element stress analysis. A nonlinear constitutive relationship (the hyperbolic model) is used to represent the mechanical behavior of the granular backfill. Any realistic modelling of the interaction problem must include some form of non-linear stress-strain relationship for the soil medium. Furthermore, it should be possible to determine the material parameters by making use of test results from conventional soil tests. The finite element analysis on which this study is based satisfies these requirements in that the hyperbolic parameters used in Table (3-1) are taken from the results of triaxial tests by Duncan and associates (1977). For this reason, the hyperbolic constitutive relationship is clearly an improvement over the linear-elastic model upon which equation (5.1) is based. Furthermore, an analytical modelling of compaction and construction processes is an important feature of the finite element analysis used in the present study. Special elements are adopted to represent the behavior at the interface between the backfill and the structure. The objective of developing a simple methodology applicable to everyday problems in soil-steel structures, is accomplished by means of the concept of dimensional analysis. By such procedure, the problem simplifies to parameters that are more readily amenable. More importantly, such simplification in no way precludes a thorough and comprehensive treatment of the problem. While the original finite element analysis incorporates the mechanical non-linearities of the soil-structure system, the final expressions for the coefficient of soil reaction contain only such simple parameters as the depth of filling, the span of the conduit, and the direction of action -- all of which can be readily defined without any ambiguity.

Experimental determinations of the coefficient of soil reaction

reported in the literature, are very limited in scope. Consistent with Marston-Spangler theory, Watkins (7) conducted model tests on flexible conduits in sand backfill and determined the coefficient of soil reaction at the springline. Meyerhof and Baike (1963) performed tests on quarter sections of circular culverts embedded in sand backfill and obtained "the average values of the soil pressure, radial deflection, and coefficient of soil reaction by dividing the total volume under the pressure and deflection curves by the area of the sheets in contact with the sand."

A graphical summary of the characteristics of the coefficient of soil reaction is given in Figures (3-7) and (3-8) and Tables (3-2) to (3-35). From these, the following observations appear valid:

1) The coefficient of soil reaction is not constant around the conduit as equation (5.1) suggests. This finding was verified experimentally by Meyerhof and Baike who noted that "the observed coefficients of soil reaction varied considerably around the sheets." It is observed in the present study that for a given conduit, the coefficient of reaction of a well-compacted granular backfill varies with the depth of filling and the direction of action, attaining a maximum value at the invert and a minimum at the crown of the conduit. The influence of depth on the coefficient of soil reaction was recognized by Terzaghi (1955) who postulated that the coefficient of horizontal soil reaction for sands, was linearly proportional to the depth of the sand backfill, and proposed the following equation

$$k_{h} = n_{h} \frac{Z}{B} \tag{5.2}$$

where n_h = constant of horizontal subgrade reaction (tons per square

foot per foot); Z = depth at which k_h is evaluated (feet), and B = width of pile (feet).

Proposed values of the coefficient of soil reaction based on load tests by Terzaghi are given in Table (4-10). However, a direct inference is impossible from these data since they refer exclusively to footings, beams and piles.

- 2) Within the range of soil displacements encountered in this study (less than 0.1 inch in all cases), the magnitude of soil displacements exerts no influence on the coefficient of soil reaction around the conduit. This is indicative of a linear load-deflection relationship (Figure (3-9)). However, the coefficient of soil reaction is influenced by changes in the direction of soil displacements. This behavior can be inferred from the work of Terzaghi (1955).
- 3) The coefficient of soil reaction is very sensitive to changes in the relative density of the backfill. This fact is clearly borne out by Tables (3-2) to (3-35) which show that k_n increases with the relative density of the backfill.
- 4) The coefficient of soil reaction is more sensitive to changes in the depth of cover when the depth ratio (the ratio of the depth of cover to the crown, to the span of the conduit) is in the neighborhood of 0.1 to 0.6.

5-2 ANALYSIS AND STABILITY

The pre-buckling deflections, moments and thrusts are summarized in Figures (4-2) and (4-3) and compared with corresponding solutions from the finite element method in Tables (4-1) to (4-3). With the exception of the elliptical sections, the two sets of results (present study versus finite element solution) show remarkable agreement. In the case

of the elliptical section, there is some discrepancy in the values of the moments at the haunches. This discrepancy may be due to the differences in the geometry of the sections used in the two solutions.

The elliptical section considered in the finite element solution is an actual model of the Adelaide Creek Culvert in Canada, and comprises sections of circular sheets fabricated to form an approximate ellipse.

In contrast, a perfectly elliptical section is considered in this study.

The study of stability is involved with the determination of the critical load (or stress) for the soil-steel structure. A detailed review of the literature on this subject is given by Leonard and Setkar (1970). As noted earlier, all theories with the exception of Kloppel and Glock, assume uniform radial boundary pressure around the conduit wall. To the author's knowledge, the present study is the first realistic attempt to consider non-uniform fill support (coefficient of soil reaction) in addition to non-uniform boundary pressures.

A summary of the theoretical buckling pressures is given in Figures (4-6b) to (4-9) and Tables (4-11) to (4-14). In Figure (4-6a) and Table (4-11) comparison is made with the results of Luscher (1960), Meyerhof and Baike (1963), Cheney (41), and Chelapati and Allgood (42). To illustrate the importance of interaction with the backfill, the critical stress for a non-supported circular ring $(P_{cr} = 3EI/R^3)$ is also plotted on the same axes (Figure (4-6a)). From such data, the following observations may be made:

1) Providing even a fair amount of elastic support increases the critical stress by an order of magnitude. The case plotted in Figure (4-6a) is for a circular conduit of diameter 120 inches, buried to a depth of 120 inches in a fill of $E_s = 20,000$ psi, and $v_s = 0.4$. The results show that the critical stress for the unsupported ring is

300 psi at EI/R³ of 100. This jumps to 1371 psi and 2380 psi for the same flexibility factor (EI/R³) when the ring is embedded respectively in a medium and a dense backfill. Evidently the substantial increase in the load carrying capacity of the structure is derived from its interaction with the surrounding fill. Accordingly the performance limit of the structure might be expected to be first reached at the point where it is least supported. Such expectation is verified from the plots of both the pre-buckling deflection (figure (4-2)) and the "relative" deflections during buckling (Figure (4-10)). (The relative nature of the deflections during buckling is emphasized because the eigenvectors satisfying a particular eigenvalue can only be determined to a multiplicative degree.) From these plots, it is clear that the maximum deflections occur at the crown of the conduit (point of least support) suggesting that instability would first initiate at that

2) At small values of the coefficient of soil reaction and the flexural rigidity of the conduit wall (EI), the conduit may fail by buckling. For larger values of these, the conduit may fail by yielding of the section. A similar conclusion was reached by Meyerhof and Baike (1963). As an illustration, the critical stress for the case considered in Figure (4-6a) is only 101 psi for $EI/R^3 = 1.0$ when the backfill is of medium relative density. With an increase in the relative density (hence an increase in K) and the stiffness of the conduit wall (say $EI/R^3 = 100$, dense soil), the critical stress is 2380 psi. The thrust corresponding to this (N \simeq PR) is 142800 lb/in and the corresponding thrust stress, N/A, (the cross-sectional areas of these thin-walled structures are much less than unity in general) is well into the inelastic range. To extend the theory to stresses in the inelastic

range, a number of approximate solutions are available. Meyerhof and Baike (1963) recommended the following equation, due originally to Timoshenko (36)

$$f_e = \frac{f_y}{1 + \frac{y}{f_{cr}}}$$
 (5.3)

where:

f = critical compressive (ring buckling) stress

 F_{y} = yield stress of conduit material

f = buckling stress obtained from analysis.

3) The critical stress, like the coefficient of soil reaction, is more sensitive to the depth of cover when the depth ratio

$$(\alpha = \frac{\text{depth to the crown}}{\text{span of the conduit}})$$

is less than or equal to 0.6 (Figure (4-8). This behavior has been verified experimentally by Donnellan (43), and Allgood (44). It may be explained by the fact that the thrust due to live load increases due to reduced arching as the depth of cover inchreases (Bakt, 1970).

4) Elliptical conduits have twice as much tendency to buckle as circular conduits of equal span and rise, under identical soil conditions.

This tendency varies inversely with the aspect ratio

Figure (4-9)). Results similar to these have been presented by Kloppel and Glock (1970) (buckling load of an elliptical conduit is half that of the circular conduit), and Marlowe and Brogan (45) (buckling load

decreases with an increase in the aspect ratio). However, the later study did not consider soil-supported conduits, and a more direct comparison is not possible.

The direct correlation between the buckling pressure of elliptical conduits and the radius of curvature at the crown, suggested by the OHBDC (equation 2.25) is not verified in the present study. For the two cases considered, the buckling pressure is 85 psi for a crown radius of 300 inches (depth to the crown of 48 inches and span of 300 inches) but increases to 108 psi for the same crown radius of 300 inches with depth to the crown of 48 inches and span of 250 inches. Clearly the critical pressure is not governed exclusively by the radius of curvature at the crown.

5) Without exception, buckling strength increases with the relative density of the backfill. This fact is clearly borne out by all the results discussed herein. Also, for a given conduit, the prebuckling deflections and the relative deflections during buckling decrease with increasing relative density.

CONCLUSIONS

The present study has been conducted in the following manner:

- a) Examine the parameters governing the coefficient of soil reaction, k_n , normal to the surface of the conduit wall as well as the coefficient, k_s , tangential to the wall surface, and develop simple formulas for their evaluation.
- b) Use these formulas in the study of both the pre-buckling and buckling behavior of the conduits.

75

On the basis of the study reported herein, the following concluding remarks may be made:

- 1) The coefficient of soil reaction is sensitive to the relative density of the soil, the depth of fill, and the direction of action.
- 2) Regarding pre-buckling and buckling analyses, the theories of variational calculus provide a useful alternative where solutions based on governing differential equations present difficulties. In particular, for the special case of uniform boundary pressures and coefficient of soil reaction, variational calculus yields identical solution to the classical approach.
- 3) The buckling pressure of a buried conduit increases with the flexural rigidity of the conduit wall. However, in the practical range, the buckling pressure does not increase in the same order of magnitude as an increase in the flexural rigidity.
- 4) A good portion of the strength of buried conduits is derived from its interaction with the surrounding fill. To this end, the quality and state of compaction of the fill are critical. Without exception, the critical pressure increases with the relative density of the fill.
- 5) For small values of the coefficient of soil reaction and the flexural rigidity of the conduit wall, a moderately sized conduit will fail by buckling. For large values of these quantities the conduit will fail by yielding of the section.
- 6) The critical pressure is more sensitive to the depth of filling when the depth to the crown is at most one-half the span of the conduit.
- 7) The shape of the conduit has an influence on its stability.

 In particular, conduits of elliptical cross-section have twice as much tendency to buckle as circular conduits.



REFERENCES

- 1. Sze'chy, K. "The art of tunnelling," Akade'miai Kiado, Budapest, Hungary, 1967.
- 2. National Cooperative Highway Research Program, Report No. 116: Structural Analysis and Design of Pipe Culverts, by R. J. Krizek et al. Washington D.C., 1971.
- 3. Corrugated Steel Pipe Institute, Ontario, Canada, Case History Bulletin No. 241.
- 4. Fitzhardinge, C. "Economical Highway Bridge Designs Using Earth and Steel," Paper presented at International Road Federation, Australian Road Conference, Melbourne, April 1978.
- 5. White, H. A., and Layer, J. P. "The corrugate metal conduit as a compression ring," Highway Research Board, Proceedings of the Annual Meeting, 39, 1960, pp. 389-397.
- 6. Spangler, M. G. "The structural design of flexible pipe culverts," Bulletin No. 153, Engineering Experiment Station, Iowa State College, 1941.
- 7. Watkins, R. K. "Failure conditions of flexible culverts embedded in soil," Proceedings of the Highway Research Board, Vol. 39, 1960, pp. 361-371.
- 8. Watkins, R. K. "Structural design of buried circular conduits," Highway Research Record, No. 185, 1967, pp. 36-50.
- 9. Duncan, J. M. "Behavior and Design of Long-Span Metal Culvert Structures," paper presented at the Technical Session on Soil-Structure Interaction for Shallow Foundations and Buried Structures, A.S.C.E., October 1977, San Francisco.
- 10. Leonards, G. A., and Stetkar, R. E. Performance of flexible conduits. Interim report, Federal Highway Administration, Purdue University, IN, 1978.
- 11. Kloeppel, K., and Glock, D. "Theoretische und experimentelle untersuchungen zu den traglastprobl emen biegeweicher," in die Evde eigenbetten Rohre. Publ. no. 10, Institut fuer Statik aund Stahhbau, T. H. Darmstadt, Germany. (Translated from the original German by Dr. G. A. Sayed.)

- 12. Hafez, H. "Stability of flexible conduits under shallow cover," a Dissertation Submitted to the Faculty of Graduate Studies through the Dept. of CE in Partial Fulfillment of the Requirements for the Degree of Doctor of Philosophy at The University of Windsor, 1982.
- 13. Desai, C. S., and Christian, J. T. "Numerical methods in geotechnical engineering," McGraw-Hill Book Company, 1977.
- 14. Hardin, B. O. "Constitutive relations for air field subgrade and base course materials," Technical Report UKY 32-71-CE5, University of Kentucky, College of Engineering, Soil Mechanics Series No. 4, Lexington, KY, 1970.
- 15. Duncan, J. H., and Chang, C. Y. "Nonlinear analysis of stress and strain in soils," Journal of the Soil Mechanics and Foundations Division, ASCE, vol. 96, no. SM5, Proc. Paper 7513, Sep. 1970, pp. 1629-1653.
- 16. Janbu, N. "Soil compressibility as determined by Dedometer and triaxial tests," Proc. Env. Conf. Soil Mech. Found. Engr., Wiesbaden, 1963, Vol. 1, pp. 19-25.
- 17. Marston, A. "The theory of loads on closed conduits in the light of the latest experiments," Proc. HRB, Vol. 9, 1930, pp. 138-170.
- 18. Spangler, M. G. "Unverground conduits -- an appraisal of modern research," Trans. ASCE, Vol. 113, 1948, pp. 316-343.
- 19. Watkins, R. K., "Structural Design of Buried Circular Conduits," Highway Research Record, No. 145, 1966, pp. 1-6.
- 20. Bakht, B. "Live load testing of soil-steel structures," Structural Research Report 80-SRR-4, Ministry of Transportation and Communications, Downsview, Ont., 1980.
- 21. Duncan, J. M. "Finite element analysis of buried flexible metal culverts," Norwegian Geotechnical Institute, OSL., Norway, 1976.
- 22. Burns, J. Q. "An analysis of circular cylindrical shells embedded in elastic media," Ph.D. thesis, University of Arizona, Tucson, Arizona.
- 23. Terzaghi, K. "Evaluation of coefficient of subgrade reaction," Geotechnique, Vol. 5, 1955, pp. 297-326.
- 24. Meyerhof, G. G., and Baike, L. D. "Strength of steel culvert sheets bearing against compacted sand backfill," HRB, Proc. of the 42nd Annual Meeting, 1963.
- 25. Luscher, U. "Buckling of soil-surrounded tubes," ASCE, Journal of Soil Mechanics and Foundations Division, 1966, pp. 211-228.
- 26. Kloeppel, K., and Glock, D. (see reference 11).

- 27. Sze'chy, K. "The art of tunnelling," Akade'miai Kiado, Budapest, Hungary, 1967.
- 28. Murphy, G. "Similitude in engineering," The Ronald Press Company, 1950.
- 29. Watkins, R. K., and Spangler, M. G. "Some Characteristics of the modulus of passive resistance of soil: a study in similtude," Proc. HRB, Vol. 37, 1958, pp. 576-583.
- 30. Bowles, J. E. "Analytical and computer methods in foundation engineering," McGraw-Hill Book Company, 1974.
- 31. Vesic, A. S. "Beams on elastic subgrade, and the Winkler hypothesis," 5th Intl. Conf. of Soil Mechanics and Fdn. Engr., Vol. 1, pp. 845-850, 1966.
- 32. Abdel-Sayed, G. "Stability of flexible conduits embedded in soil," Canadian Journal of Civil Engineering, 5, 1978, pp. 324-334.
- 33. Brush, D. O., and Almroth, B. O. "Buckling of bars, plates and shells," McGraw-Hill Book Company, 1975.
- 34. Langhaar, H. L. "Energy methods in applied mechanics," John Wiley and Sons, Inc., 1962.
- 35. Ghobrial, M. M. "Analysis and stability of othotropic cylindrical cantilever shells," Ph.D. Thesis, University of Windsor, 1977.
- 36. Timoshenko, S., and Gere, J. M. "Theory of elastic stability," McGraw-Hill Book Company, New York, 1961.
- 37. Almroth, B. O. "Buckling of a cylindrical shell subjected to non-uniform external pressure," Journal of Engr. Mechanics Division, ASCE, Vol. 29, Dec. 1962.
- 38. Hornbeck. R. W. "Numerical methods," Quantum Publishers, Inc., New York, 1975.
- 39. Yao, J. C., and Jenkins, W. C. "Buckling of elliptical cylinders under normal pressure," AIAA Journal, Vol. 8, No. 1, Jan. 1970, pp. 22-27.
- 40. Watkins, R. K., and Muser, A. P. "The structural performance of buried corrugated steel pipes," Research Report, Engr. Expt. Station, Utah. State University, Logan, Utah, 1965.
- 41. Cheney, J. A. "Buckling and soil-surrounded tubes," Journal of Engr. Mech. Division, ASCE, Vol. 97, EM4, 1963, pp. 333-343.
- 42. Chelapati, C. V., and Allgood, J. R. "Buckling of cylinders in a confining medium," Highway Research Record, No. 413, 1964, pp. 77-88.

- 43. Donnellan, B. A. "The response of buried cylinders to quasistatic overpressures," Proc. of the Symposium of Soil-Structure Interaction, University of Arizona, Tucson, 1964.
- 44. Allgood, J. R. "The behavior of shallow buried cylinders," Proc. of the Symposium on Soil-Structure Interaction, University of Arizona, Tucson, 1964.
- 45. Marlowe, M. B., and Brogan, F. A. "Collapse of elliptical cylinders under uniform external pressure," AIAA. Journal, Vol. 9, pp. 2264-2266, 1971.
- 46. Norris, C. H., Wilbur, J. B., and Utku, S. "Elementary Structural Analysis," McGraw-Hill Book Company, New York, 1960, pp. 547-555.
- 47. Bathe, K. J., and Wilson, E. L. "Numerical methods in finite element analysis," Prentice-Hall, 1976.

TABLE 3-1: HYPERBOLIC PARAMETERS USED

Parameter	Symbol	Dense	Medium
Angle of Internal Friction	ф	45 ⁰	45 ⁰
Friction Angle	Δ	23 ⁰	23 ⁰
Failure Ratio	$\mathtt{R}_{\mathbf{f}}$	0.92	0.85
Failure Ratio	R _{fs}	0.834	0.834
Modulus Parameter	K	3100	1200
Modulus Parameter	ĸ	43070	43070
Modulus Number	n	0.52	0.48
Modulus Number	n s	0.60	0.60
Poisson's Number	G	0.34	0.34
Poisson's Ratio Number	đ	75.9	11.7
Poisson's Ratio Number	F	0.12	0.23

TABLE 3-2: RESULTS FOR P = 33.3 #, H_C = 4 AND DIAMETER=100 INCHES

Interface Element	Soil Node	Δx (inch)	ΔY (inch)	AN (inch)	o (psi)	k _n (#/in ³)
1	59		00026	.00026	.247	950.0
2	58	00016818	00025043	.0002901	.247	851.4
3	60	.00016492	00025064	.0002893	.247	854.0
4	77	00031227	00019012	.0003373	.249	738.3
5	78	.00030938	00019079	.0003361	.252	750.0
6	80	00042372	000068541	.000383	.235	613.5
7	82	.00042633	000064530	.0003828	.240	627.0
8	84	00049414	.00011161	.0004354	.217	498.4
9	86	.00049972	.00012581	.0004364	.214	490.4
10	110	00052079	.00033654	.00052079	.198	380.3
11	114	.00051877	.00033176	.00051877	.182	351.0
14	148	00050685	.00058760	.0006636	.160	241.1
15	153	.00050623	.00058379	.0006618	.161	243.3
18	186	00045735	.00082611	.0008555	.170	198.7
19	196	.00045952	.00082343	.0008557	.171	199.8
22	233	00035016	.0010899	.0010875	.157	144.4
23	234	.00035012	.0010894	.0010872	.156	143.5
26	237	00019972	.0012751	.0012744	.152	119.3
27	238	.0001976	.0012747	.0012733	.153	120.2
30	241	0000013188	.00013416	.0013416	.100	74.5

TABLE 3-3: RESULTS FOR P = 33.3 $^{\#}$, H_C = 6.4 $^{\prime}$ AND DIAMETER=100 INCHES

Interface Element	Soil Node	ΔX (inch)	ΔY (inch)	AN (inch)		k _n (#/in ²)
1	59		0003216	.0003216	.320	995
2	58	00017306	00027905	.0003188	.285	894
3	60	.00017284	00027924	.0003191	.285	893
4	77	0003271	00021404	.0003654	.287	785.4
5	78	.00032634	00021465	.0003654	.288	788.3
6	80	0004434	00008808	.0004104	.269	655.5
7	82	.00044529	000086	.0004107	.269	655
8	84	00051287	.000090983	.0004596	.246	535.2
9	86	.00051367	.000092635	.0004599	.244	530.6
10	110	00053657	.00029474	.00053657	.228	425
11	114	.00053719	.00029502	.00053719	.213	396.6
14	148	00052955	.00053449	.0006687	.189	282.7
15	153	.00053232	.00053607	.0006719	.189	281.3
18	186	00047981	.00075969	.0008346	.201	240.8
19	196	.00048761	.00076159	.000842	.200	237.5
22	233	00036693	.001003	.001025	.181	176.6
23	234	.00037252	.0010058	.0010327	.181	175.3
26	237	00020617	.0011529	.0011602	.179	154.3
27	238	.00020833	.0011563	.0011641	.179	154
30	241		.0012062	.0012062	.116	96.2

TABLE 3-4: RESULTS FOR P=300#, H_C=6.4 AND DIAMETER=200 INCHES

Interface Element	Soil Node	Δx (inch)	ΔY (inch)	\Delta N (inch)	o N (psi)	k _n (#/in ³)
1	59	.000050102	0039209	.0039209	2.55	650.36
2	58	0027646	0040328	.0046846	2.43	518.72
3	60	.0028501	0040290	.0047098	2.42	513.82
4	77	0052202	0028986	.0054312	2.34	430.85
5	78	.0052075	0029261	.0054257	2.31	425.73
6	80	0071361	00066596	.0061539	2.18	354.25
7	82	.0071212	00072177	.0061807	2.16	349.48
8	84	0080793	.0023202	.006952	1.93	277.09
9	86	.0079864	.0020641	.0069564	1.92	276.01
10	110	0082896	.0058275	.0082896	1.69	203.87
11	114	.0082773	.0057982	.0082773	1.58	190.88
14	148	0077296	.0096365	.0115511	1.45	125.53
15	153	.0077142	.0097402	.0116468	1.47	126.21
18	186	0071128	.013418	.0136414	1.41	103.36
19	196	.0070769	.013460	.0136375	1.42	104.13
22	233	0058268	.017595	.0176607	1.34	75.87
23	234	56883	.017614	.0175945	1.32	75.02
26	237	0035325	.021208	.0212621	1.26	59.26
27	238	.00334468	.021112	.0211125	1.27	60.15
30	241	000093378	.022550	.02255	1.18	52.33

TABLE 3-5: RESULTS FOR P=300[#], H_C=8⁻, AND DIAMETER=200 INCHES

1 59 .000033532 0040 2 58 0027698 0041 3 60 .0028226 0041 4 77 0052264 .0030 5 78 .0051903 003 6 80 0071199 00083 7 82 .0070996 00086 8 84 0080635 .0021 9 86 .0079921 .0019		651.78
3 60 .00282260041 4 770052264 .0030 5 78 .0051903003 6 80007119900083 7 82 .007099600088 8 840080635 .0021 9 86 .0079921 .0019	1634 0048188 2 54 5	
4 770052264 .0030 5 78 .0051903003 6 80007119900083 7 82 .007099600088 8 840080635 .0021 9 86 .0079921 .0019	1034 .0040100 2.34 3	527.105
5 78 .0051903003 6 80007119900083 7 82 .007099600088 8 840080635 .0021 9 86 .0079921 .0019	1683 .0048402 2.53	522.7 0
6 80007119900083 7 82 .007099600088 8 840080635 .0021 9 86 .0079921 .0019	0372 .0055272 2.46	445.08
7 82 .007099600088 8 840080635 .0021 9 86 .0079921 .0019	3069 .0055285 2.43	439.54
8 840080635 .0021 9 86 .0079921 .0019	3707 .0062545 2.30	367.73
9 86 .0079921 .0019	3093 .00626 2.27	362.62
	1158 .0070165 2.04	290.74
10 110	9241 .0070043 2.02	288.39
10 1100082943 .0055	5483 .0082943 1.80	217.02
11 114 .008264 .0055	5223 .008264 1.67	202.08
14 1480078180 .0092	2910 .0103061 1.56	151.37
15 153 .0077744 .0093	3617 .0102861 1.57	152.63
18 1860071755 .012	2966 .0134266 1.52	113.21
19 196 .0071248 .012	2989 .0133997 1.52	113.44
22 2330059106 .017	7056 .0172719 1.45	83.95
23 234 .0057976 .017	7079 .0172247 1.43	83.02
26 2370035282 .020	0384 .0204755 1.37	66.91
27 238 .0033798 .020		67.154
30 241000086828 .021	0353 .0204008 1.37	

TABLE 3-6: RESULTS FOR P=300[#], H_C=11.73⁻, AND DIAMETER=200 INCHES

Interface Element	Soil Node	Δx (inch)	ΔY (inch)	\DN	σ ·	k _n
1	59	.000047599	0043184	.0043184	2.86	662.28
2	58	0027249	0044086	.0050321	2.75	546.49
3	60	.0028077	0044055	.0050593	2.74	541.58
4	77	0051652	0033284	.0057313	2.66	464.12
5	78	.0052011	0033399	.0057651	2.65	459.61
6	80	0070506	0012136	.0064147	2.52	392.85
7	82	.0070999	0012209	.0064595	2.51	388.58
8	84	008034	.0016336	.0071402	2.27	317.92
9	86	.0080629	.0015495	.0068433	2.24	327.33
10	110	0082767	.0049080	.0082767	2.55	308.09
11	114	.0083615	.0049140	.0083615	2.55	304.97
14	148	0079099	.0085114	.0101535	1.75	172.35
15	153	.0080362	.0085804	.0102947	1.75	169.99
18	186	0072285	.012028	.0129191	1.78	137.781
19	196	.0073878	.012080	.0130778	1.77	135.344
22	233	0059498	.015889	.0163516	1.66	101.52
23	234	.0060773	.015957	.0164808	1.64	99.51
26	237	0033962	.018591	.0187297	1.60	85.43
27	238	.0034842	.018646	.0188091	1.58	84.00
30	241	.000023878	.019409	.019409	1.50	77.28

TABLE 3-7: RESULTS FOR P=300[#], H_C=4⁻, AND DIAMETER=300 INCHES

Interface Element	Soil Node	Δx (inch)	ΔΥ (inch)	\Delta N (inch)	
1	59	.00017183	-10045713	0.0045713	2.19 479.10
2	58	0035477	0047731	.005636	2.13 377.94
3	60	.0037625	0047416	.005672	2.09 368.46
4	77	0069716	0031147	.0066176	2.01 303.73
5	78	.0068574	0032158	.0066323	1.94 292.51
6	80	0090851	00026326	.0075047	1.85 246.51
7	82	.0087169	00060459	.0074075	1.86 251.10
8	84	010251	.0039504	.0074309	1.75 235.5
9	86	.010296	.0041711	.007358	1.74 234.0
10	110	010311	.0090090	.0085285	1.62 189.95
11	114	.010116	.0082438	.0085032	1.61 189.34
14	148	0087211	.014442	.012757	1.07 83.87
15	153	.0085260	.014538	.0126012	1.18 93.64
18	186	0078839	.019924	.0180892	0.923 51.02
19	196	.0074904	.020259	.017968	0.973 54.15
22	233	0062997	.026951	.0255067	0.831 32.58
23	234	.0059800	0.027372	.025659	0.844 32.89
26	237	0050464	.036875	.0366296	0.740 20.20
27	238	.0045887	.03694	.03655	0.757 20.71
30	241	0002251	.042842	0.042842	0.603 14.07

TABLE 3-8: RESULTS FOR P=100[#], H_C=6.39⁻, AND DIAMETER=300 INCHES

Interface Element	Soil Node	ΔX (inch)	ΔY (inch)	ΔN (inch)	o N (psi)	k _n (lb/in ³)
1	59	.0000309	001634	.001634	0.766	468.79
2	58	0012128	0016917	.00198368	0.755	380.61
3	60	.0012511	0016902	.0019940869	0.744	373.103
4	77	0023234	0011561	.002300965	0.724	314.651
5	78	.0022441	0011992	.02289222	0.717	313.207
6	80	0031401	00013816	.0026216027	0.675	257.47 6
7	82	.0031361	00013995	.0026194187	0.680	259.60
8	84	0035277	.0012691	.0027530	0.621	225.57
9	86	.0035245	.0012464	.0026817	0.625	233.06
10	110	00296287	.0012691	0.00296287	0.591	199.47
11	114	.00296684	.0012464	0.00296684	0.574	193.47
14	148	0032068	.0046003	.00447142	0.381	85.21
15	153	.0032035	.0045885	.00446463	0.390	87.35
18	186	0028777	.0064217	.0061026888	0.402	65.87
19	196	.0027696	.0064494	.0060315157	0.442	73.282
22	233	0023757	.0085633	.0082912195	0.401	48.364
23	234	.0022859	.0085656	.0082733343	0.407	49.194
26	237	0016466	.011007	.0109771065	0.384	34.982
27	238	.0015125	.010928	.0108605339	0.399	36.739
30	241	000065664	.012077	.012077	0.324	26.828

TABLE 3-9: RESULTS FOR P=300[#], H_C=6.39' AND DIAMETER=300 INCHES

Interface	Soil	$\Delta \mathbf{x}$	ΔΥ	$ \Delta \mathbf{n} $	$ \sigma_N $	k _n
Element	Node	(inch)	(inch)	(inch)	(psi)	(#/in ³)
1	59	.00005462	0048582	.0048582	2.306	474.66
2	58	003704	0050239	.0050751838	2.235	440.38
3	60	.0037608	0050446	.0051356005	2.204	429.161
4	77	0070803	0033983	.0069109784	2.114	305.89
5	78	.0068201	0035655	.0068932962	2.107	305.66
6	80	0095874	00033132	.007951114	1.965	247.135
7	82	.0095557	00035528	.007939552	1.99	250.644
8	84	0107767	.0039203	.007465	1.701	225.4
9	86	.010775	.0038635	.0074618	1.664	223.0
10	110	0107767	.0087567	.0107767	1.701	188.21
11	114	.0107751	.0081836	.0107751	1.664	183.79
14	148	0098827	.0140118	.0137288906	1.152	83.91
15	153	.009884	.0138563	.0136820748	1.183	86.463
18	186	0088131	.0194707	.018574538	1.147	61.751
19	196	.0084133	.0193734	.0181939016	1.219	67.00
22	233	0071488	.0257293	.0250174002	1.113	44.489
23	234	.0068133	0.255476	.0246731998	1.136	46.042
26	237	0050035	.033097	.0329393195	1.075	32.636
27	238	.0045219	.032668	.0324664502	1.106	34.066
30	241	000226644	.036314	.036314	0.950	26.16

TABLE 3-10: RESULTS FOR P=500[#], H_C=6.39⁻, AND DIAMETER=300 INCHES

Interface Element		Δx (inch)	ΔY (inch)	AN (inch)	o	k _n (#/in³)
					(20-7	
1	59	.0000435	0080794	.0080794	3.906	483.45
2	58	0062038	0049478	.0098632098	3.765	381.72
3	60	.0062192	0083615	.0098740976	3.724	377.148
4	77	0117905	0056169	.0114744496	3.55	309.383
5	78	.011356	0058769	.0114294013	3.557	311.215
6	80	0158648	00056265	.0131607375	3.295	250.37
7	82	.0158311	00055436	.0131334736	3.340	254.312
8	84	0178266	.0064599	.0149537753	2.851	225.4
9	86	.0178151	.0064732	.014942838	2.804	227.0
10	110	0181039	.0144563	.0181039	3.452	190.65
11	114	.0180509	.0137286	.0180599	3.387	187.65
14	148	016414	.0232855	.0228062569	1.942	85.152
15	153	.0163736	.0229394	.0226608833	1.971	86.978
18	186	0145946	.0323827	.0308413529	1.905	61.768
19	196	.01395948	.0321004	.0301615983	1.985	65.812
22	233	011807	.0426376	.0414345235	1.821	43.949
23	234	.0111635	.0423886	.0408863264	1.852	45.296
26	237	0083913	.055433	.0553129701	1.752	31.674
27	238	.007515	.054586	.0542375847	1.779	32.80
30	241	000403744	.061116	.061116	1.550	25.36

TABLE 3-11: RESULTS FOR P=100[#], H_C=8', AND DIAMETER=300 INCHES

		· · · · · · · · · · · · · · · · · · ·				
Interface	Soil	$\Delta \mathbf{x}$	ΔΥ	DN	$ \sigma_{N} $	k_n
Element	Node	(inch)	(inch)	(inch)	(psi)	(#/in ³)
1	59	.000028014	0016759	.0016759	.782	466.61
2	58	0011882	0017386	.0020206	.774	383.05
3	60	.0012209	0017410	.002033	.767	377.27
4	77	002302	0012144	.0023354	.742	317.72
5	78	.0022683	0012572	.0023501	.729	310.19
6	80	0030369	00028237	.0026228	.713	271.84
7	82	.0029669	0037272	.0026192	.721	275.29
8	84	0034626	.0010872	.0026589	.634	238.44
9	86	.0034853	.0011289	.0026835	.636	237
10	110	0026689	.0026790	.0026689	.59 5	223.0
11	114	.0022137	.0025606	.0022137	.493	222.9
14	148	0031627	.0043421	.0043458	.435	100.10
15	153	.0031299	.0043814	.0043306	.450	103.91
18	186	0028802	.006077	.0059026	.447	75.73
19	196	.0028551	.0061103	.0059013	.471	79.81
22	233	0023384	.0081602	.0079761	.434	54.41
23	234	.002363	.0082352	.0080513	.445	55.27
26	237	0016453	.010541	.0105334	.404	38.35
27	238	.0015679	.010391	.0104413	.421	40.31
30	241	000030801	.011796	.011796	.328	27.81

TABLE 3-12: RESULTS FOR P=300[#], H_C=8⁻, AND DIAMETER=300 INCHES

Interface Element	Soil Node	Δx (inch)	ΔY (inch)	\Delta N (inch)	o (psi)	k n (#/in ³)
1	59	.000084073	0050273	.0050273	2.37	471.43
2	58	0035645	0052154	.0060613	2.32	382.75
3	60	.0036625	0052224	.0060984	2.29	375.5
4	77	0069058	0036425	.0070059	2.23	318.3
5	78	.0068049	0037708	.0070505	2.18	309.2
6	80	0091104	00084629	.007838	2.08	265.37
7	82	.0089003	0011174	.0078572	2.09	266.00
8	84	010387	.0032627	.0078481	1.86	236.68
9	86	.010455	.0033876	.008137	1.87	233.35
10	110	0076783	.0080383	.0076783	1.61	209.68
11	114	.0072312	.0076828	.0072312	1.52	210.20
14	148	0094873	.013028	.0130487	1.35	103.46
15	153	.0093885	.013146	.0129915	1.42	109.10
18	186	0086398	.018235	.0177079	1.26	71.15
19	196	.0085646	.018332	.0177041	1.30	73.43
22	233	0070148	.024482	.0239295	1.17	48.89
23	234	.0070887	.024707	.024155	1.18	48.85
26	237	0049359	.031624	.0316014	1.10	34.81
27	238	.0047038	.031175	.0311026	1.11	35.69
30	241	000092391	.03539	.035390	.995	28.12

TABLE 3-13: RESULTS FOR P=500[#], H_C=8⁻, AND DIAMETER=300 INCHES

Interface	Soil Node	Δx (inch)	ΔY (inch)	AN (inch)	o N (psi)	k _n (#/in ³)
			· · · · · · · · · · · · · · · · · · ·		(PSI)	\#/ ±11 /
1	59	.00013998	0083794	.008794	3.93	469
2	58	0059410	008693	.0101037	3.86	382.04
3	60	.0061041	0087048	.0101672	3.82	375.72
4	77	011510	0060718	.0116789	3.70	316.81
5	78	.011342	0062855	.0117491	3.64	309.81
6	80	015185	0014115	.0131179	3.42	260.71
7	82	.014834	0018633	.0130887	3.46	264.35
8	84	017313	.0054365	.014219	3.35	235.6
9	86	.017426	.0056447	.0141525	3.34	236.0
10	110	0147868	.013396	.0147868	3.09	208.97
11	114	.0147868	.012803	.0148279	3.10	209.07
14	148	015814	.021711	.021749	2.25	103.45
15	153	.015649	.021908	.021653	2.35	108.53
18	186	.014401	.030389	.029513	2.07	70.14
19	196	.014275	.030553	.029507	2.13	72.19
22	233	011692	.04080	.03988	1.90	47.64
23	234	.0011815	.041177	.0402576	1.92	47.69
26	237	-,0082268	.052705	.052603	2.74	52.08
27	238	.0078396	.051956	.051834	2.96	57.10
30	241	00015426	.058976	.058976	1.61	27.3

TABLE 3-14: RESULTS FOR P=300[#], H_c=11.73⁻, AND DIAMETER=300 INCHES

Interface Element	Soil Node	Δx (inch)	Δy (inch)	AN (inch)	o (psi)	k _n (#/in³)
1	59	.000042057	0053059	0053059	2.5	471.17
2	58	0035472	0054881	.0063171	2.45	387.83
3	60	.0035794	0055009	.0063367	2.43	383.48
4	77	0068180	0039850	.0073091	2.38	325.62
5	78	.0067174	0041046	.0072668	2.35	323.39
6	80	0090511	0012555	.0080552	2.23	276.84
7	82	.0088860	0014689	.0080601	2.26	280.39
8	84	010345	.0027247	.0089978	2.03	225.61
9	86	.010372	.0027988	.008998	2.03	225.60
10	110	0090825	.0072660	.0090825	1.98	218.5
11	114	.0091030	.007048	.0091030	1.97	216.41
14	148	0097181	.012024	.0129576	1.55	119.62
15	153	.0096215	.012111	.0128935	1.59	123.32
18	186	0088170	.016958	.0171	1.46	85.38
19	196	.0087444	.016963	.0170456	1.49	87.41
22	233	0073139	.022869	.022797	1.36	59.66
23	234	.0073027	.022891	.0228111	1.35	59.18
26	237	0048773	.029165	.0292449	1.28	43.77
27	238	.0047265	.028960	.0290025	1.29	44.48
30	241	.000076984	.031616	.031616	1.19	37.64

TABLE 3-15: RESULTS FOR P=500[#], H_c=11.73⁻, AND DIAMETER=300 INCHES

						· · · · · · · · · · · · · · · · · · ·
Interface	Soil	Δχ	ΔΥ .	$ \Delta n $	σ _N	k _n
Element	Node	(inch)	(inch)	(inch)	(psi)	(#/in ³)
1	59	.000069958	0088437	.0088437	4.51	509.97
2	58	005912	0091473	.0105289	4.09	388.45
3	60	.0059657	0091687	.010564	4.05	383.38
4	77	011364	0066422	.0109489	3.95	360.77
5	78	.011196	0068416	.0110603	3.92	354.42
6	80	015086	0020931	.013309	3.69	277.26
7	82	.014810	0024489	.0134166	3.73	278.01
8	84	017243	.0045403	.0149968	3.36	224.05
9	86	.017287	.0046636	.015	3.37	224.65
10	110	0146103	.013371	.0146103	3.15	215.6
11	114	.0146906	.011746	.0146906	3.13	213.06
14	148	016198	.020039	.0208844	2.57	123.06
15	153	.016037	.020184	.0214894	2.63	122.39
18	186	014696	.028263	.0285022	2.40	84.2
19	196	.014574	.028271	.0284078	2.44	85.89
22	233	012190	.038114	.0380001	2.23	58.68
23	234	.012171	.038151	.0386184	2.20	57.87
26	237	0081290	.048607	.0487402	3.11	63.81
27	238	.0078773	.048265	.0483374	3.09	63.93
30	241	00012855	.052691	.052691	1.93	36.63

TABLE 3-16: RESULTS FOR P=100[#], H_c=12.64', AND DIAMETER=300 INCHES

Interface Element	Soil Node		ΔY (inch)	AN (inch)	o (psi)	k _n (#/in³)
1	59	.000022804	0017898	.0017898	.845	472.12
2	58	0011797	0018350	.002109736	.833	394.836
3	60	.0012097	0018382	.00212205	.825	388.775
4	77	002250	0013442	.0024099975	.806	334.44
5	78	.0022055	0013855	.0024172534	.803	332.20
6	80	0030602	00039592	.0027084697	.769	283.92
7	82	.0030718	00039702	.0027185009	.781	287.29
8	84	0034731	.000391435	.0030205647	.692	229.096
9	86	.0034867	.00090934	.0030350473	.627	223.061
10	110	0035311	.0023952	.0035311	0.783	221.87
11	114	.0035638	.0023441	.0035638	.0784	220.00
14	148	0033129	.0040112	.0043902841	.490	111.61
15	153	.0033684	.0039849	.0044349406	.496	111.84
18	186	0029663	.0056637	.0057288264	.526	91.82
19	196	.0029666	.0056702	.0057328898	.540	94.193
22	233	0024646	.0075662	.0075698399	.508	67.108
23	234	.0024891	.0075599	.0075791439	.514	67.82
26	237	0015874	.0094846	.0095106993	.502	52.783
27	238	.0015859	.0094734	.0094998089	.485	51.05
30	241	000061849	.010179	.010179	.414	40.67

TABLE 3-17: RESULTS FOR P=300[#], H_C=12.64⁻, AND DIAMETER=300 INCHES

Interface	Soil	_ Δ x	ΔΥ	\DN	$ \sigma_{\mathbf{N}} $	k _n
Element	Node	(inch)	(inch)	(inch)	(psi)	(#/in ³)
1	59	.000053251	0053675	.0053675	2.515	468.56
2	58	0035984	0055206	.0063582	2.443	384.23
3	60	.0036624	0055303	.0063903	2.435	381.05
4	77	0068433	0040479	.0072941	2.346	321.63
5	78	.0067285	0041674	.0073291	2.343	319.68
6	80	009395	00119198	.0083096	2.219	267.04
7	82	.0094021	00117974	.0083	2.241	270.00
8	84	0106951	.00276945	.0083709	1.982	236.77
9	86	.0107088	.00278804	.0083479	1.957	234.43
10	110	0084878	.0072697	.0084878	1.866	219.843
11	114	.0083183	.0071629	.0083183	1.850	222.399
14	148	0104319	.0121985	.0136905	1.484	106.40
15	153	.010563	.0121212	.013792	1.483	107.53
18	186	0092295	.0171087	.0175217	1.536	87.83
19	196	.0091387	.0170832	.0174344	1.539	. 88.27
22	233	0075166	.0225502	.0226617	1.463	64.56
23	234	.0075973	.0226119	.0227587	1.477	64.90
26	237	0047871	.0280616	.0281672	1.426	50.63
27	238	.0047553	.0279904	.0280822	1.415	50.39
30	241	000085927	.029827	.029827	1.241	41.61

TABLE 3-18: RESULTS FOR P=500[#], H_C=12.64', AND DIAMETER=300 INCHES

Interface Element	Soil Node	Δx (inch)	ΔΥ (inch)	ΔN (inch)	o (psi)	k _n (#/in ³)
1	59	.000066903	0089462	.0089462	4.235	473.39
2	58	0060072	0091764	.0105843	4.103	387.65
3	60	.00608	009196	.0106265	4.095	385.36
4	77	0114235	0067075	.0121413	3.926	323.36
5	78	.0112138	0069029	.0121941	3.933	322.53
6	80	0155825	00197999	.0137681	3.719	270.12
7	82	.0156176	00194048	.013774	3.751	272.32
8	84	0177317	.00458435	.0154477	3.312	214.4
9	86	.0177871	.00462614	.0154864	3.277	211.61
10	110	0141202	.0120369	.0181934	2.901	205.45
11	114	.0125235	.0119156	.0184068	2.59	206.81
14	148	0173477	.0202857	.0227669	2.504	109.98
15	153	.0176041	.0201032	.0229547	2.493	108.61
18	186	0152567	.0284197	.029048	2.546	87.65
19	196	.0152182	.0283352	.0289669	2.549	88.00
22	233	0124199	.0374982	.0376343	2.427	64.49
23	234	.0125928	.0374689	.0377151	2.444	64.80
26	237	0079349	.0468046	.0469662	2.336	49.74
27	238	.0079419	.0466114	.0467845	2.324	49.67
30	241	000071623	.049955	.049955	2.053	41.097

TABLE 3-19: RESULTS FOR P=100[#], H_C=20.36', AND DIAMETER=300 INCHES

Interface Element	Soil Node	Δx (inch)	ΔY (inch)	AN (inch)		k _n (1/in ³)
1	59	.000018863	0018853	.0018853	.914	484.8
2	58	0011380	0019258	.0021830108	.904	414.11
3	60	.001164	0019226	.002188197	.896	409.47
4	77	0021735	001472	.0024684243	.880	356.503
5	78	.0021481	0014966	.0024733963	.878	354.98
6	80	0029563	00058928	.002738067	.851	310.803
7	82	.0029716	00057688	.0027431564	.859	313.143
8	84	0033793	.00062751	.003019994	.776	256.954
9	86	.0033962	.00064060	.0030320219	.766	252.637
10	110	0034615	.0020021	.0034615	.709	245.82
11	114	.0035135	.0020015	.0035135	.604	241.908
14	148	0033386	.0035291	.0042657557	.584	136.90
15	153	.0033989	.0035288	.0043230051	.578	133.703
18	186	0030254	.0050853	.0054366643	.635	116.80
19	196	.0030565	.0051098	.0054619244	.624	114.245
22	233	0025392	.0068367	.0070235108	.602	85.172
23	234	.0025933	.0068732	.0070848391	.615	86.81
26	237	0015169	.0082832	.0083465392	.576	69.011
27	238	.0015604	.0083363	.0084104825	.586	69.68
30	241 -	000011195	.0086433	.0086433	.503	58.195

TABLE 3-20: RESULTS FOR P=300[#], H_C=20.36⁻, AND DIAMETER=300 INCHES

Interface	Soil	Δχ	ΔΥ	An	o	k _n
Element	Node	(inch)	(inch)	(inch)	(psi)	(#/in ³)
1	59	.0000380246	0056853	.0056853	2.704	475.61
2	58	0034771	0058279	.006618	2.634	398.00
3	60	.0035591	005821	.0066387	2.616	394.06
4	77	0066767	0044763	.0075478	2.55	337.85
5	78	.0066063	0045427	.0075543	2.538	335.97
6	80	0091339	00181318	.0084506	2.441	288.85
7	82	.009175	00175938	.0084601	2.459	290.66
. 8	84	0104978	.00188551	.0094017	2.236	237.83
9	86	.0105467	.0019496	.0094306	2.196	232.86
10	110	0108156	.0060866	.0108156	1.999	230.82
11	114	.01098	.006118	.01098	1.794	229.39
14	148	0105507	.0107586	.0133587	1.714	128.31
15	153	.0107536	.0107803	.013558	1.698	125.24
18	186	0093311	.0153283	.0165593	1.825	110.20
19	196	.0094449	.0154218	.0167057	1.794	107.39
22	233	0075791	.0202447	.0208323	1.752	84.1
23	234	.0077786	.0203642	.021047	1.765	83.86
26	237	0044847	.0244542	.024643	1.686	68.42
27	238	.0046587	.0246173	.024852	1.696	68.24
30	241	.000056851	.0256633	.0256623	1.543	60.127

TABLE 3-21: RESULTS FOR P=500[#], H_C=20.36⁻, AND DIAMETER=300 INCHES

Interface	Soil	Δχ	ΔΥ	\DN	σ _N	k _n
Element	Node	(inch)	(inch)	(inch)	(psi)	$(\#/in^3)$
1	59	.0000626316	0095354	.0095354	4.524	474.443
2	58	0058178	0097463	.0110648	4.404	398.02
3	60	.0059355	0097344	.0110906	4.376	394.57
4	77	0111236	0074674	.0125776	4.25	337.9
5	78	.0110182	0075676	.0125986	4.248	337.18
6	80	0151772	00304058	.0140612	4.071	289.52
7	82	.0152539	00293418	.0140671	4.109	292.10
8	84	0174337	.00309491	.0156257	3.736	239.09
9	86	.0175218	.0032144	.0156715	3.676	234.57
10	110	0179928	.0100552	.0179928	3.329	226.00
11	114	.0182591	.0101146	.0182591	3.024	225.616
14	148	0175919	.0178588	.0222497	2.874	129.17
15	153	.0179251	.0178831	.0225739	2.848	126.16
18	186	0154891	.0254233	.0274743	3.025	110.103
19	196	.0156918	.0255618	.0277194	2.984	107.65
22	233	0125678	.0335787	.0345523	2.912	84.28
23	234	.0129131	.0337812	.0349191	2.915	83.48
26	237	0074576	.0406872	.0410016	2.806	68.44
27	238	.0077971	.0410613	.0414611	2.806	67.68
30	241	.000011403	.0427413	.0427413	2.563	59.97

TABLE 3-22: LOADING SCHEDULE

(1b) (ft) (1b) (ft) (100 4.0 4.0 100 6.4 6.4 200 8.0 300 8.0 5	
100 6.4 6.4 200 8.0 300 8.0 5	P H lb) (ft)
200 8.0 300 8.0 5	4.0
	6.4
	00 8.0
11.73 11.73	11.73
12.64 12.64	12.64
300 20.36 20.36	20.36

TABLE 3-23: RECOMMENDED VALUES OF K, AND n, (AFTER TERZAGHI 1955)

Relative Density	Loo	se	Medi	um	Dense	е
of Sand	K	n h	K	n h	K 1	ⁿ h
Dry or Moist Sand [Test Results)	20-60	7	60-300	21	300-1000	56
Proposed Values	40	7	130	21	500	56
Sumbmerged Sand	25	5	80	14	300	34

TABLE 3-24: RESULTS FOR $H_C = 4$, DIAMETER=200 INCHES, AND P=50 LBS

Inter- face	Soil	Δ x	ΔΥ	$ \Delta_{N} $	$ \sigma_{_{ m N}} $	k*
Element	Node	(inch)	(inch)	(inch)	psi	(#/in ³)
1	59	.000029927	.00050551	.00050551	.282	557.86
2	58	00045902	00062578	.00073691	.262	355.54
3	60	.00048482	00062470	.00074392	.251	337.41
4	77	00093804	00054158	.00098935	.247	249.66
5	78	.00089854	00054569	.00096939	.229	236.23
6	80	0013941	00024788	.0012734	.207	162.55
7	82	.0013119	00027817	.0012247	.210	171.5
8	84	0017267	.00029879	.0015499	.156	100.65
9	86	.0017063	.00030157	.0015333	.168	109.56
10	110	0017780	.0010639	.0017780	.105	• 59.6
11	114	.0017842	.0011183	.0017842	.108	60.5
14	148	0014884	.0017388	.0019521	.108	55.32
15	153	.0014778	.0018419	.0019746	.117	59.25
18	186	0013688	.0024113	.0025246	.103	40.8
19	196	.0013661	.0025072	.0025788	.109	42.3
22	233	0010664	.0030591	.0030878	.0998	32.32
23	234	.0010162	.0031465	.0031428	.102	32.45
26	237	00065706	.0036543	.0036783	.153	41.59
27	238	.00057482	.0036661	.0036642	.169	46.12
30	241	000042342	.0039512	.0039512	.0708	17.92

LEGEND: (Tables 3-24 to 3-35): $k \atop n$ refers to the dense soil and $k \atop n$ to the medium dense.

TABLE 3-25: RESULTS FOR H_c = 4; DIAMETER =200 INCHES AND P=100 LBS

Inter- face	Soil	Δχ	ΔΥ	$ \Delta_{\mathbf{N}} $	$ \sigma_{_{ m N}} $	k* n
Element	Node	(inch)	(inch)	(inch)	psi	(#/in ³)
1	59	.000059859	0010112	.0010112	.563	556.76
2	58	00091808	0012518	.0014741	.526	356.8
3	6 0	.00096968	0012496	.001488	.504	338.7
4	77	0018761	0010834	.0019791	. 493	249.1
5	78	.0017971	0010916	.0019393	.458	236.16
6	80	0027883	00049598	.0025472	.411	161.35
7	82	.0026238	00055659	.0024497	.417	170.22
8	84	0034534	.00059732	.0030999	.343	110.65
9	86	.0034126	.00060288	.0030593	.358	117.02
10	110	0035560	.0021275	.0035560	.283	79.5
11	114	.0035685	.0022364	.0035685	.285	79.9
14	148	0029769	.0034772	.0039056	.218	55.82
15	153	.0029558	.0036834	.0039493	.233	59.00
18	186	0027377	.0048222	.0050491	.202	40.01
19	196	.0027324	.0050140	.0051576	.287	55.64
22	233	0021330	.0061179	.0062031	.272	43.85
23	234	.0020324	.0062923	.0062851	.267	42.48
26	237	0013142	.0073080	.0073564	.235	31.94
27	238	.0011496	.0073318	.0073281	.251	34.25
30	241	.000084729	.0079019	.0079019	.153	19.4

TABLE 3-26: RESULTS FOR H_C = 6.4, DIAMETER=200 INCHES, AND P=100 LBS

Inter- face	Soil	$\Delta \mathbf{x}$	ΔΥ	ΔN	$ \sigma_{_{ m N}} $	k* n	$\frac{\frac{k^*}{n}}{k}$
Element	Node	(inch)	(inch)	(inch)	psi	(#/in ³)	n
1	59	.000029493	0011352	.0011352	0.61	537.35	0.826
2	58	00097073	0013599	.0015933	0.57	357.75	0.69
3	60	.00098489	0013619	.0015976	0.557	348.6	0.68
4	77	0019555	0011694	.0020954	0.533	254.4	0.590
5	78	.0018866	0011756	.0020599	0.512	248.5	0.584
6	80	0028679	00057812	.0026599	0.444	166.9	0.471
7	82	.0027369	00062167	.0025795	0.451	174.8	.500
8	84	0035132	.00049894	.0031870	0.386	121.12	0.43
9	86	.0034481	.00049948	.0031249	0.382	122.24	0.443
10	110	003617	.0019777	.003617	0.318	87.9	0.431
11	114	.0035867	.0020456	.0035867	0.312	86.9	0.456
14	148	0031524	.0033036	.0040189	0.231	57.5	0.458
15	153	.0030786	.0034255	.0039864	0.243	60.96	0.483
18	186	0028955	.0046136	.0050542	0.255	50.45	0.488
19	196	.0028393	.0047247	.0050741	0.260	51.44	0.494
22	233	0022034	.0057964	.0059844	0.319	53.3	0.703
23	234	.0021045	.0059409	.0060432	0.331	54.8	0.73
26	237	0012923	.006705	.0067761	0.312	46.04	0.777
27	238	.0011508	.0067432	.0067686	0.315	46.58	0.774
30	241	00007752	.0067852	.0067852	0.216	31.83	0.608

TABLE 3-27: RESULTS FOR $H_C = 8$, DIAMETER=200 INCHES, AND P=100 LBS

Inter- face	Soil	Δx	ΔΥ	AN	$ \sigma_{_{ m N}} $	k* n	k* n
Element	Node	(inch)	(inch)	(inch)	psi	(#/in ³)	k _n
1	59	.000037088	.0012186	.0012186	0.631	517.81	0.794
2	58	00096915	0014345	.0016636	0.593	356.4	0.676
3	60	.0010062	0014319	.0016726	0.583	348.5	0.669
4	77	0019834	0012210	.0021536	0.554	257.2	0.578
5	78	.0019560	0012202	.0021367	0.539	252.2	0.574
6	80	0028730	00062744	.002693	0.466	173.	0.488
7	82	.0028027	00065473	.0026522	0.471	177.6	0.49
8	84	0035138	.00043141	.0032084	0.398	124.05	0.427
9	86	.0034956	.00043522	.0031899	0.406	127.3	0.441
10	110	0036171	.0018795	.0036171	0.340	93.99	0.433
11	114	.0036316	.0019352	.0036316	0.334	91.97	0.455
14	148	0032013	.0031901	.0040304	0.255	63.27	0.418
15	153	.0032028	.0032867	.0040616	0.264	65.00	0.426
18	186	0029222	.0044736	.0049935	0.287	57.5	0.508
19	196	.0029223	.0045608	.0050449	0.291	57.7	0.508
22	233	0022161	.0056071	.0058387	0.371	63.54	0.757
23	234	.0021776	.0057128	.0059016	0.362	61.34	0.739
26	237	0012769	.0063999	.0064812	0.348	53.69	0.802
27	238	.0012034	.0064228	.0064802	0.339	52.31	0.779
30	241	000042355	.0067075	.0067075	0.238	35.48	0.597

TABLE 3-28: RESULTS FOR H_{C} = 11.23, DIAMETER=200 INCHES, AND P=100 LBS

Inter- face	Soil	$\Delta \mathbf{x}$	ΔΥ	DN	$ \sigma_{_{ m N}} $	k* n	k*
Element	Node	(inch)	(inch)	(inch)	psi	(#/in ³)	k _n
1	59	.0000061507	00067431	.00067431	.327	484.9	0.732
2	58	00050981	0007536	.00087421	.309	353.5	0.647
3	60	.00051757	000757	.00087978	.305	346.67	0.64
4	77	0010223	00063033	.0011107	.293	263.79	0.568
5	78	.0010055	0006327	.0011027	.288	261.16	0.568
6	80	0014426	00032957	.0013607	.254	186.66	0.48
7	82	.0014147	00032911	.0013378	.255	190.6	0.49
8	84	0017515	.00018711	.0016081	.202	125.6	0.395
9	86	.0017430	.00019236	.0015778	.204	129.29	0.395
10	110	0018013	.00089023	.0018013	0.240	133.36	.433
11	114	.0017955	.00090366	.0017407	0.235	135.0	0.443
14	148	0016340	.0015355	.0020284	.163	80.36	0.47
15	153	.0016079	.0015600	.0020111	.165	82.04	0.483
18	186	0014613	.0021490	.0024453	.171	69.93	0.508
19	196	.0014345	.0021740	.0024383	.172	70.54	0.522
22	233	0011007	.0026860	.0028199	.164	58.16	0.573
23	234	.0010779	.0027315	.0027596	.164	59.43	0.597
26	237	00063637	.0030510	.0030982	.155	50.03	0.586
27	238	.00060049	.0030662	.0032561	.155	47.6	0.567
30	241	000020220	.0032287	.0032287	.139	43.05	0.557

TABLE 3-29: RESULTS FOR $H_C = 4$, DIAMETER=300 INCHES, AND P=100 LBS

Inter-	Soil	Δχ	ΔΥ	DN	σ _N	k* n	k* n
Element	Node	(inch)	(inch)	(inch)	psi	(#/in ³)	k _n
1	59	.000013627	0015101	.0015101	0.514	340.4	0.71
2	58	0014546	0017836	.0021457	0.489	227.9	0.603
3	60	.0014798	0017403	.0021123	0.505	239.1	0.649
4	77	0027329	0013282	.0026808	0.490	182.8	0.602
5	78	.0027165	0012906	.0026407	0.456	172.7	0.590
6	80	0037695	00042411	.0032987	0.455	137.93	0.559
7	82	.0036848	00052689	.0032906	0.414	126.0	0.502
8	84	0047874	.0011527	.0049092	0.337	68.6	0.291
9	86	.004684	.0010696	.0047852	0.334	69.8	0.298
10	110	0049494	.0033180	.0049494	0.253	51.1	0.27
11	114	.0048809	.0032587	.0048809	0.254	52.0	0.275
14	148	0039658	.0051774	.0053715	0.175	32.6	0.387
15	153	.0039325	.0052085	.0053495	0.190	35.5	0.379
18	186	0035455	.0070683	.0070229	0.241	34.3	0.672
19	196	.0033999	.0070588	.0068991	0.251	36.4	0.672
22	233	0026482	.0089225	.0087749	0.198	22.6	0.693
23	234	.0026423	.0090292	.0088578	0.201	22.7	0.69
26	237	0018645	.011563	.011573	0.171	14.78	0.73
27	238	.0017454	.011412	.0113928	0.175	15.36	0.74
30	241	000055753	.012610	.012610	0.127	10.1	0.740

TABLE 3-30: RESULTS FOR H = 6.4, DIAMETER=200 INCHES, AND P=50 LBS

Inter-	Soil	Δχ	ΔΥ	AN	$ \sigma_{\mathbf{N}} $	k*	k* n
Element	Node	(inch)	(inch)	(inch)	psi	(#/in ³)	k _n
1	59	00000050803	.00080059	.00080059	.268	334.8	0.714
2	58	00073085	00091764	.0010984	.259	235.78	0.619
3	60	.00072528	00089965	.0010796	.266	246.37	0.660
4	77	0013932	00069191	.0013786	.258	187.14	0.595
5	78	.0013673	00067356	.0013484	.240	179	0.568
6	80	0018952	00022674	.0016664	.227	136.21	0.529
7	82	.0018434	00026717	.0016482	.209	126.8	0.488
8	84	0023754	.00054046	.0020920	.165	78.87	0.350
9	86	.0023262	.00051513	.0020531	.172	83.77	0.359
10	110	0024468	.0015873	.0024468	.178	72.75	0.365
11	114	.0024175	.0015756	.0024175	.180	74.46	0.385
14	148	0019823	.0025046	.0026592	.111	41.74	0.49
15	153	.0019824	.0025248	.0026655	.117	43.89	0.503
18	186	0017975	.0034530	.0034837	.113	32.44	0.492
19	196	.0017343	.0034425	.0034264	.116	33.85	0.462
22	233	0012854	.0043289	.0042589	.134	31.5	0.651
23	234	.0013103	.0043868	.0043191	.138	31.95	0.65
26	237	00087272	.0055085	.0055085	.133	24.14	0.69
27	238	.00084651	.0054744	.0054679	.139	25.4	0.691
30	241	000010261	.0060132	.0060132	.115	19.12	0.713

TABLE 3-31: RESULTS FOR H_C = 8, DIAMETER=300 INCHES, AND P=50 LBS

Inter-	Soil	Δχ	ΔΥ	Δη	$ \sigma_{N} $	k* n	k* n
Element	Node	(inch)	(inch)	(inch)	psi	(#/in ³)	k _n
1	59	.00000072793	00084071	.00084071	.275	327.1	0.702
2	58	00072799	00094901	.0011316	.266	235.06	0.614
3	60	.00072614	00093273	.001114	.272	244.73	0.649
4	77	0013848	00073527	.0014149	.265	187.3	0.589
5	78	.0013780	00070927	.0013836	.247	178.5	0.575
6	80	0019187	00025457	.0017018	.233	136.9	0.504
7	82	.0018572	00029503	.0016755	.217	129.51	0.470
8	84	0023648	.00049886	.0020948	.186	88.8	0.373
9	86	.0023247	.00048478	.0020612	.191	92.7	0.391
10	110	0024472	.0015190	.0024472	.227	92.7	0.307
11	114	.0024137	.0015221	.0024137	.224	93.0	0.303
14	148	0020755	.0024337	.0027259	.126	46.22	0.462
15	153	.0020283	.0024548	.0026875	.128	47.63	0.458
18	186	0017135	.0031421	.003233	.128	39.59	0.523
19	196	.0017913	.0033644	.0034266	.131	38.23	0.48
22	233	0013421	.0041894	.0041781	.159	38.0	0.699
23	234	.0013652	.0042958	.0042778	.162	37.9	0.686
26	237	00086544	.0052082	.0052207	.146	28.0	0.73
27	238	.00085203	.0052355	.005242	.156	29.8	0.739
30	241	0000096557	.0055777	.0055777	.108	19.36	0.733

TABLE 3-32: RESULTS FOR H_C = 8, DIAMETER=300 INCHES, AND P=100 LBS

Inter-	Soil	Δχ	ΔΥ	An	o _N	k* n	k*
face Element	Node	(inch)	(inch)	(inch)	psi	(#/in ³)	k _n
1	59	.0000013838	0016984	.0016984	.556	327.4	0.702
2	58	0014548	0019084	.0022636	.532	235.0	0.613
3	60	.0014511	0018758	.0022323	.543	243.2	0.645
4	77	0027677	0014780	.0028225	.530	187.8	0.591
5	78	.0027542	001426	.0027724	.493	177.8	0.573
6	80	0038348	00051525	.0034050	.497	140.7	0.518
7	82	.0037121	00059606	.003502	.462	138.0	0.501
8	84	0047251	.00099301	.0039384	.371	94.2	0.395
9	86	.0046450	.00096487	.0041157	.382	98.82	0.417
10	110	0048888	.0030339	.0030339	.198	65.3	0.303
11	114	.004822	.0030401	.0030401	.197	64.8	0.300
14	148	0041451	.0048642	.0054452	.222	40.8	0.408
15	153	.0040507	.0049063	.0053685	.228	42.5	0.409
18	186	0037527	.0067296	.0069915	.313	44.8	0.592
19	196	.0035827	.0067291	.0068537	.317	46.3	0.58
22	233	0026845	.0083797	.0083571	.316	37.8	0.695
23	234	.0027306	.0085924	.0085563	.316	36.9	0.668
26	237	₹.0017311	.010417	.0104379	.290	27.8	0.725
27	238	.0017042	.010472	.010486	.309	29.5	0.732
30	241	000019334	.011156	.011156	.227	20.4	0.733

TABLE 3-33: RESULTS FOR H_C = 11.23, DIAMETER=300 INCHES, and P=50 LBS

Inter-	Soil	Δχ	ΔΥ	DN	$ \sigma_{_{ m N}} $	k*	$\frac{\frac{k_n^*}{n}}{k_n}$
Element	Node	(inch)	(inch)	(inch)	psi	(#/in ³)	k _n
1	59	000019174	00090706	.00090706	.287	316.43	0.67
2	58	00073930	00098955	.0010088	.278	275.6	0.711
3	60	.00071096	00099146	.00098243	.283	288.1	0.751
4	77	0013787	00077617	.0014382	.275	191.2	0.587
5	78	.0013812	00077292	.001437	.262	182.31	0.564
6	80	0019496	00027019	.0017360	.242	139.4	0.504
7	82	.0018860	00033920	.0017251	.231	133.9	0.478
8	84	0023627	.00046098	.0021046	.187	88.85	0.394
9	86	.0023250	.00041982	.0020813	.194	93.21	0.413
10	110	0024381	.0014397	.0024381	.193	79.16	0.362
11	114	.0023939	.0014026	.0023939	.195	81.46	0.380
14	148	0021822	.0023499	.0028014	.146	52.12	0.436
15	153	.0021106	.0023105	.0027212	.150	55.12	0.447
18	186	0019739	.0032590	.0028848	.151	52.34	0.613
19	196	.0018404	.0031793	.0028602	.154	53.84	0.616
22	233	0014826	.0040828	.0041744	.162	38.8	0.65
23	234	.0013473	.0039992	.0040272	.155	38.5	0.65
26	237	00092491	.0048724	.0049197	.151	30.7	0.701
27	238	.00078875	.0047875	.0047968	.149	31.10	0.699
30	241	000063658	.0051058	.0051058	.130	25 .4 6	0.695

TABLE 3-34: RESULTS FOR H_C = 12.64, DIAMETER=300 INCHES, AND P=50 LBS

Inter-	Soil	Δχ	ΔΥ	DN	$ \sigma_{\mathbf{N}} $	k* k* n n
Element	Node	(inch)	(inch)	(inch)	psi	(#/in ³) k _n
1	59	000015181	00093959	.00093959	.291	309.73 0.661
2	58	00073537	0010191	.0011963	.284	237.38 0.618
3	60	.00071515	0010176	.0011887	.287	241.43 0.634
4	77	0013798	00080903	.0014654	.278	189.70 0.59
5	78	.0013885	00079432	.0014587	.268	183.72 0.575
6	80	0019528	00030431	.0017584	.246	139.89 0.524
7	82	.0019038	00035324	.0017477	.237	135.60 0.502
8	84	0023485	.00043318	.0020997	.192	91.44 0.386
9	86	.0023289	.00039733	.0020921	.198	94.64 0.404
10	110	0024142	.0013860	.0024142	.211	87.4 0.396
11	114	.0023991	.0013614	.0023991	.209	87.1 0.392
14	148	0021897	.0022893	.0027899	.154	55.2 0.509
15	153	.0021435	.0022618	.0027374	.157	57.35 0.533
18	186	0019633	.0031787	.0034567	.162	46.87 0.534
19	196	.0018612	.0031170	.0033377	.163	48.83 0.553
22	233	0012932	.0035842	.0036597	.133	36.3 0.563
23	234	.0013844	.0039359	.0039978	.140	35.2 0.542
26	237	00089233	.0047140	.004759	.147	30.9 0.610
27	238	.00081654	.0046816	.0047047	.148	31.46 0.624
30	241	000035976	.0049623	.0049623	.142	28.62 0.687

TABLE 3-35: RESULTS FOR H = 12.64, DIAMETER=300 INCHES, AND P=100 LBS

Inter-	Soil	Δχ	ΔΥ	\DN	$ \sigma_{\mathbf{N}} $	k*	k*
face Element	. Node	(inch)	(inch)	(inch)	psi	(#/in ³)	$\frac{\frac{k_n^*}{n}}{\frac{k_n}{n}}$
1	59	000030511	0018964	.0018964	0.588	310.1	0.66
2	58	0014695	0020485	.0024022	0.566	235.6	0.597
3	60	.0014291	0020459	.0023873	0.574	240.43	0.618
4	77	0027577	0016255	.0029359	0.557	189.7	0.567
5	78	.0027750	0015963	.0029224	0.535	183.1	0.551
6	80	0039030	00061476	.0035188	0.524	148.9	0.524
7	82	.0038051	00071263	.003497	0.504	144.1	0.502
8	84	0046927	.00086165	.0047291	0.406	85.9	0.375
9	86	.0046533	.00078985	.0046695	0.414	88.7	0.398
10	110	0048232	.0027679	.0048232	0.358	74.22	0.335
11	114	.0047929	.0027185	.0047929	0.360	75.11	0.341
14	148	0043744	.0045754	.005741	0.282	50.6	0.453
15	153	.0042819	.0045203	.0054691	0.289	52.84	0.472
18	186	0039267	.0063575	.0069136	0.368	53.4	0.582
19	196	.0037224	.0062339	.0066756	0.375	56.2	0.597
22	233	0029234	.0079447	.0081456	0.374	45.9	0.716
23	234	.0027688	.0078720	.007996	0.379	47.4	0.699
26	237	0017847	.0094287	.0095187	0.370	38.9	0.74
27	238	.0016332	.0093638	.0094101	0.374	39.7	0.78
30	241	000071912	.0099247	.0099247	0.291	29.32	0.72

TABLE 3-36: COMPARISON OF PROPOSED AND FEM RESULTS FOR MEDIUM SOIL (CIRCULAR)

	Crown: θ = 0°						
Diameter (inches)	Hc (ft)	$\sqrt{\frac{H}{D}}$	Coeffic Soil Re (#/i	action			
			Proposed	FEM			
200 300 300	8.0 8.0 12.64	0.6928 0.5657 0.71105	40. 22.9 33.6	35.5 19.4 28.62			
	Spri	Springline: $\theta = 90^{\circ}$					
200 300 300	8.0 8.0 12.64	0.9899 0.906 1.003	97.7 90.6 100	94.0 92.7 87.4			
200 300 300	8.0 8.0 12.64	1.2165 1.149 1.227	450 364 388	517 327 310			

TABLE 3-37: COMPARISON OF PROPOSED AND FEM RESULTS FOR DENSE SOIL (CIRCULAR)

		Invert	: θ = 180			
Diameter (inches)	Hc (ft)	$\sqrt{\frac{H}{D}}$	Coefficie Soil Reac (#/in ³	tion	% Difference	
			Proposed*	FEM		
100	4.0	1.2415	834	950	12.2	
100	6.4	1.3293	893	995	10.2	
200	11.73	1.305	689	662	4.4	
300	8.0	1.1489	441	466.6	5.5	
300	12.64	1.227	471	468		
	Springline: θ = 90°					
		Springline:	, 			
100	4.0	0.99	385	380		
100	6.4	1.126	437	425	7.4	
200	11.73	1.097	335	308	8.8	
300	8.0	1.003	222	223		
300	12.64	0.9066	201.3	210	4.3	
		Crown: θ	= 0°			
100	4.0	0.6928	73	74.5		
100	6.4	0.8764	92.4	74.5 96.2	4.0	
200	11.73	0.8389	69.3	77.3	10.3	
300	8.0	0.5657	33.9	27.81	22.0	
300	12.64	0.71105	42.66	40.67	5.0	

^{*}Based on a unit weight of soil Y of 120 pcf.

TABLE 4-1: THEORETICAL PRE-BUCKLING THRUSTS

Section	Relative Density	Diameter (inches)	Location	Thrust (Compression) (lb/in)	FEM
Circular	Dense	300	Haunch	212 188	216 180
Circular	Dense	200	Haunch	142 134	141
Circular	Dense	150	Haunch	110 101	134 115
Circular	Medium	300	Haunch	212.13 73.44	
Ellipse	Dense		Haunch	221 162.6	2 4 6 156

†Semi-minor axis: 75 inches Semi-major axis: 150 inches

TABLE 4-2: THEORETICAL PRE-BUCKLING DEFLECTIONS

Section	Relative Density	Diameter (inch)	Location	Deflection (inch)	FEM
Circular	Dense	300	Crown Spring-Line Invert	03 .008 .0056	0314 .005 .004
Circular	Dense	200	Crown Spring-Line Invert	017 .005 .0032	0178 .0035 .0037
Circular	Dense	150	Crown Spring-Line Invert	0134 .004 .003	017 .0036 .0048
Circular	Medium	300	Crown Spring-Line Invert	048 .01 .002	
Ellipse [†]	Dense		Crown Spring Line Invert	064 .015 .0012	063 .01 .0018

†Semi-minor axis: 75 inches Semi-major axis: 150 inches

TABLE 4-3 THEORETICAL PRE-BUCKLING MOMENTS

Section	Relative Density	Diameter (inches)	Location	Moments (lb-in/in)	FEM
Circular	Dense	300	Crown Haunch Spring-Line Invert	19.70 -7.4 -2.52 1.0	20 -5.5 -2.36 1.37
Circular	Dense	200	Crown Haunch Spring-Line Invert	17.85 -10.0 -2.0 1.0	18.11 -6.031 -2.75 1.27
Circular	Dense	150	Crown Haunch Spring-Line Invert	23.4 -10.75 -3.75 2.13	19 -7.4 -2.5 2.0
Circular	Medium	300	Crown Haunch Spring-Line Invert	47.6 -30.5 -3.17 1.59	
Ellipse [†]	Dense		Crown Haunch Spring-Line Invert	23 -100 -63 3.31	32 -62.3 -40.5 3.91

Semi-minor axes: 75 inches Semi-major axes: 150 inches

TABLE 4-4: VARIATION OF λ WITH SPAN

Diameter (inches)	K _{Ni} #/in ³	K s #/in ³	$\lambda = \frac{K_s}{K_{N_1}}$
300	413.6	75	0.18
200	587.7	125	0.21
50	689.34	145	0.21

TABLE 4-5: COMPARISON OF PROPOSED AND FEM RESULTS FOR DENSE SOIL (ELLIPTICAL)

			Coefficien Soil React (#/in ³)	ion
H _C (ft)	Node Number	$\sqrt{\frac{H}{D}}$	Proposed	FEM
4	59	0.855	343	319
6 8		0.903 0.948	363 381	333 353
4	60	0.646	336	390
6 8		0.707 0.765	357 376	397 4 10
4 6 8	241	0.41 0.502 0.57	25.9 31.7 36.6	16 25 30
6	58	0.707	357	397

Semi-minor axis: b = 80.5 inches Semi-major axis: a = 143 inches

Span: D = 286 inches

TABLE 4-6: COMPARISON WITH TEST RESULTS

Investi-	Nominal Sand Density and		Soil Ring Thickness	Uniform Applied Buckling Pressure	Pres Stu (ps	ıdy
gator	Void Ratio		(in)	(psi)	Dense	Medium
	Medium-Dense, (0.50	3/8	9.0	7.72	5.17
	Medium-Dense, C	0.50	3/8	12.4	7.72	3.17
Luscher	Medium-Dense, C	0.4 8	2/3	14.2		
					8.09	5.45
	Medium-Dense, C	0.48	2/3	12.4		
	Medium-Dense, C	0.47	2/3	9.9		

⁽a) All tests on aluminum tubes with constant radius (0.815 in.) and constant stiffness ($EI/R^3 = 0.042$).

TABLE 4-7: COMPARISON WITH TEST RESULTS

Investi-	Area (in ² /in)	Radius (in)	EI R ³	Thrust Stress at Failure (psi)	Present Critical Pressure (psi)	Study Thrust Stress at Failure (psi)
	.013 ^a	12.9	.0057	5,780	6.9	6,697
	.0328 ^a	12.9	.086	7,850	22.41	8,813
Meyerhof	.0328 ^a	25.6	.011	5,600	9.55	7,454
and	.0328 ^a	12.0	0.11	6,350	19.5	7,134
Baike	.018 ^b	12.0	1.3	41,400	106.11	70,740
	.0162 ^b	24.0	0.2	26,100	22.92	33,956

⁽a) Plain Sheets

⁽b) Corrugated Sheets

TABLE 4-8: COMPARISON WITH TEST RESULTS

Investi-	Radius	Soil D	ensity	Critical	Present (ps	_
gator	(in)	Pcf	% Std. AASHTO	Pressure (psi)	Dense	Medium
Watkins	30	101.7	83	111	151	131.4
and	30	118.4	97	132		
Moser	30	129	106	97		

TABLE 4-9: COMPARISON OF THEORETICAL FORMULATIONS OF COEFFICIENT OF SOIL REACTION (SOIL SUPPORT MODULUS)

Investigator	Suggested Expression for k
Luscher	$\frac{E_{\mathbf{g}}\left[1-\left(\frac{R_{\mathbf{i}}}{R_{\mathbf{o}}}\right)^{2}\right]}{\left(1+\mu_{\mathbf{g}}\right)^{2}\left\{1+\left[\frac{R_{\mathbf{i}}}{R_{\mathbf{o}}}\right]^{2}-\left(1-2\mu_{\mathbf{g}}\right)^{2}\right\}} R$
Meyerhof and Baike	E _S 2(1-μ _S ²) R
Kloppel and Glock	E _S R(1+µ _S)
Present Study	$k_{n} = \beta^{*} c_{D} c_{\theta} \sqrt{\frac{H}{D}}$
	k _s = 0.2 k n

TABLE 4-10: VALUES OF K IN TONS/CU. FT FOR SQUARE PLATES,

1 FT X 1 FT, OR BEAMS 1 FT WIDE, RESTING ON SAND

(AFTER TERZAGHI, 1955)

Relative Density of Sand	Medium	Dense
Dry or moist sand, Limiting values for K	60 - 300	300 - 1000
Dry or moist sand, Proposed values	130	500
Submerged sand, Proposed values	80	300

¹ ton/cu. ft = 1.1574 pci

TABLE 4-11: COMPARISON OF THEORETICAL CRITICAL PRESSURES (CIRCULAR)

Investigato	or	EI/R³	f _{cr} (psi)	EI/R³	f _{:cr} (psi)	EI/R³	f cr (psi)
Meyerhof and Baike		1.0	107.3	10	611	100	930
Luscher		1.0	391.9	10	878.4	100	3675.7
Chelapati and Allgood		1.0	440.54	10	927	100	4410.0
Cheney		1.0	884	10	1945.2	100	4103.0
Present Study	Dense	1.0	180.9	10	1073.2	100	2380.4
	Medium	1.0	116.84	10	757.4	100	1371.33

TABLE 4-12: VARIATION OF CRITICAL PRESSURE WITH $\frac{P}{P_o}$

P_1	(psi) Critical Pressure		
P _o	Dense	Medium	
0	254	187	
0.25	217	165.6	
0.33	210	146	
0.50	184	126	
1.0	165	101	

Span = 300 inches

 $\alpha = 0.16$

TABLE 4-13: VARIATION OF CRITICAL PRESSURES WITH ASPECT RATIO (ELLIPTICAL SECTION)

Aspect	(psi) Critical Pressure			
Ratio, B/A	Medium	Dense		
0.2	12.3	22.0		
0.3	21.1	37.5		
0.5	48.7	85.0		
1.0	106.03	159.96		

Span, D = 300 Inches

 $\alpha = 0.16$

$$\frac{P_1}{P_2} = 1.0$$

TABLE 4-14: VARIATION OF CRITICAL PRESSURE WITH DEPTH

Davids Davids	Critical Pressure (psi)		
Depth Ratio α	Dense	Medium	
0.16	165	101	
0.3	175.3	107.2	
0.5	187.2	111.5	
0.7	198	150	
0.9	207	155.12	
1.0	211.5	157.5	

TABLE 4-15: VARIATION WITH DEPTH OF RALATIVE CROWN DEFLECTION DURING BUCKLING (CIRCULAR)

	Crown Deflection (inches)		
Depth Ratio α	Dense	Medium	
0.16	1.59	2.63	
0.3	1.67	2.71	
0.5	1.78	2.98	
0.7	2.39	3.15	
0.9	2.41	3.30	
1.0	2.51	3.36	

TABLE A-1: DATA REDUCTION

Conduit	Di	lameter =	: 300	Inches
---------	----	-----------	-------	--------

		Conduit		= 300 inch	es		
θ = π* θ =		θ =	ο.9π		θ = 0.8π		
H D	1	<u>K</u> Y	H D	$\frac{\mathbf{K}}{\mathbf{\gamma}}$		H D	$\frac{\mathbf{K}}{\mathbf{Y}}$
1.256	3.9	96	1.23	3.17		1.16	2.62
1.256	4.0		1.23	3.18		1.16	2.54
1.32	3.8		1.296	3.19		1.225	2.64
1.32	3.9		1.296	3.19		1.225	2.65
1.32	3.9		1.296	3.18		1.225	2.63
1.4692	3.9		1.445	3.23		1.374	2.71
1.4692 1.5056	4.3		1.445	3.24		1.374	3.00
1.5056	3.9 3.9		1.481 1.481	3.29 3.20		1.410	2.78
1.5056	3.9		1.481	3.23		1.410 1.410	2.68 2.69
1.8144	4.0		1.790	3.45		1.719	2.09
1.8144	3.9		1.790	3.32		1.719	2.80
1.8144	3.9		1.790	3.32		1.719	2.80
		Conduit I	Diameter =	= 200 Inch	es		
1.383	5.4	12	1.359	4.32		1.288	3.59
1.48	5.4		1.455	4.39		1.384	3.71
1.704	5.5	52 	1.679	4.55		1.608	3.87
		Conduit I	Diameter =	= 300 Inch	es		
$\theta = 0.7\pi$ $\theta = 0.$		0.6π	$\theta = 5.0\pi$		$\theta = 0.4\pi$		
H/D	K/Y	H/D	K/Y	H/D	K/Y	H/D	K/γ
1.049	2.09	0.910	1.66	0.756	1.29	0.601	0.73
1.049	2.12	0.910	1.57	0.756	1.09	0.601	0.72
1.049	2.16	0.910	1.59	0.756	1.09	0.601	0.73
1.114	2.29	0.975	1.80	0.82	1.37	0.665	0.87
1.114	2.22	0.975	1.75	0.82	1.28	0.665	0.91
1.114	2.20	0.975	1.74	0.82	1.26	0.665	0.90
1.263	2.33	1.124	1.88	0.969	1.41	0.815	1.03
1.263	2.33	1.124	1.87	0.969	1.39	0.815	1.03
1.299	2.39	1.160	1.91	1.0056	1.47	0.851	0.93
1.299	2.25	1.160	1.77	1.0056	1.33	0.851	0.90
1.299	2.27	1.160	1.79	1.0056	1.33	0.851	0.92
1.608	2.61	1.469	2.14	1.3144	1.71	1.16	1.14
1.608	2.42	1.469	1.98	1.3144	1.52	1.16	1.07
1.608	2.43	1.469	1.99	1.3144	1.54	1.16	1.08

^{*} θ in radians

TABLE A-1: DATA REDUCTION (continued)

Conduit Diameter = 200 Inches							
1.177	2.91	1.038	2.31	0.883	1.70	0.729	1.05
1.274	3.02	1.134	2.42	0.980	1.81	0.825	1.27
1.498	3.24	1.358	2.73	1.204	2.05	0.825	1.44

Conduit Diameter = 300 Inches

$\theta = 0.3\pi$		$\theta = 0.2\pi$		$\theta = 0.1\pi$		$\theta = 0.0$	
H/D	$\frac{\mathbf{K}}{\mathbf{Y}}$	H/D	$\frac{\mathbf{K}}{\mathbf{Y}}$	H/D	<u>K</u>	H/D	<u>K</u> Y
0.461	0.61	0.351	0.41	0.28	0.31	0.256	0.22
0.461	0.56	0.351	0.38	0.28	0.28	0.256	0.22
0.461	0.55	0.351	0.38	0.28	0.27	0.256	0.21
0.526	0.67	0.415	0.46	0.24	0.34	0.32	0.23
0.526	0.61	0.415	0.41	0.344	0.30	0.32	0.23
0.526	0.60	0.415	0.40	0.344	0.48	0.32	0.23
0.675	0.73	0.565	0.49	0.494	0.37	0.469	0.31
0.675	0.73	0.565	0.49	0.494	0.57	0.469	0.30
0.073	0.72	0.601	0.49	0.434	0.33	0.409	0.34
0.712	0.73	0.601	0.54	0.53	0.42	0.5056	0.34
0.712	0.73	0.601	0.54	0.53	0.42	0.5056	0.33
1.021							
	0.97	0.91	0.72	0.839	0.58	0.8144	0.49
1.021	0.92	0 91	0.70	0.839	0.57	0.8144	0.50
1.021	0.92	0.91	0.70	0.839	0.57	0.8144	0.50
		Conduit D	iameter =	200 Inch	les		
0.589	0.87	0.479	0.63	0.408	0.50	0.383	0.44
0.686	0.95	0.575	0.70	0.504	0.56	0.48	0.50
0.909	1.15	0.799	0.85	0.728	0.71	0.704	0.64

TABLE A-2: DATA REDUCTION

$\frac{H}{D} = 1.$	0	$\frac{H}{D} = 0.5$	
θ (radians)	$\frac{\mathbf{K}}{\mathbf{\gamma}}$	θ (radians)	<u>K</u>
0	0.54	o	0.33
. 2π	0.75	.2π	0.46
.4π	1.08	.4π	0.71
.6π	1.75	.6π	1.08
.8π	2.42	.8π	1.5
1.0π	3.29	1.0π	2.08

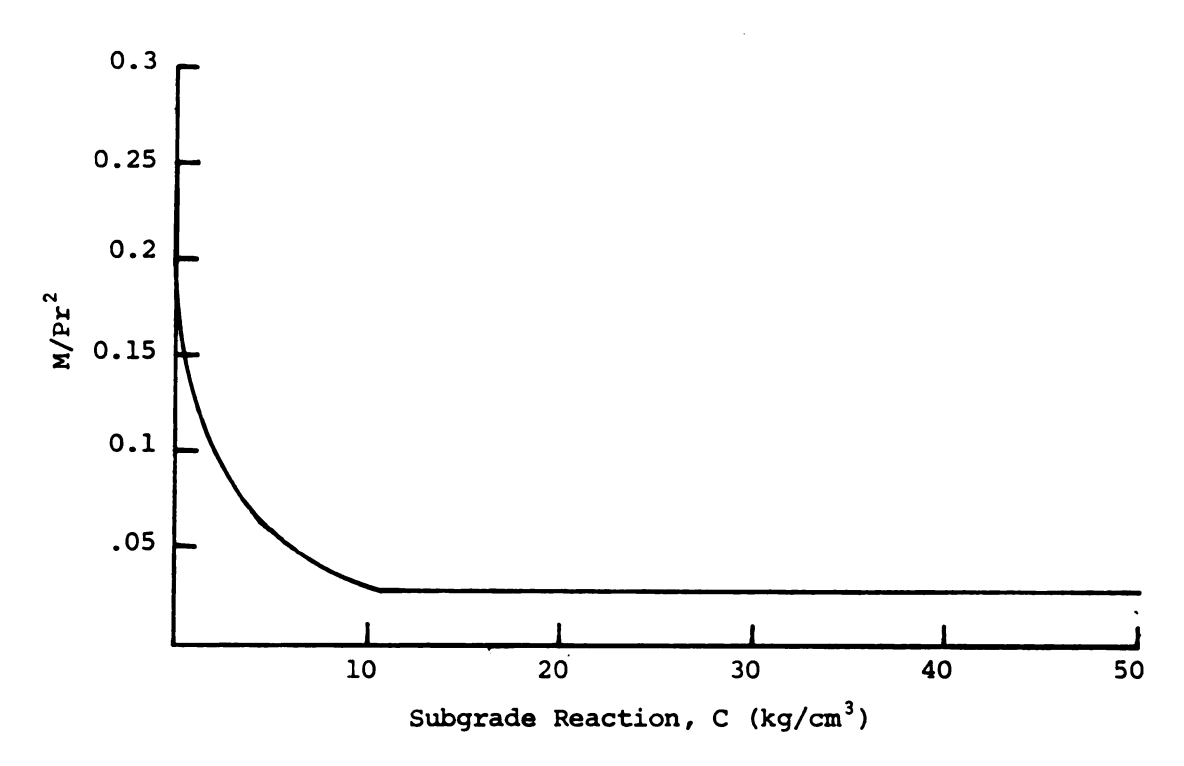


FIGURE 1-1: VARIATION OF THE CROWN MOMENT AS A FUNCTION OF SUBGRADE REACTION*

*Source: Reference (1)

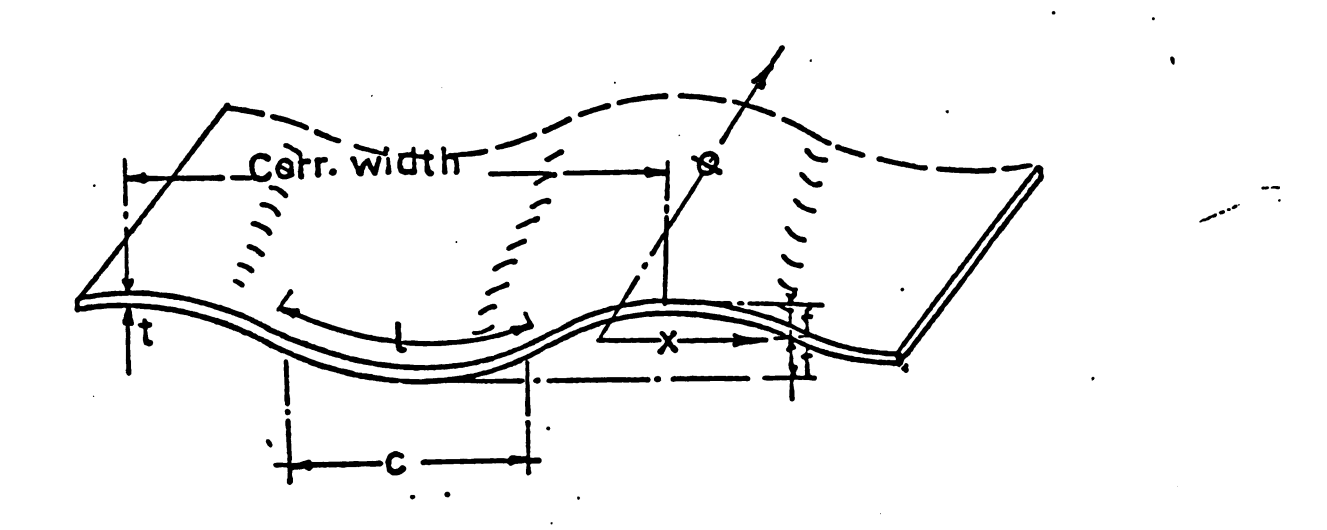


Fig.(2-1) Geometry of Corrugation

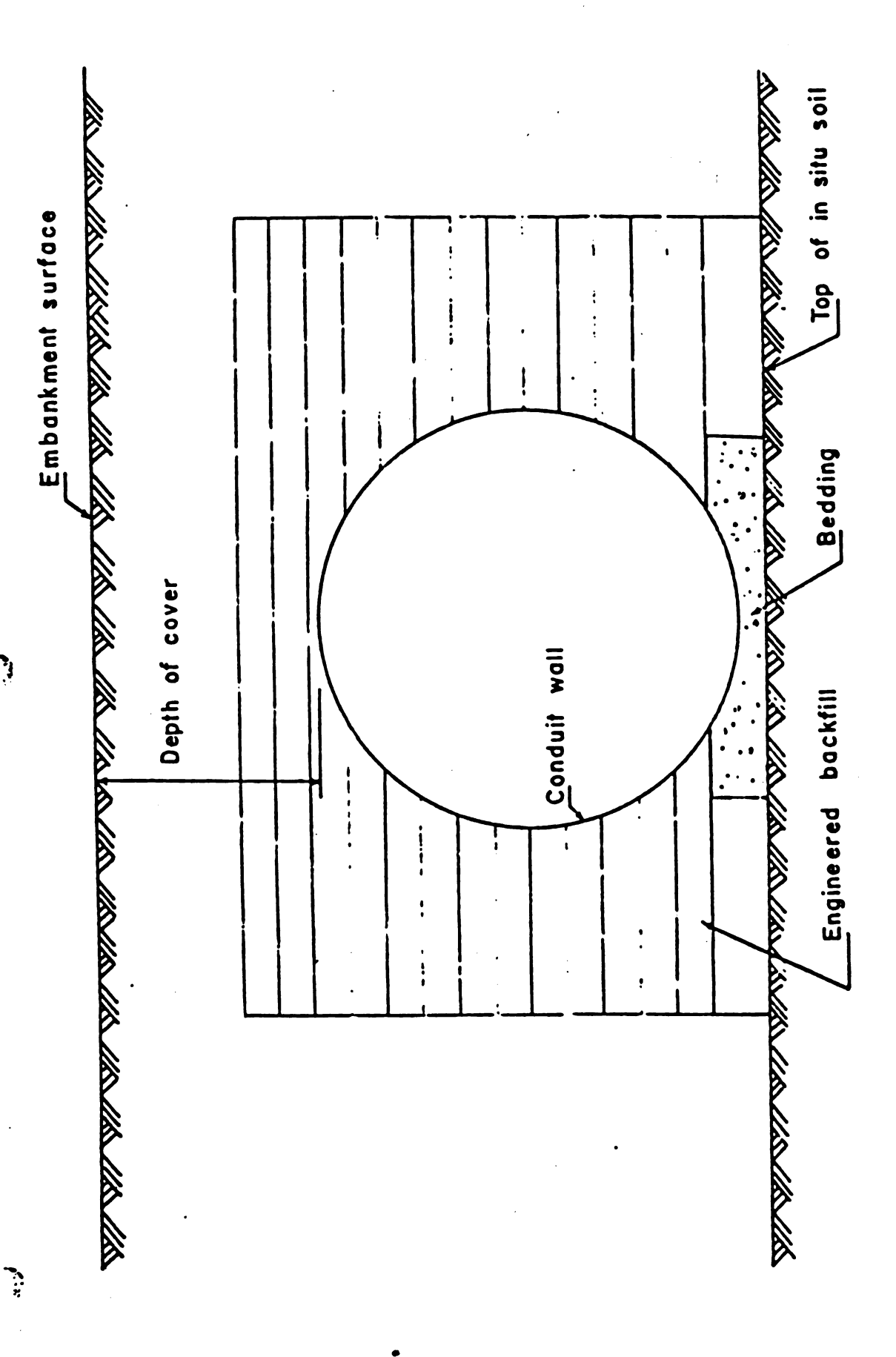


Fig. 2-2 Soil Bedding and Engineered Backfill Around the Conduit

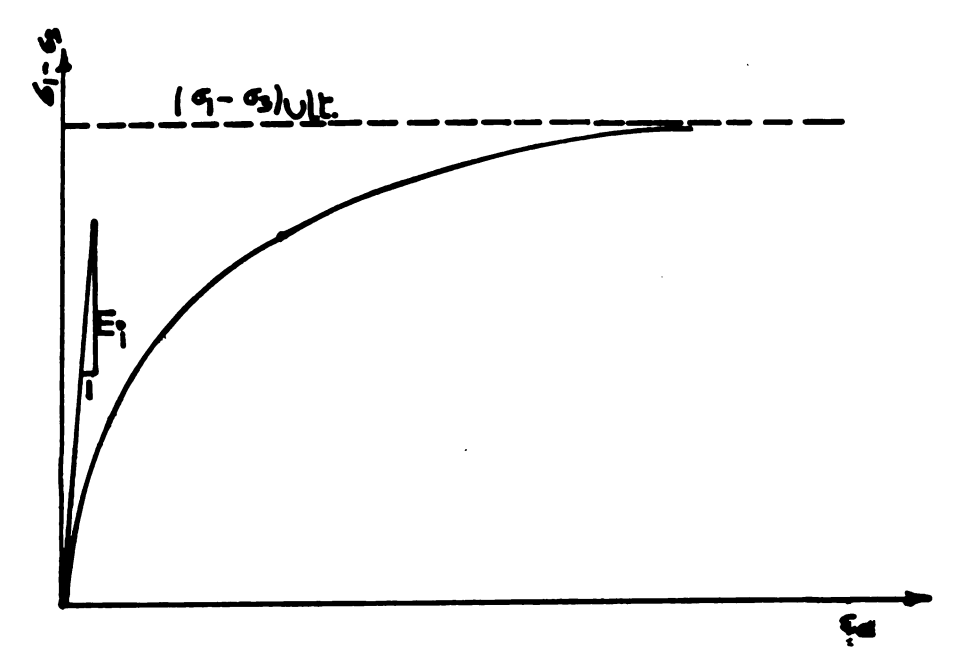


FIGURE 2-3a: HYPERBOLIC STRESS-STRAIN RELATIONSHIP

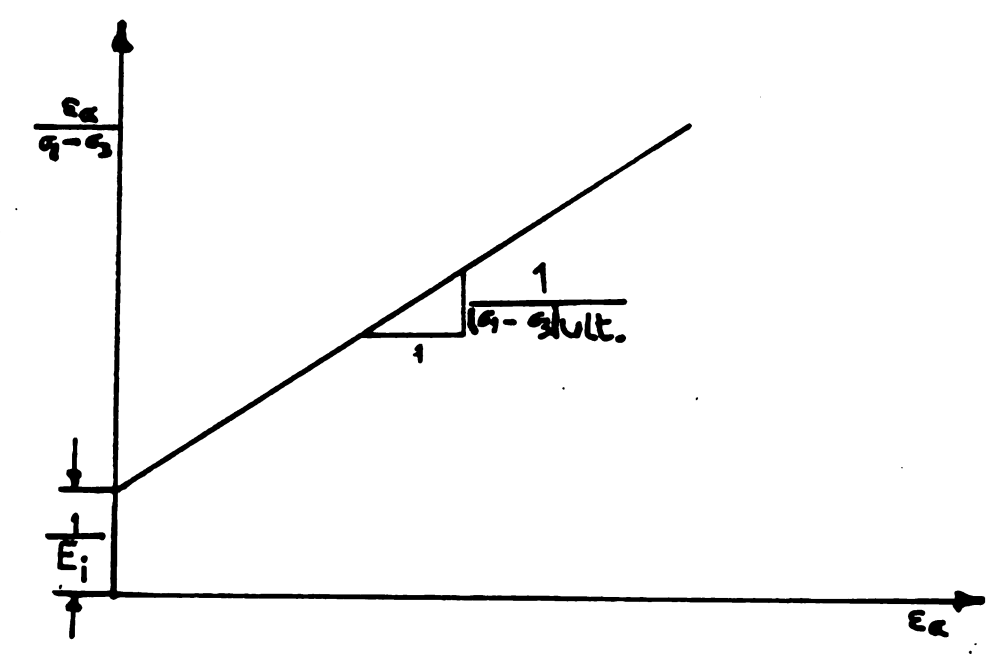


FIGURE 2-3b: TRANSFORMED HYPERBOLIC STRESS-STRAIN RELATIONSHIP

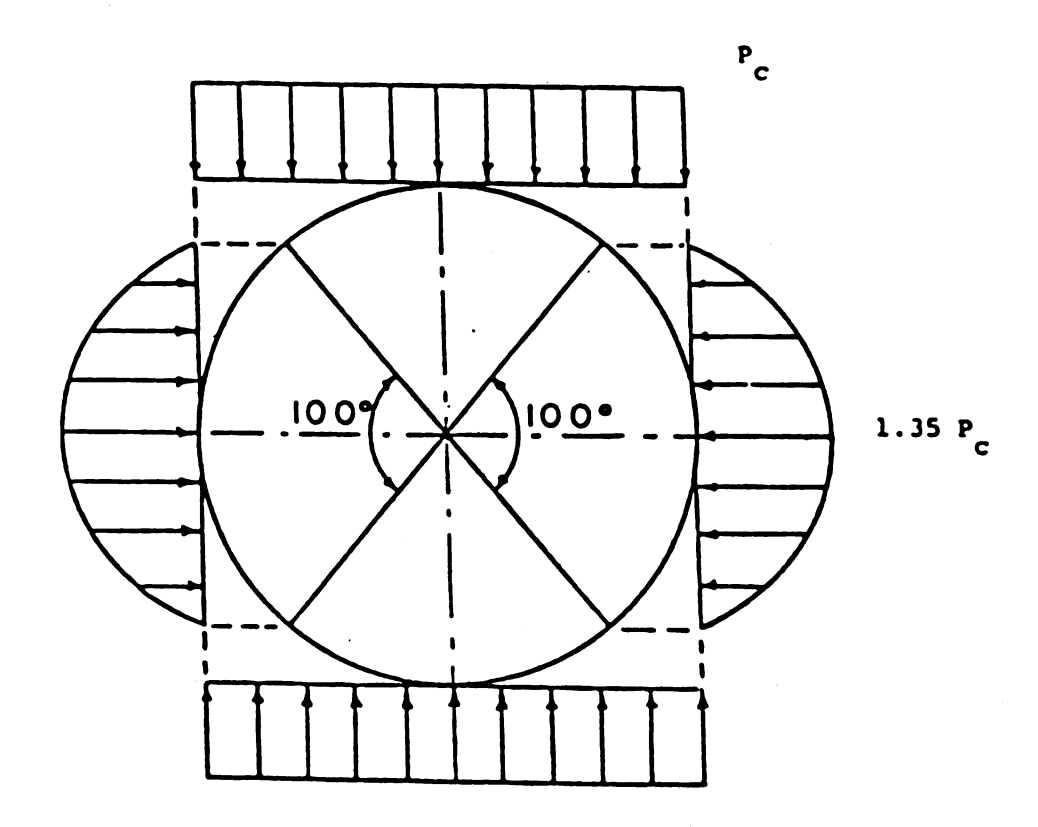


Fig. 2-4 Pressure Distribution Assumed in the Marston-Spangler Theory

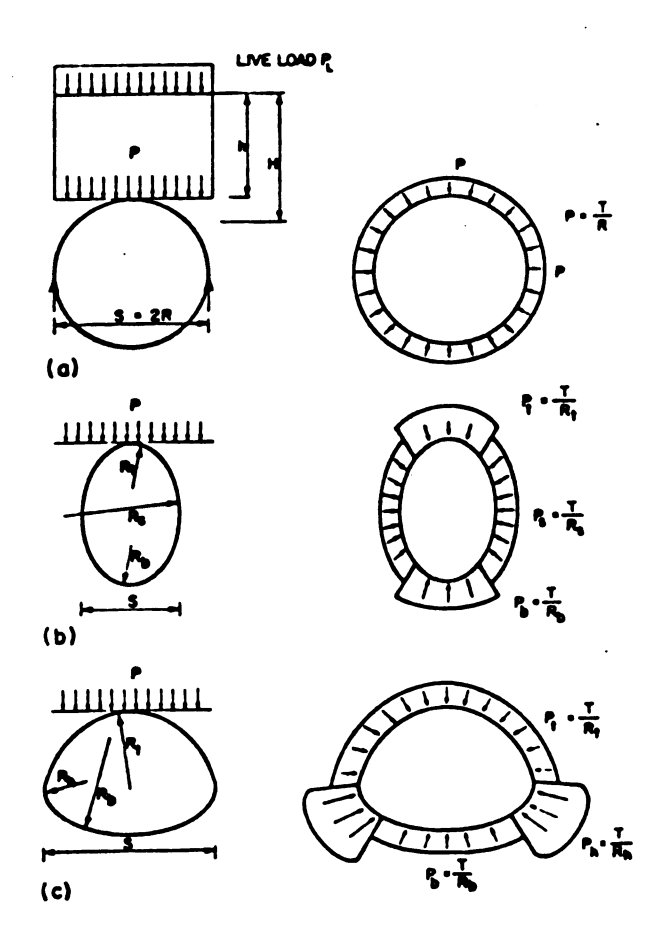


FIG. 2-5. SOIL PRESSURE DISTRIBUTION ACCORDING
TO THE RING COMPRESSION THEORY:
(a) CIRCULAR SECTION; (b) ELLIPTICAL
SECTION; (c) PIPE-ARCH

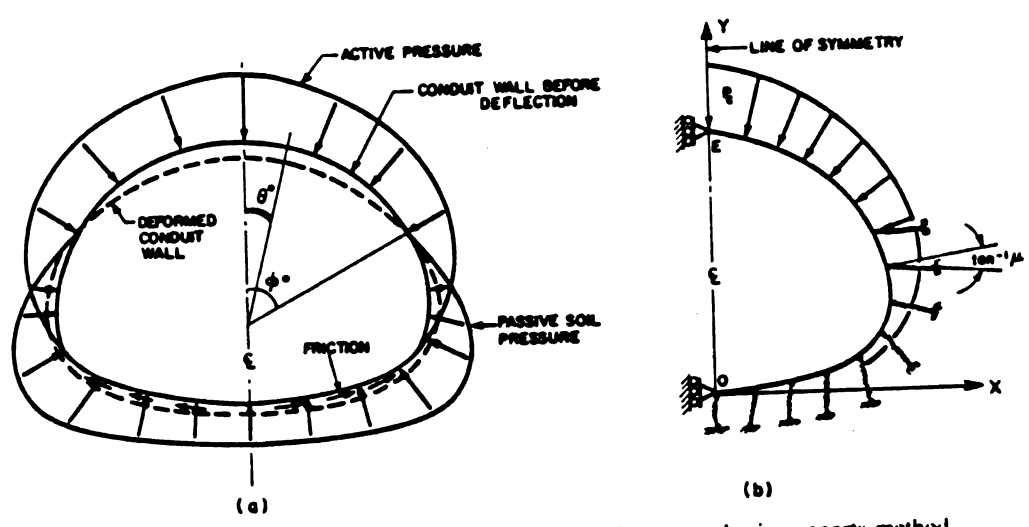


FIG 2-6: Idealisation of the structure for analysis by frame-on-clastic supports method.

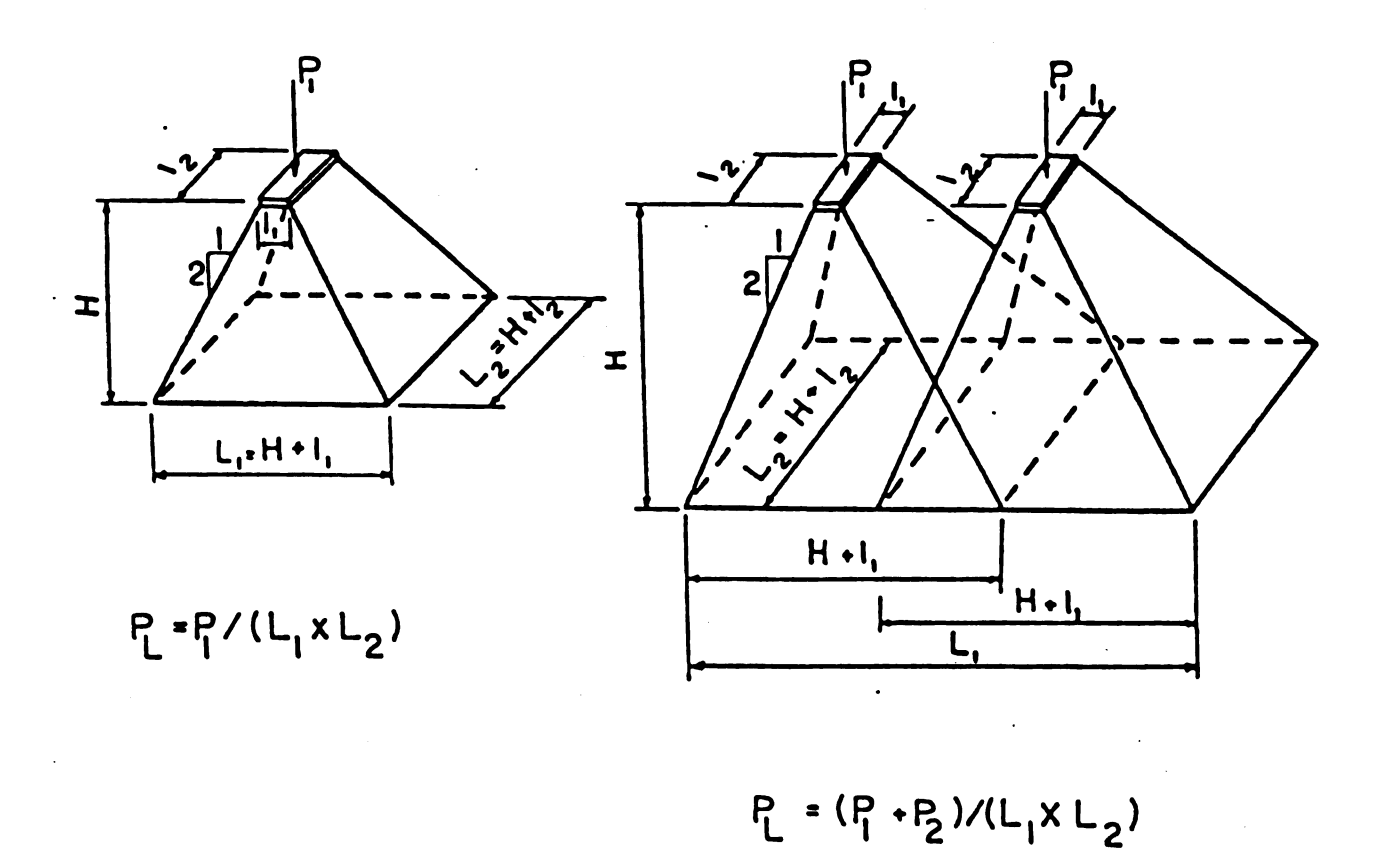


FIG. 2-7 Dispersion of Live Load Through the Soil-Fill

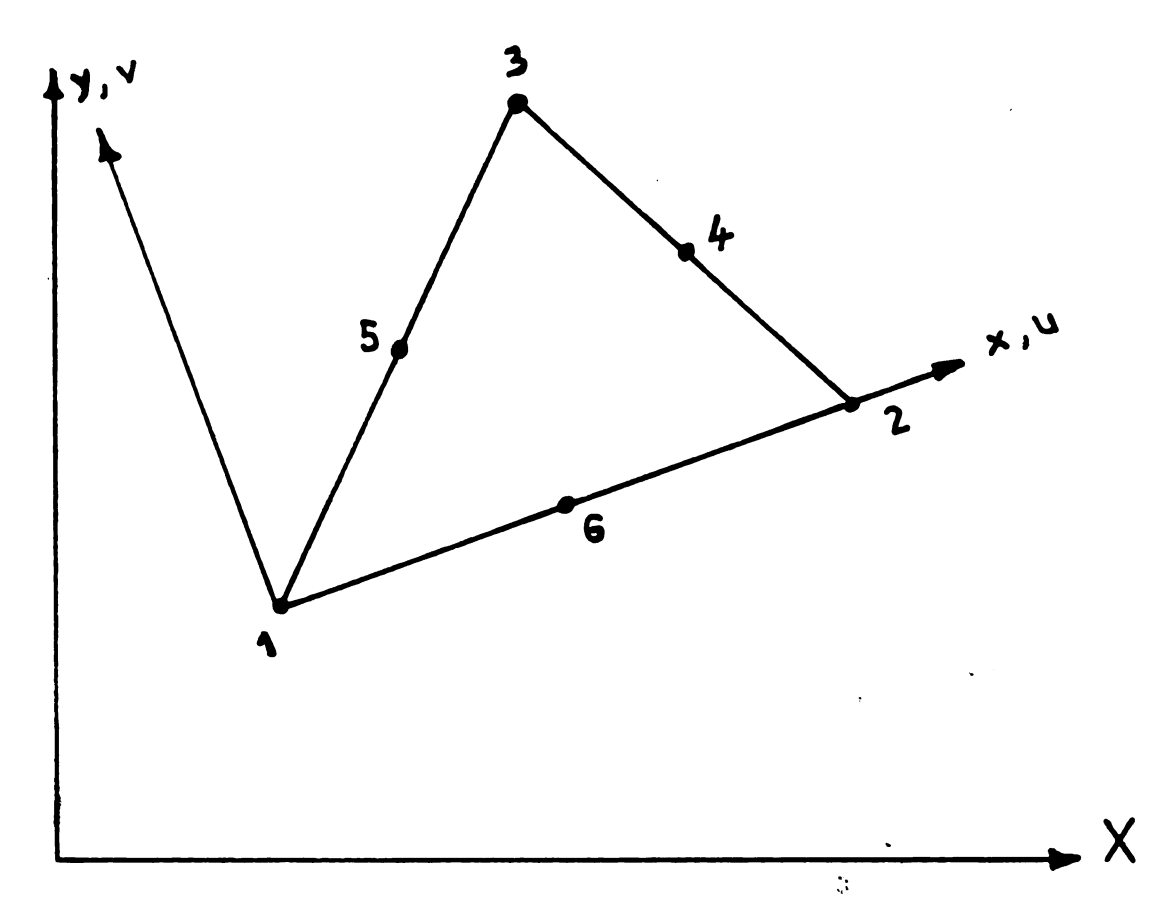


FIGURE 3-1: LINEAR STRAIN TRIANGULAR ELEMENT



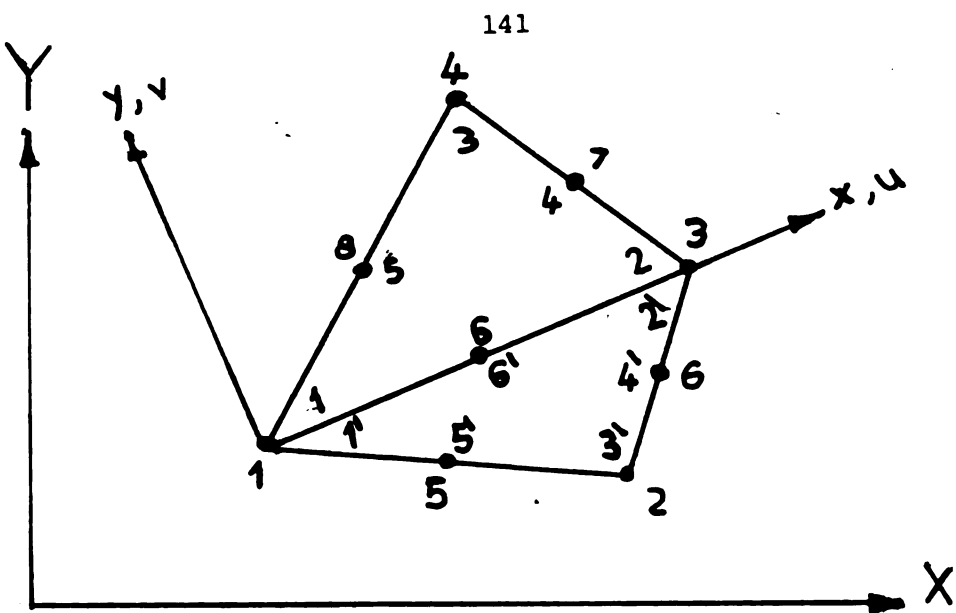


FIGURE 3-2a: 9-NODE QUADRILATERAL ELEMENT

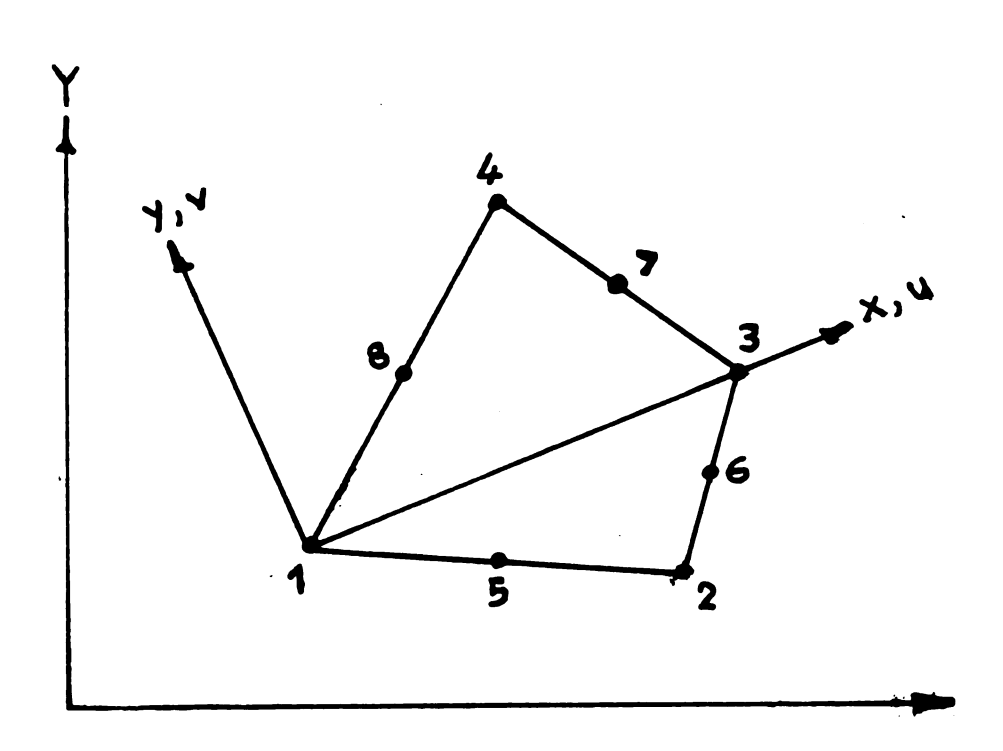


FIGURE 3-2b: 8-NODE QUADRILATERAL ELEMENT

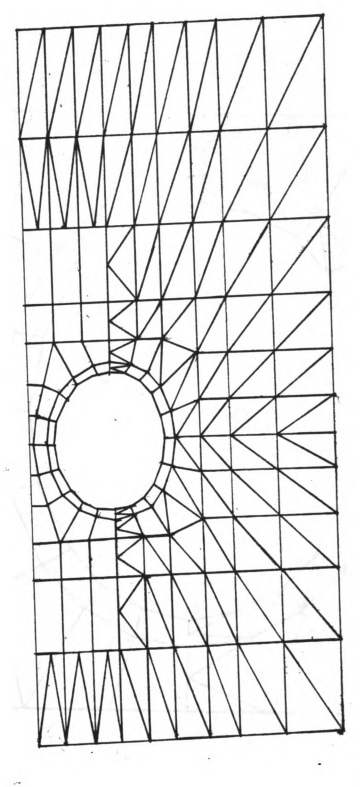


FIGURE 3-3: FINITE ELEMENT MESH

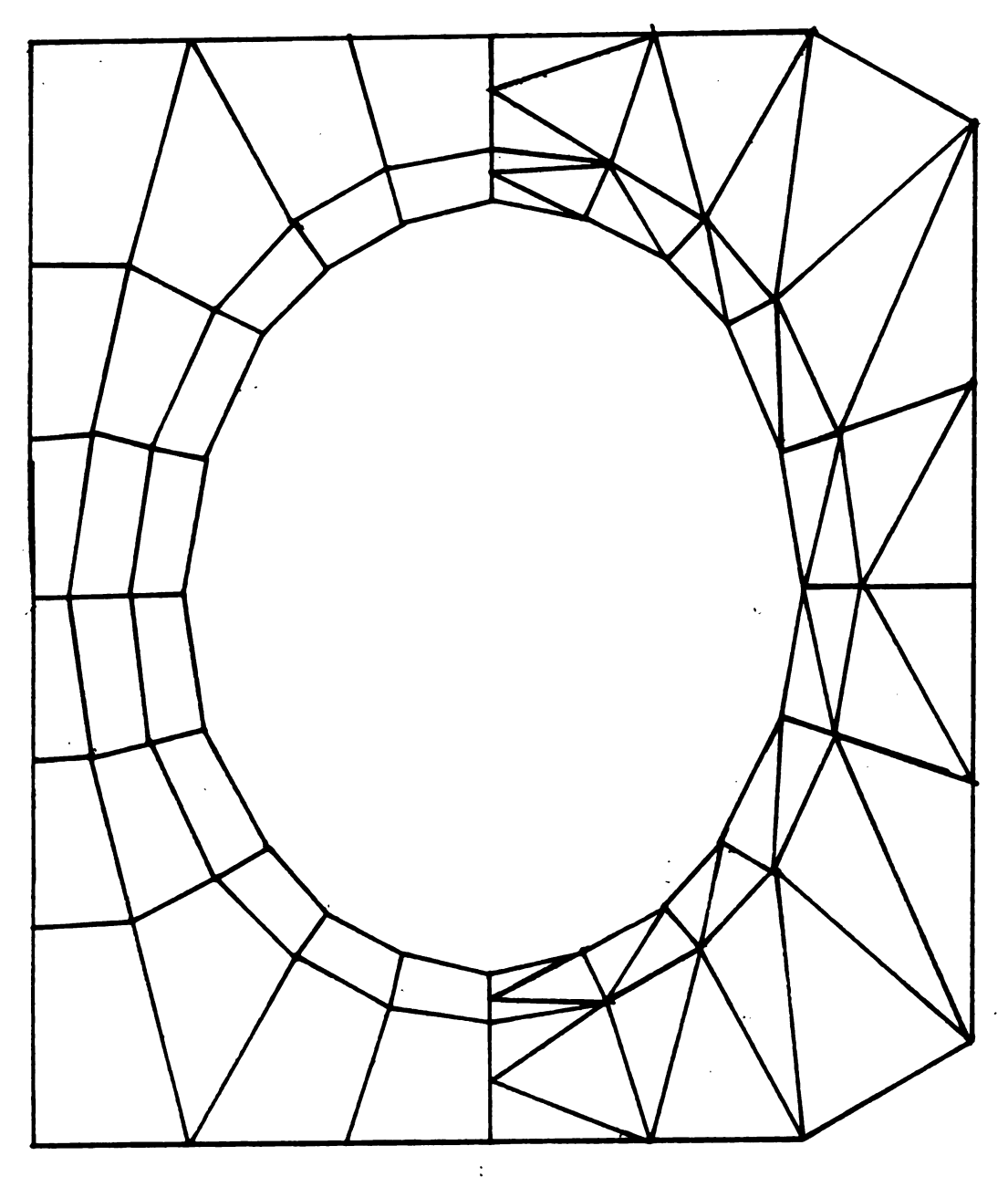


FIGURE 3-4: FINITE ELEMENTS AROUND THE CONDUIT

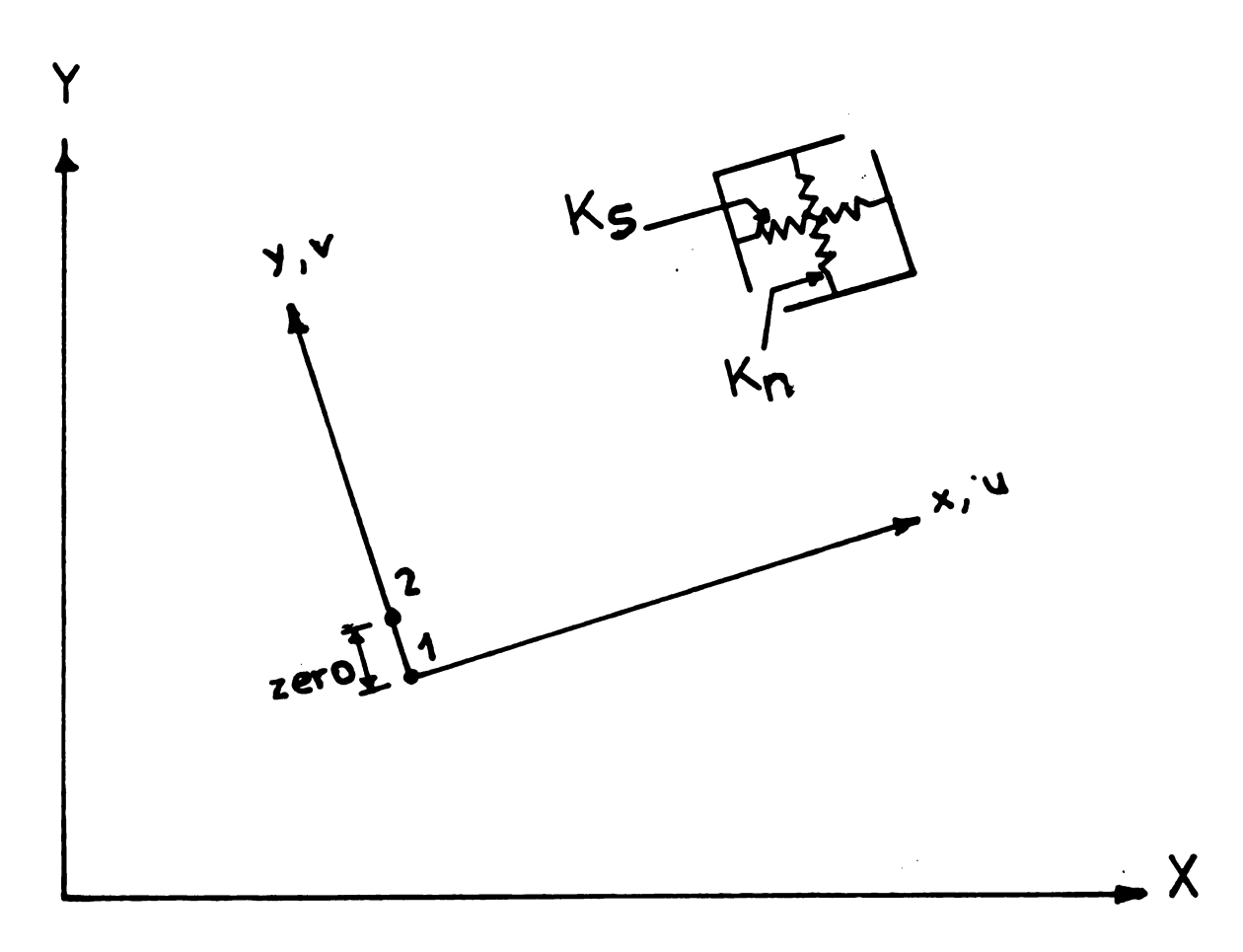


FIGURE 3-5: INTERFACE ELEMENT

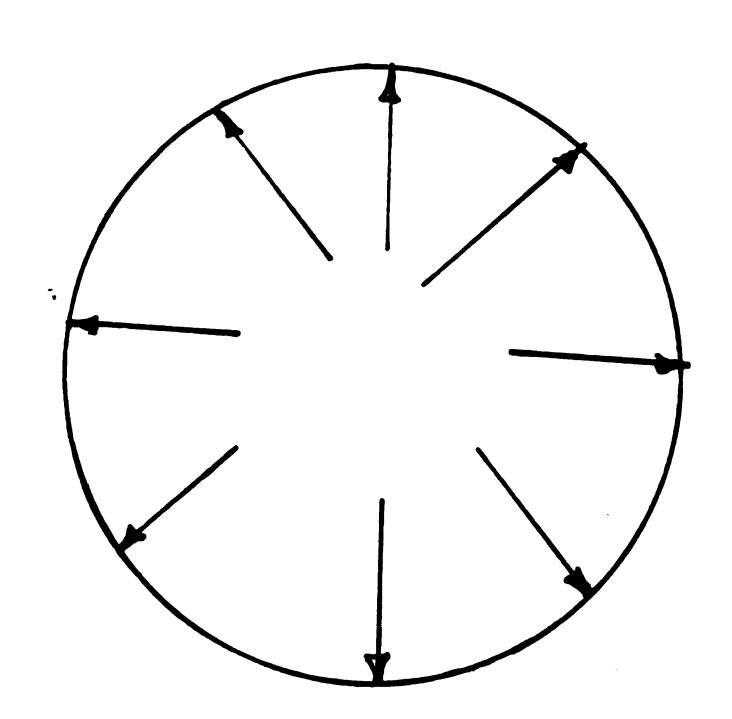


FIGURE 3-6: LOADING SCHEME

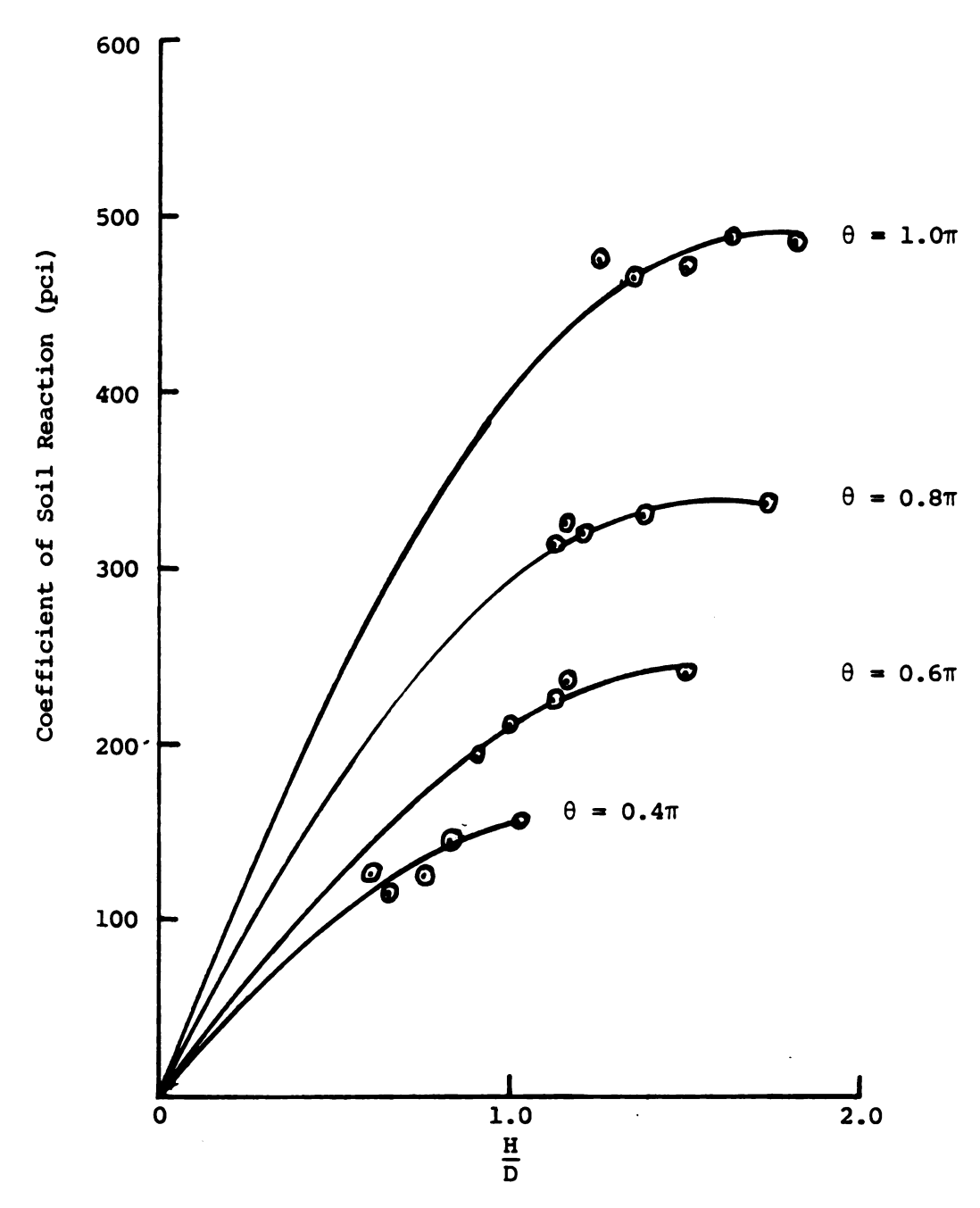


FIGURE 3-7: VARIATION OF COEFFICIENT OF SOIL REACTION WITH DEPTH (300 INCH SPAN)

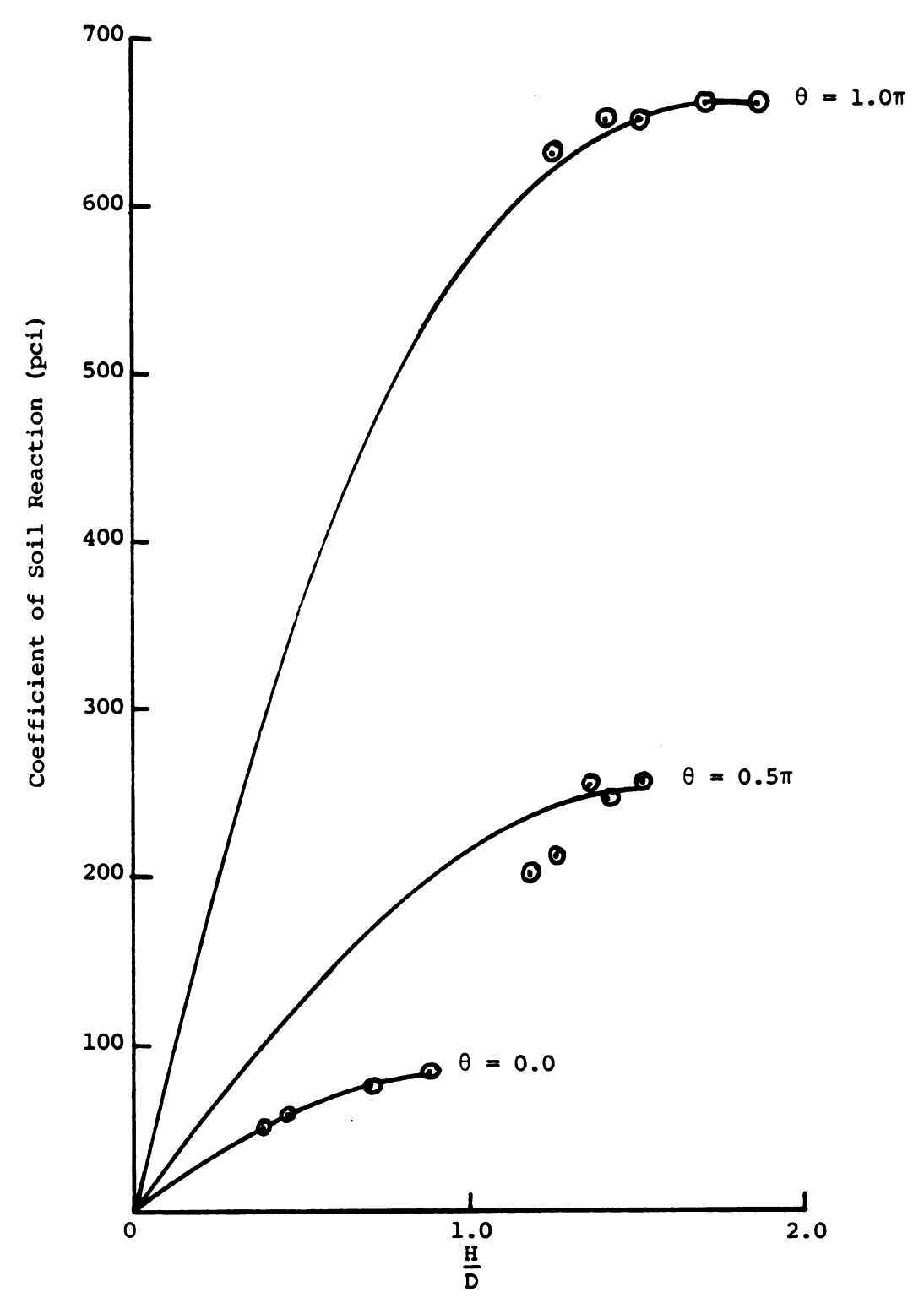


FIGURE 3-8: VARIATION OF COEFFICIENT OF SOIL REACTION WITH DEPTH (200 INCH SPAN)

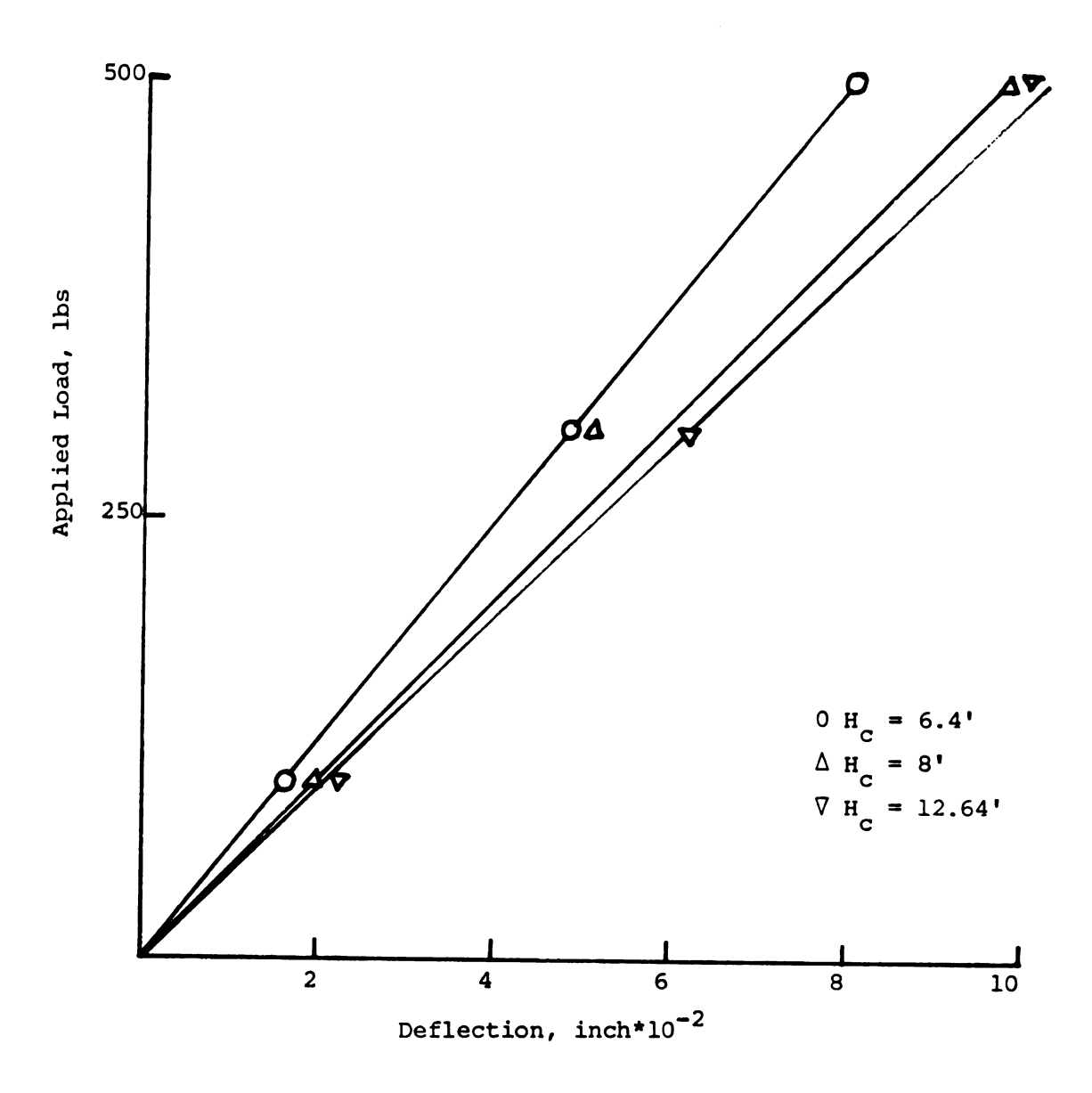


FIGURE 3-9: LOAD-DEFLECTION CURVE

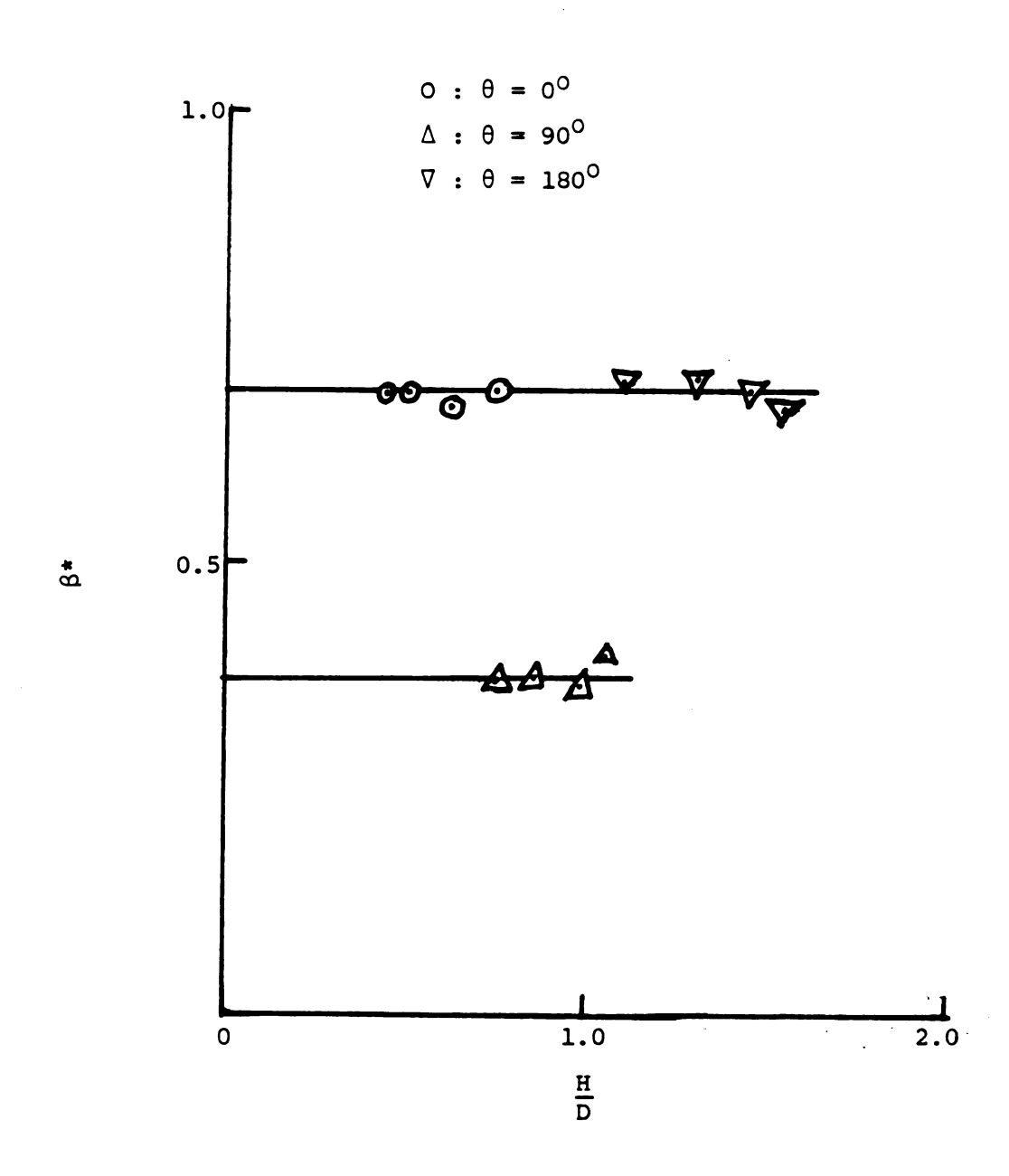


FIGURE 3-10: VARIATION OF β^* with $\frac{H}{D}$.

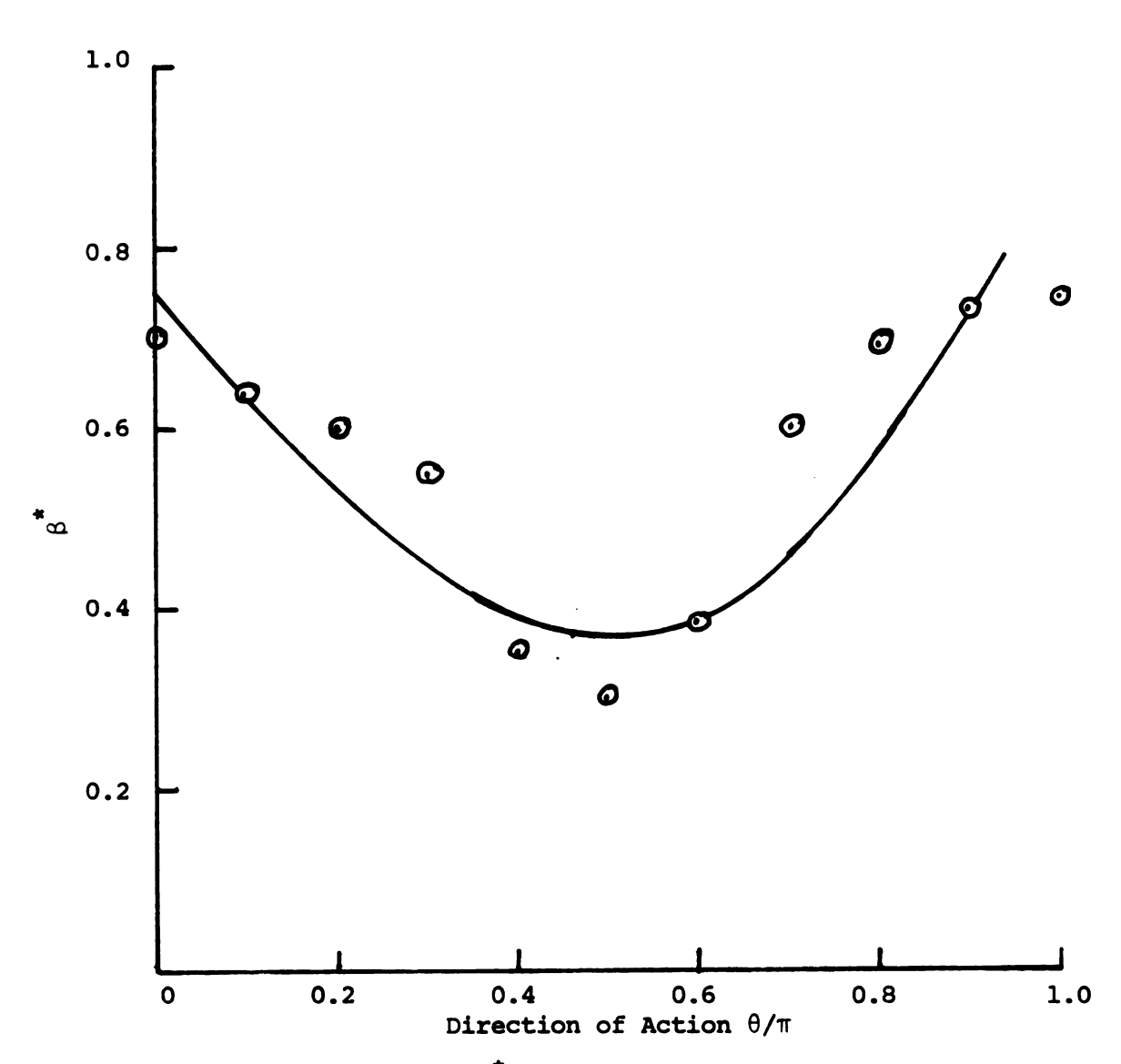


FIGURE 3-lla: VARIATION OF β^{\bigstar} WITH θ FOR 300 INCH SPAN

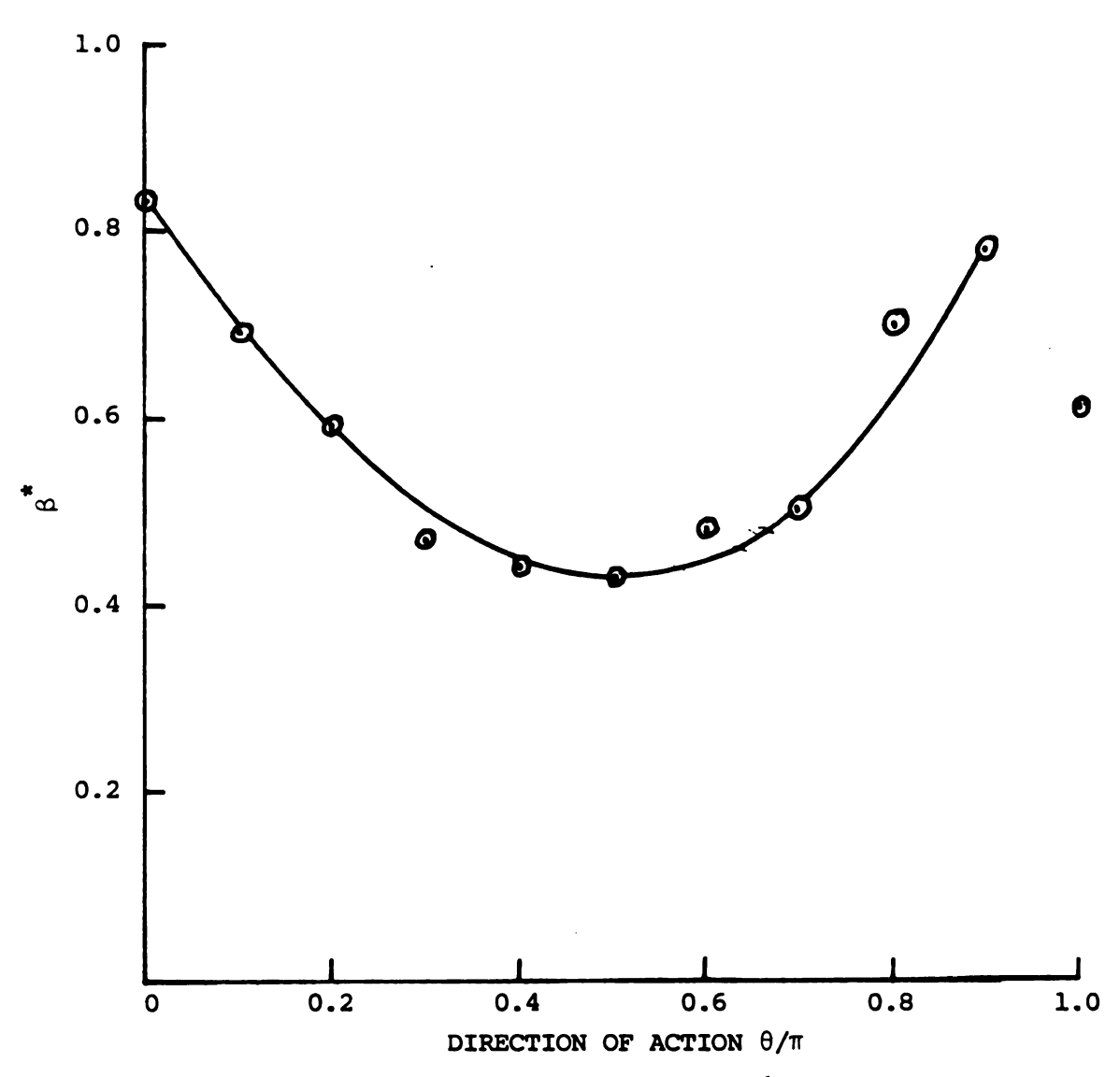
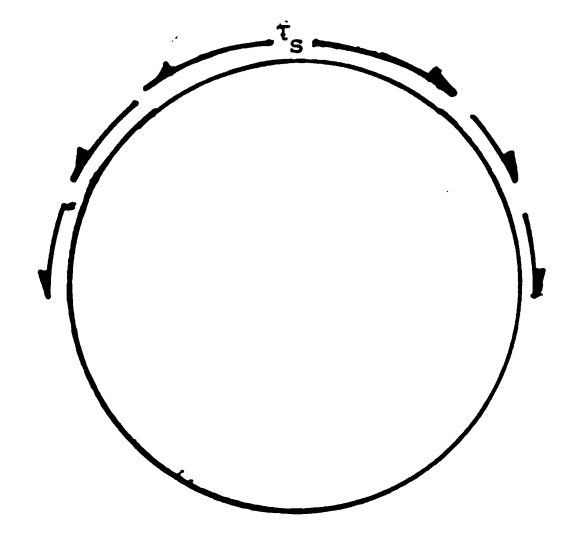
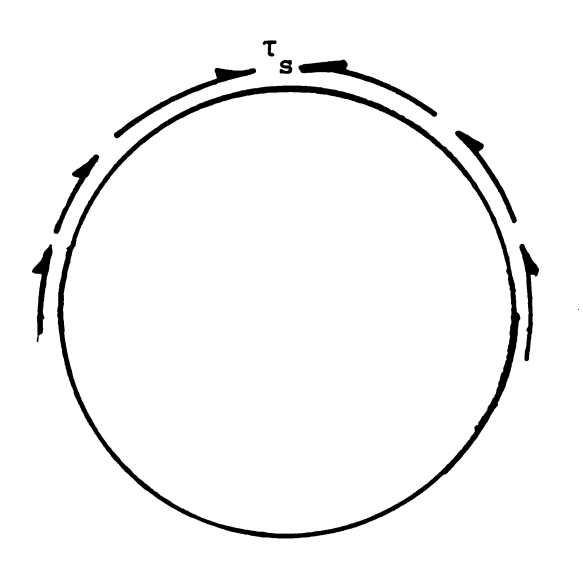


FIGURE 3-11b: VARIATION OF β^* WITH θ FOR 200 INCH SPAN



(a) Due to Loading



(b) Due to Deformation

FIGURE 4-1: SHEAR INTERACTION MODEL (AFTER KLOPPEL AND GLOCK, 1970).

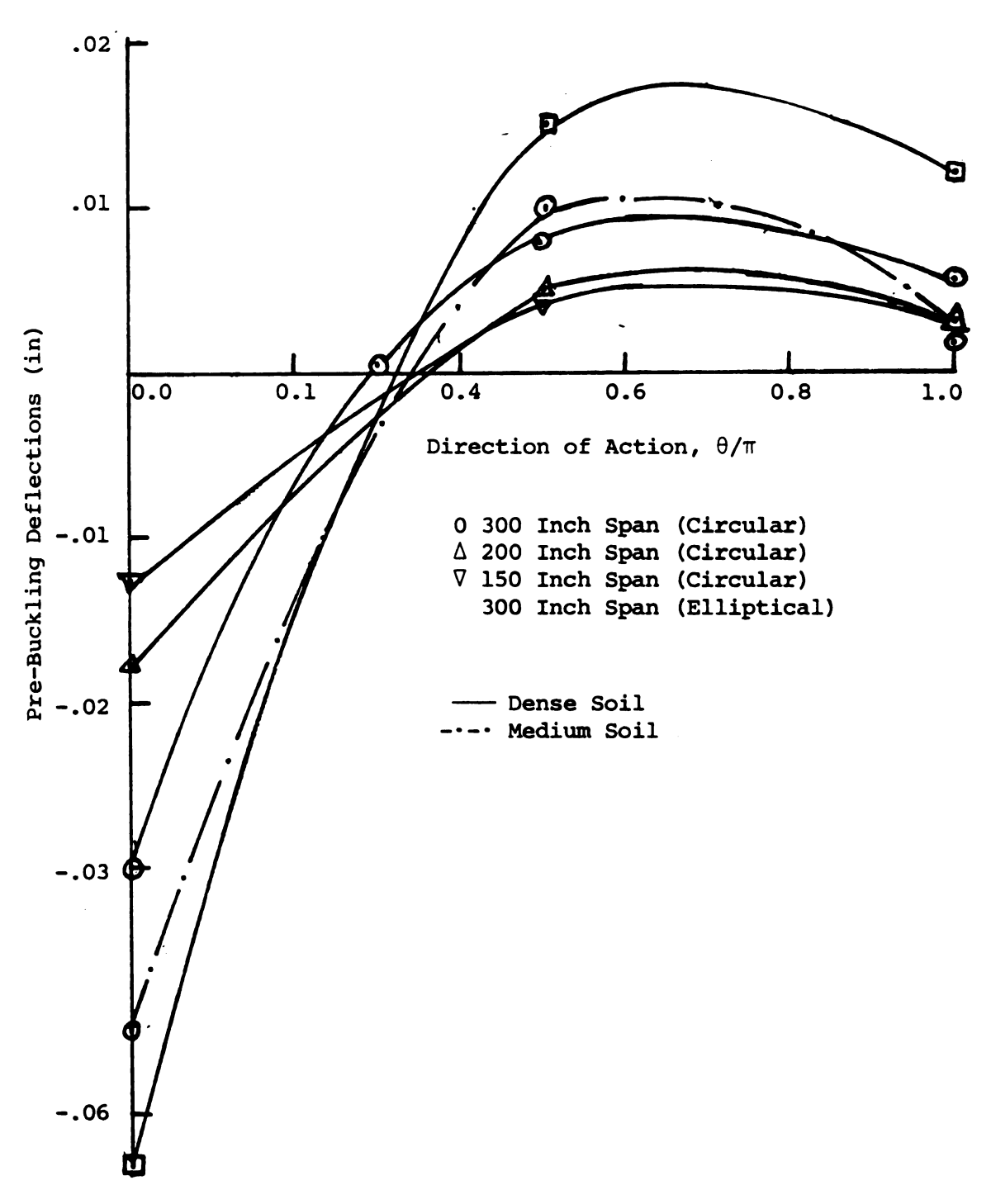
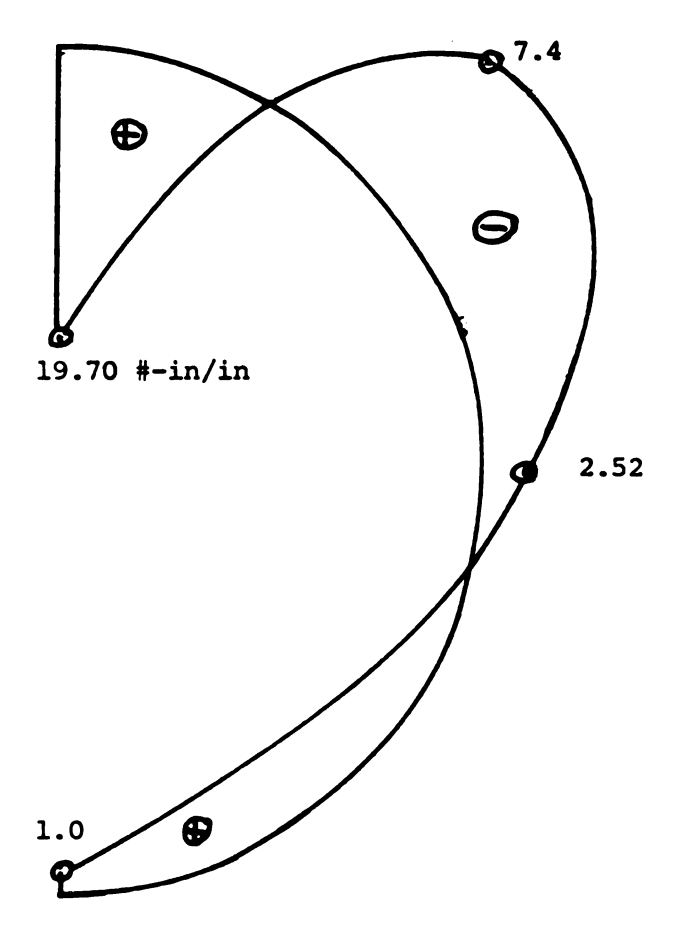


FIGURE 4-2: VARIATION OF THEORETICAL PRE-BUCKLING DEFLECTION WITH θ



300 Inch Span (Circular)
Dense Soil

FIGURE 4-3: VARIATION OF MOMENTS AROUND CONDUIT (TYPICAL)

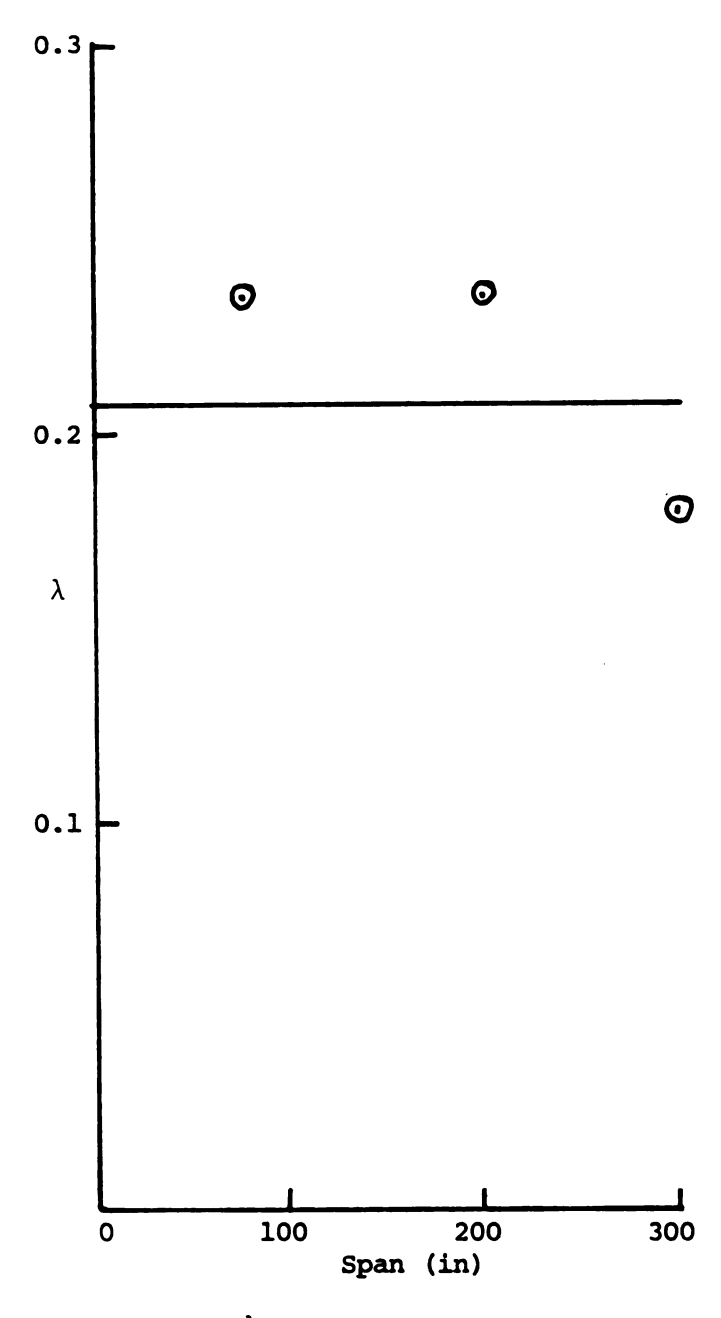


FIGURE 4-4: VARIATION OF λ WITH SPAN

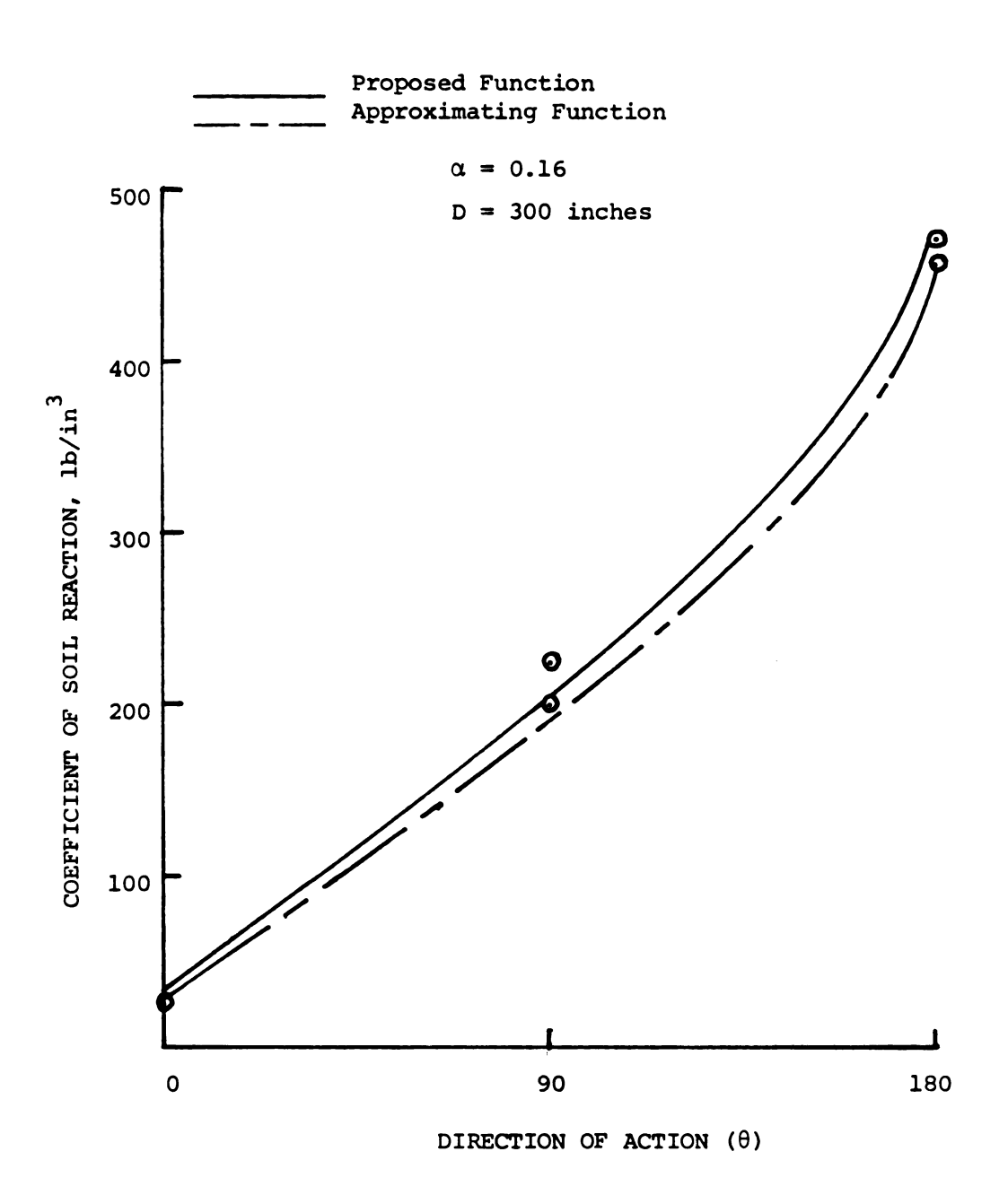


FIG. 4-5: VARIATION OF COEFFICIENT OF SOIL REACTION AROUND CONDUIT (CIRCULAR, DENSE).

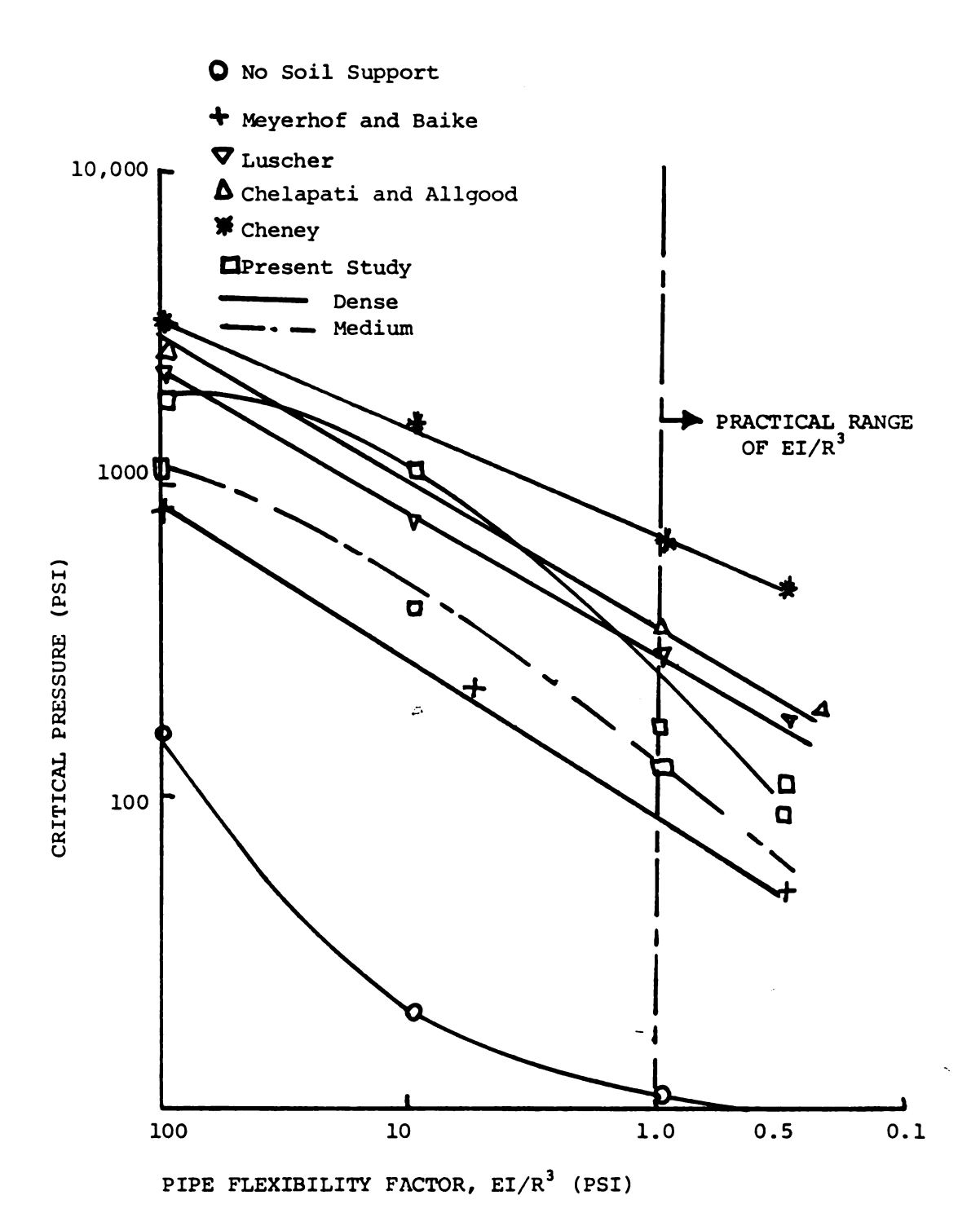


FIGURE 4-6a: COMPARISON OF THEORETICAL BUCKLING PRESSURES (CIRCULAR).

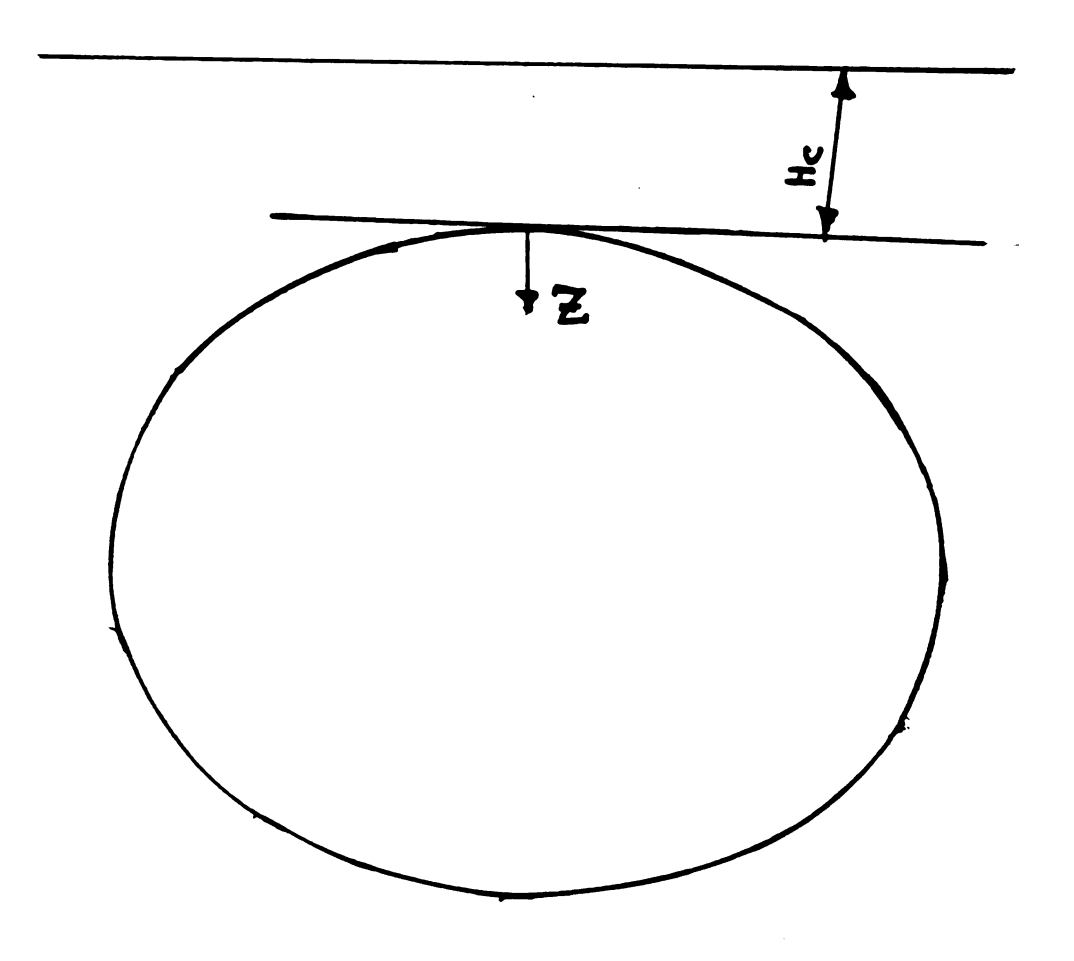


FIGURE (4-6b): ELLIPTICAL CONDUITS.

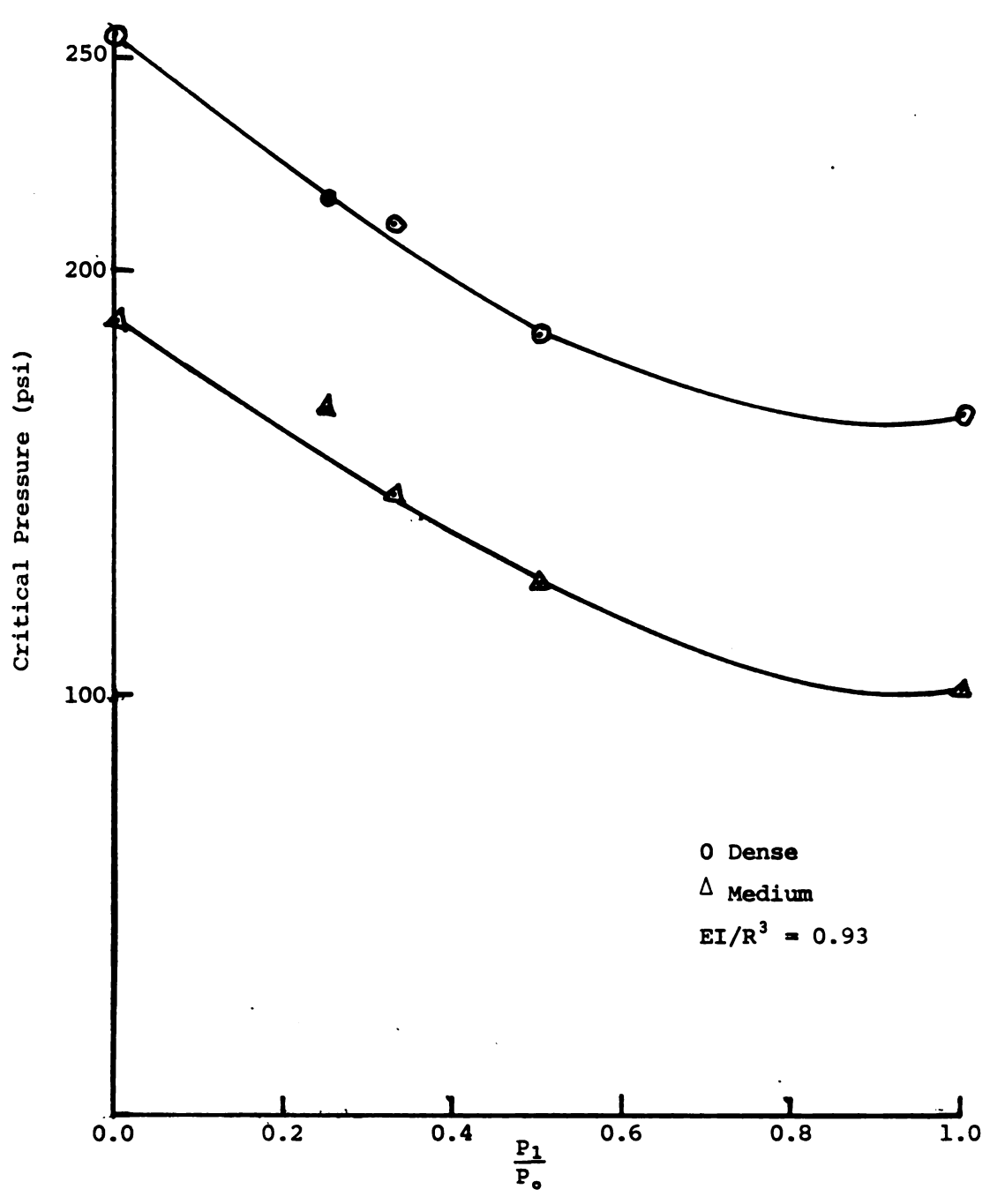


FIGURE 4-7: VARIATION OF CRITICAL PRESSURE WITH P_1/P_o

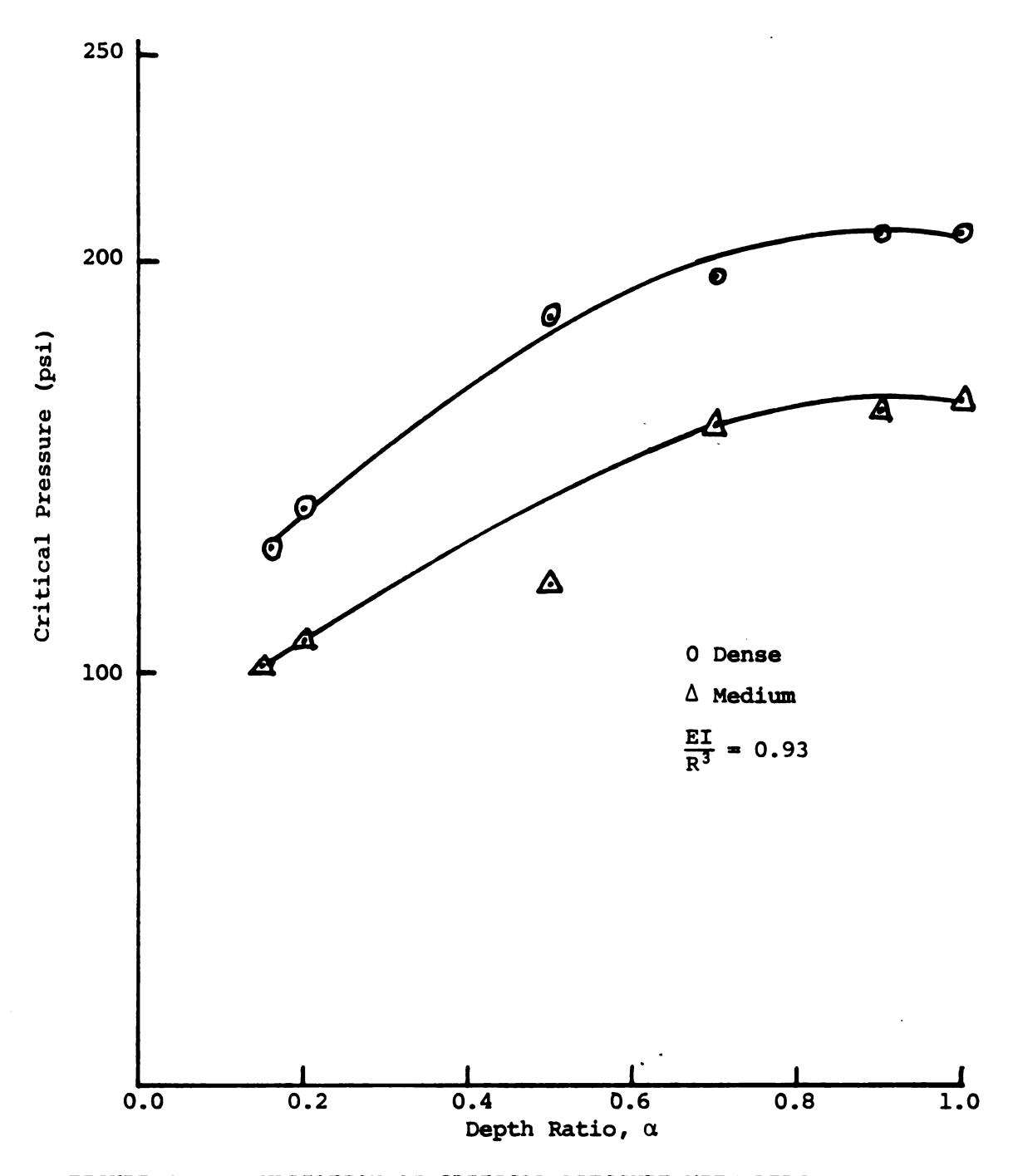


FIGURE 4-8: VARIATION OF CRITICAL PRESSURE WITH DEPTH

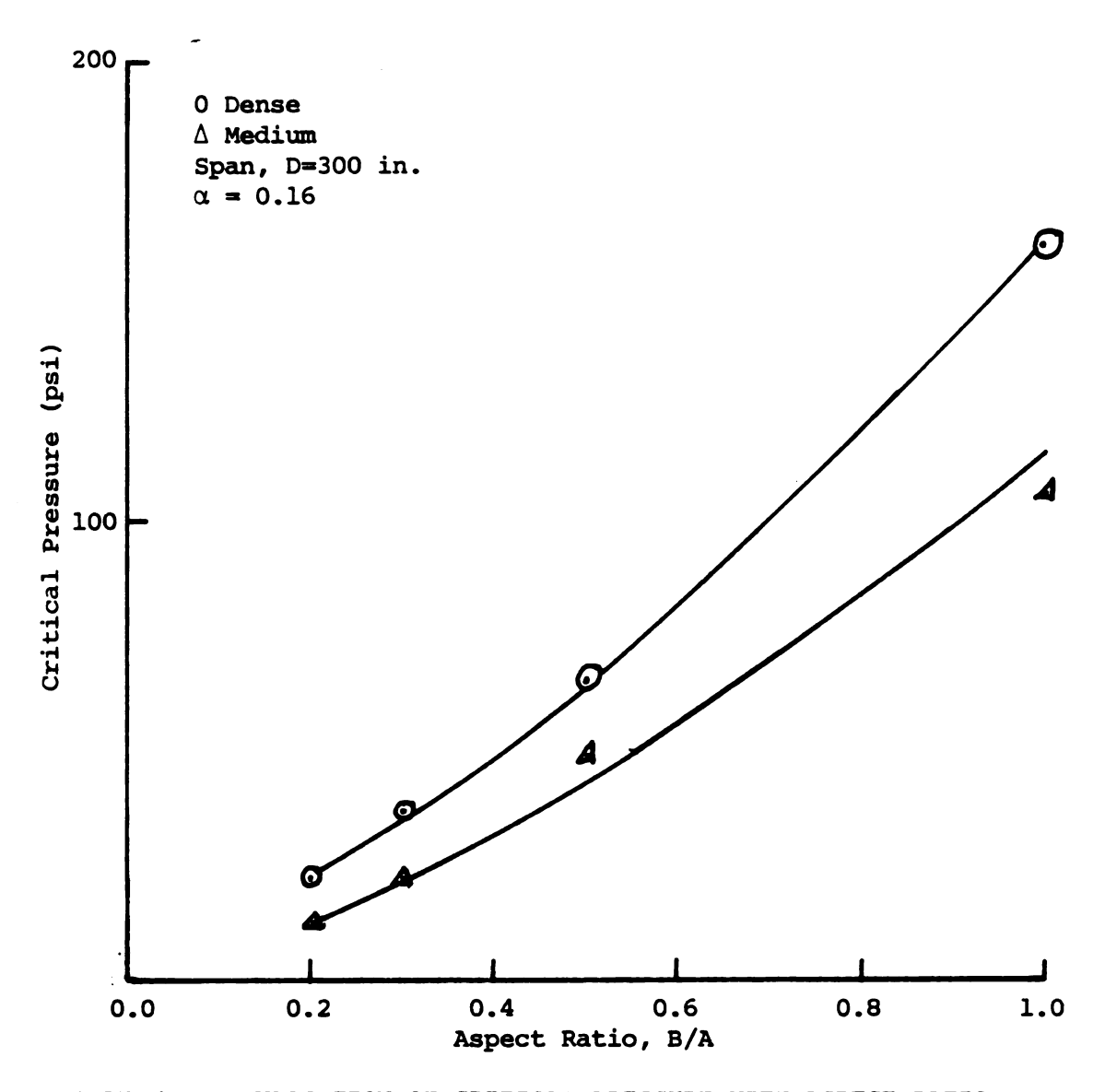


FIGURE 4-9: VARIATION OF CRITICAL PRESSURE WITH ASPECT RATIO (ELLIPTICAL SECTION)

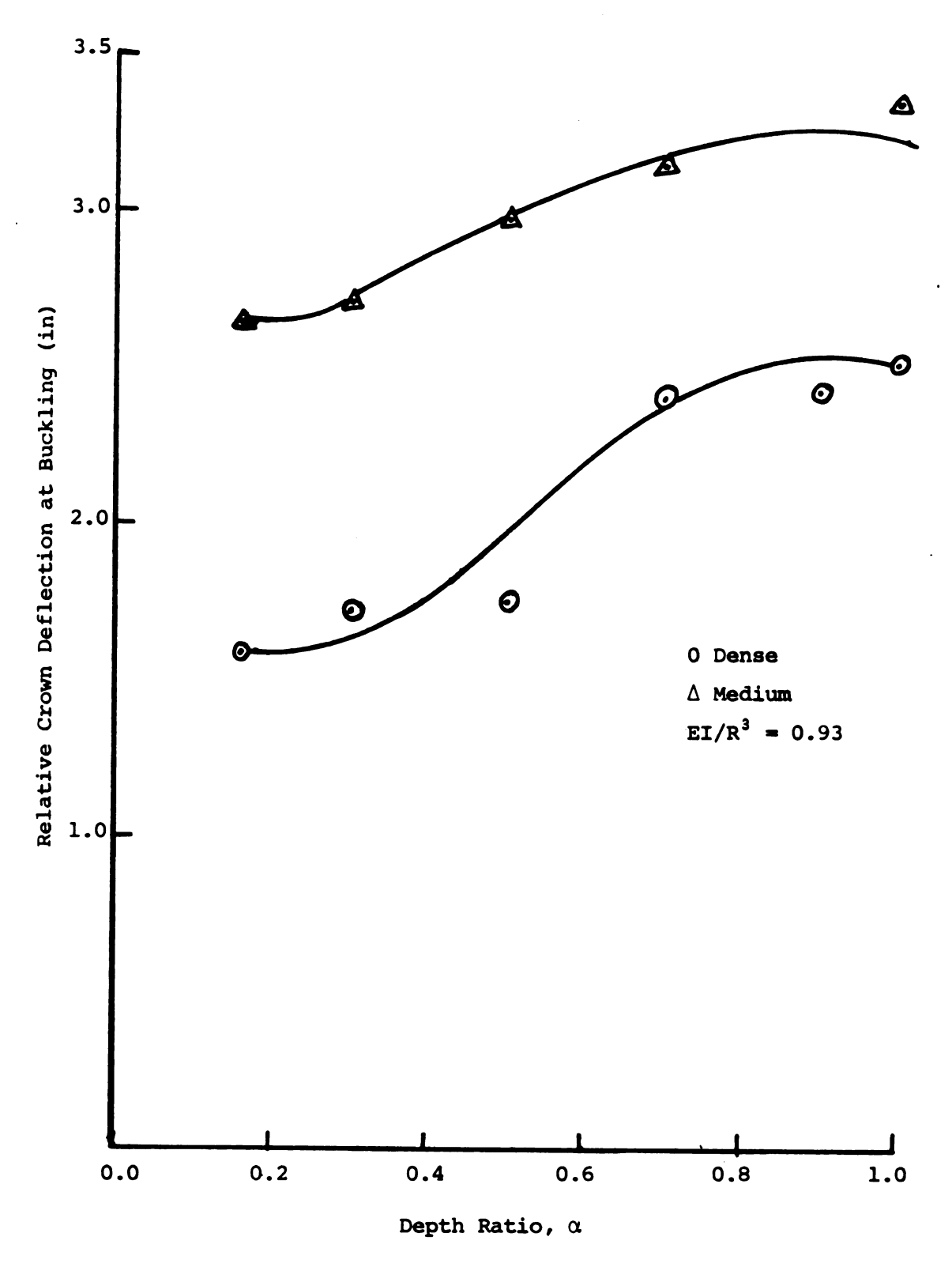


FIGURE 4-10a: VARIATION OF RELATIVE CROWN DEFLECTION AT INITIATION OF BUCKLING WITH DEPTH.

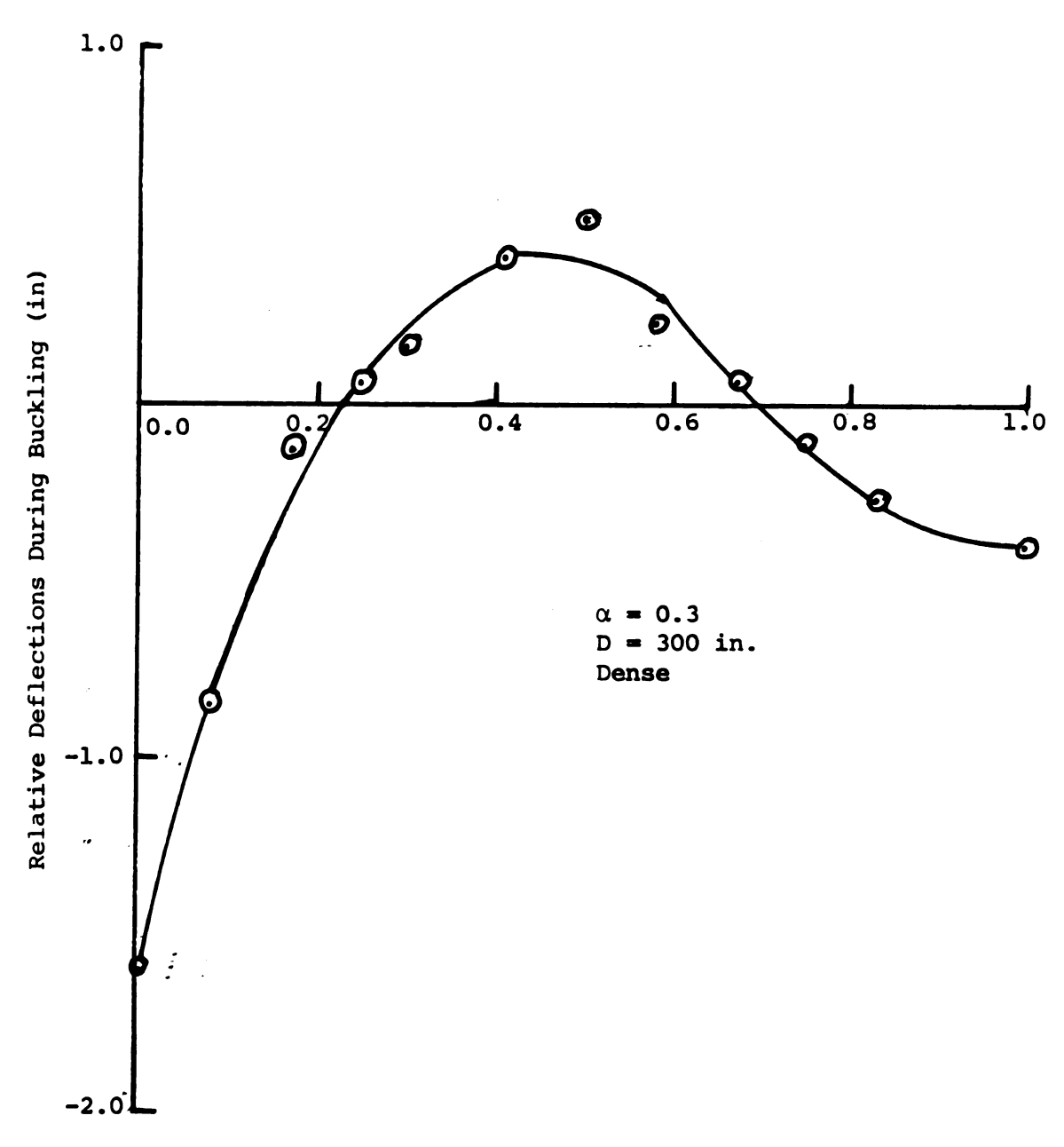


FIGURE 4-10b: APPROXIMATE BUCKLING CONFIGURATION (TYPICAL)

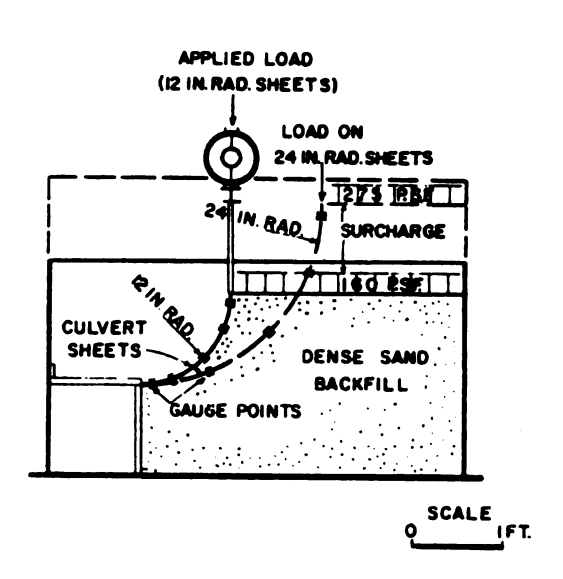


FIGURE 4-11: Meyerhoff and Baike's Loading Tests.

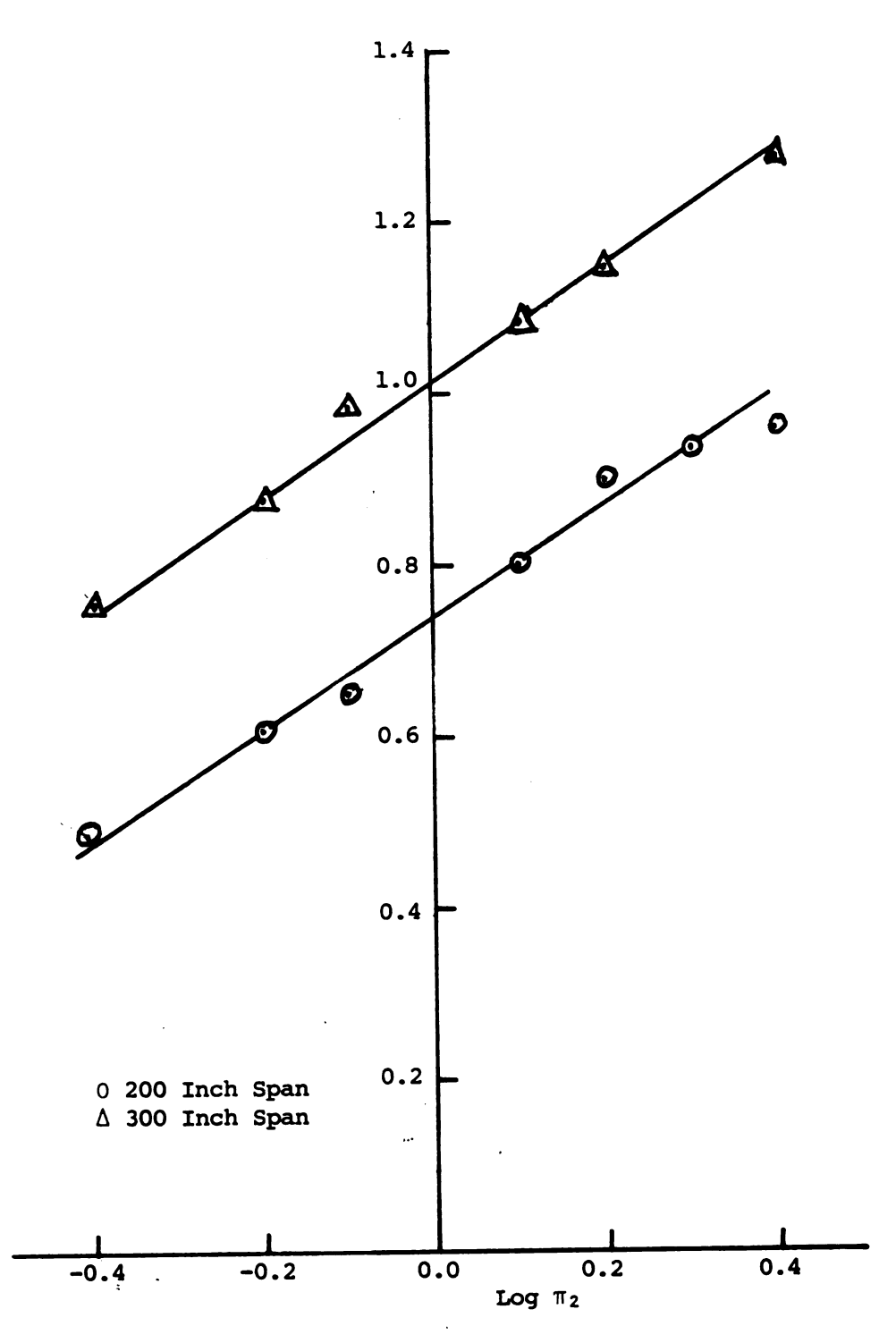
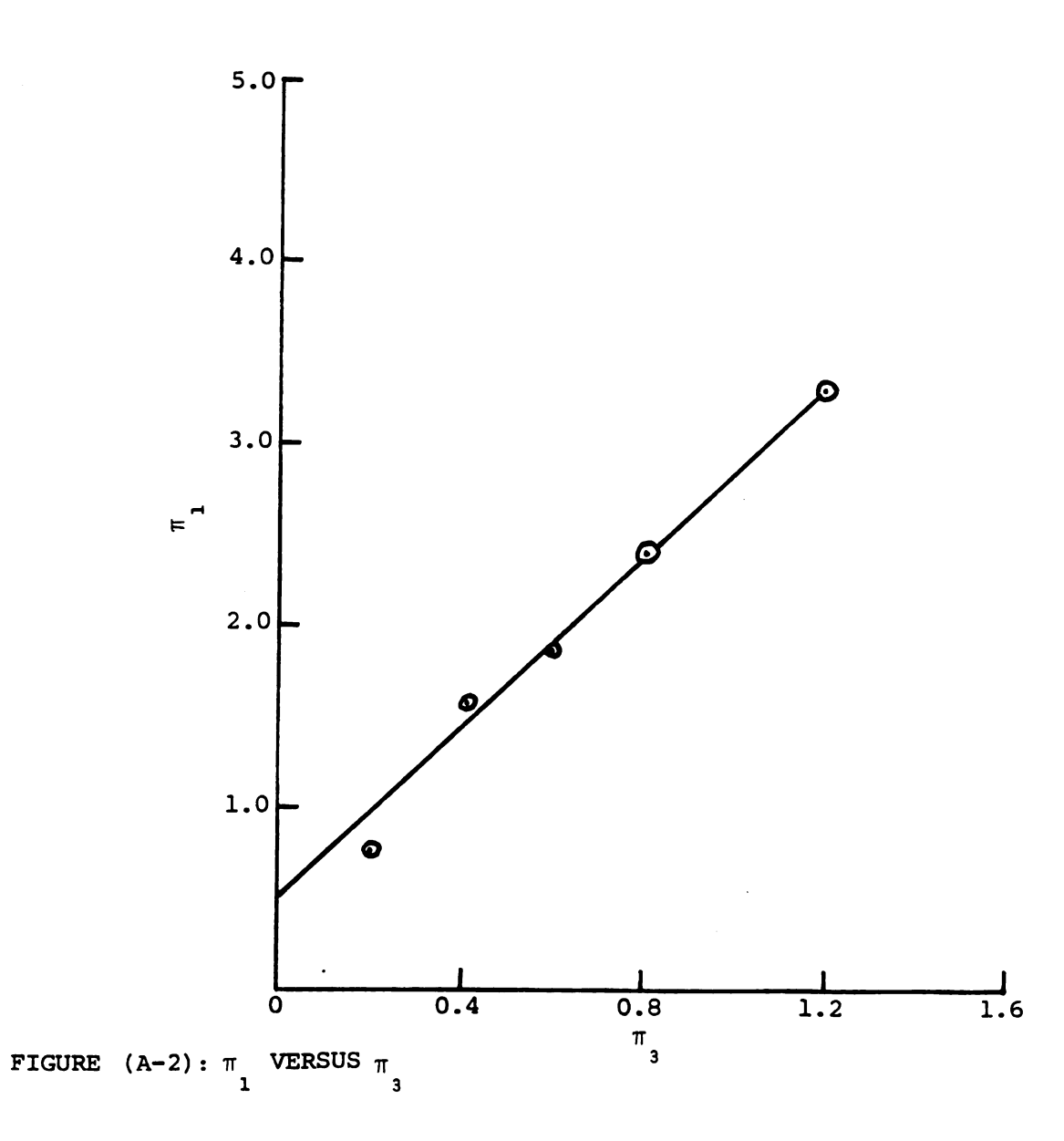


FIGURE (A-1): LOG π_1 VERSUS LOG π_2



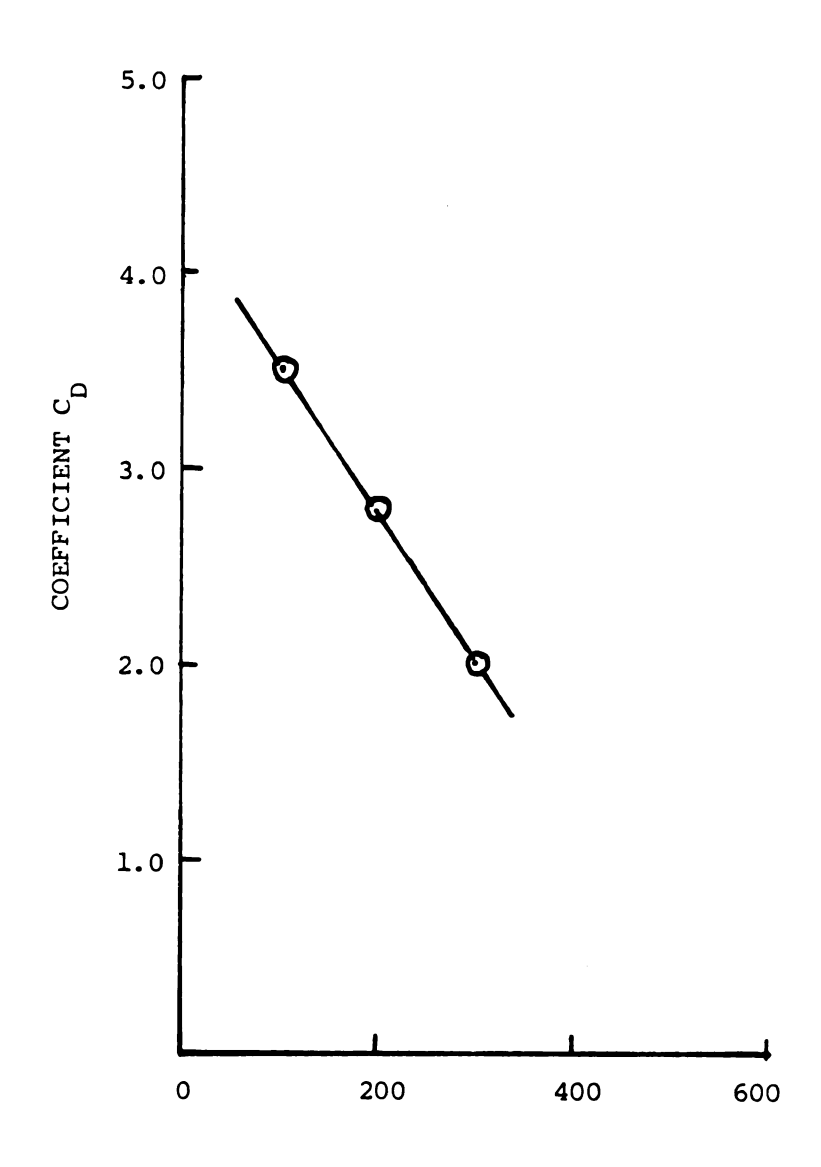


Figure A-3: variation of $\mathbf{C}_{\mathbf{D}}$ with span

-h. (i :):

APPENDIX A

APPENDIX A

THEORY OF DIMENSIONAL ANALYSIS

The theory of dimensional analysis is a useful tool in designing an experimental investigation, developing equations from a collection of data, and establishing the principles of model design, operation and interpretation. It is based on two fundamental axioms:

- (1) Absolute numerical equality exists only when the quantities concerned are similar qualitatively. That is, for a general relationship to exist between two quantities they must have the same dimensions (28).
- (2) The ratio of the magnitudes of two like quantities is independent of the units used in their measurement, provided that the same units are used for evaluating each (28).

These two axioms lead directly to an important theorem.

THEOREM 1:

Let α be some quantity which we wish to predict (also called a secondary quantity); and let a_i , i=1, n be a set of those quantities which affect the magnitude of α (the a_i are called primary quantities). If $\alpha = f$ (a_1, a_2, \ldots, a_n) , then

$$\alpha = C_{\alpha} a_1^{c_2} a_2^{c_2} \dots a_n^{c_2}$$
 (A.1)

where:

C_{\(\text{o}\)} = Dimensionless coefficient

C;, i=1, n = Dimensionless exponents

The theorem is proved by considering two systems of the same kind but different in magnitude.

That is:

$$\alpha = f(a_1, a_2, \dots, a_n)$$
 lst system
$$(A.2 a-b)$$
 $\beta = f(b_1, b_2, \dots, b_n)$ 2nd system

where β and b_1 , b_2 , . . ., b_n are the secondary and primary quantities respectively of the second system and a_i are the same as b_i except in magnitude.

Expressing the above equations in a different unit of measurement, we may write:

$$\alpha^{f} = f(x_1 a_1, x_2 a_2, \dots, x_n a_n)$$

$$\beta' = f(x_1 b_1, x_2 b_2, \dots, x_n b_n)$$
(A.3 a-b)

where x_i are the ratios of the magnitudes of the two systems of units employed. Then from axiom (2) we get:

$$\frac{\alpha'}{\alpha} = \frac{\beta'}{\beta}$$
or $\alpha' = \frac{\alpha\beta'}{\beta}$
(A.4)

Substituting into (A.3) we get:

$$f(x_{1}^{a}, x_{2}^{a}, \dots, x_{n}^{a}) =$$

$$\frac{f(a, a, \dots, a)}{f(b_{1}, b_{2}, \dots, b_{n})} f(x_{1}^{b}, x_{2}^{b}, \dots, x_{n}^{b})$$

(A.5)

(A.6)

Differentiating (A.5) with respect to x:

$$\frac{\frac{a_{1} + \frac{a_{1} + \frac{a_{2} + \cdots + \frac{a_{n}}{n}}{a_{1}}}{\frac{\partial (x_{1} + x_{1})}{a_{1}}}}{\frac{f(a_{1}, a_{2}, \dots, a_{n})}{F(b_{1}, b_{2}, \dots, b_{n})}} = \frac{\frac{f(a_{1}, a_{2}, \dots, a_{n})}{\frac{\partial f(x_{1} + \frac{a_{1}}{n}, x_{2}, \dots, x_{n}, x_{n})}{\frac{\partial f(x_{1} + \frac{a_{1}}{n}, x_{2}, \dots, x_{n}, x_{n})}{\frac{\partial (x_{1} + \frac{a_{1}}{n}, x_{2}, \dots, x_{n}, x_{n})}{\frac{\partial (x_{1} + \frac{a_{1}}{n}, x_{2}, \dots, x_{n}, x_{n}, x_{n})}{\frac{\partial (x_{1} + \frac{a_{1}}{n}, x_{2}, \dots, x_{n}, x$$

Now let all the x's equal unity. [That is, we are restricting them to the same set of units. This should not hurt the generality of the proof.]

Thus:

$$\frac{a_{1} \frac{\partial f(a_{1}, a_{2}, \dots, a_{n})}{\partial (a_{1})} = \frac{f(a_{1}, a_{2}, \dots, a_{n})}{f(b_{1}, b_{2}, \dots, b_{n})} = \frac{\partial f(b_{1}, b_{2}, \dots, b_{n})}{\partial (b_{1})}$$
(A.7)

Separating the variables:

$$\frac{\frac{\partial f(b_{1}, b_{2}, \dots, b_{n})}{\partial b_{1}}}{f(b_{1}, b_{2}, \dots, b_{n})}$$

(A.8)

For any given value of b_i , the right-hand side of (A.8) is a constant and may be designated as C_i .

$$a_{1} \frac{\partial f(a_{1}, a_{2}, \ldots, a_{n})}{\partial a_{1}} = C_{1}$$

$$f(a_{1}, a_{2}, \ldots, a_{n})$$

Rearranging:

$$\frac{\partial f(a_1, a_2, \dots, a_n)}{f(a_1, a_2, \dots, a_n)} = C_1 \frac{\partial a_1}{a_1}$$

(A.9)

Integrating:

$$\log_{e(1)} f(a_1, a_2, \dots, a_n) = C_1 \log_{e(1)} (da_1)$$

where d_1 is a constant of integration. If the same procedure is carried out in succession by differenting (A.5) with respect to x_2, x_3, \ldots, x_n , a set of particular solutions will result:

$$\ln_{(2)} f(a_1, a_2, \dots, a_n) = C_2 \ln(d_2 a_2)$$

$$\ln_{(3)} f(a_1, a_2, \dots, a_n) = C_3 \ln(d_3 a_3)$$

$$\vdots$$

$$\ln_{(n)} f(a_1, a_2, \dots, a_n) = C_n \ln(d_n a_n)$$

where the subscript 1, 2, 3, . . ., n denote that (A.5) is differented with respect to x_1 , x_2 , . . ., x_n .

The complete solution is obtained by summing all the particular solutions.

Hence:

$$\ln f(a, a, \ldots, a_n) = \\
\ln f(d_1 a_1)^{C_1} (d_2 a_2)^{C_2} \ldots (d_n C_n)^{C_n} \\
\text{or} \\
f(a_1, a_2, \ldots, a_n) = \\
(d_1^{C_1} d_2^{C_2} \ldots d_n^{C_n}) a_1^{C_1} a_2^{C_2} \ldots a_n^{C_n} \\
= C_{\alpha} a_1^{C_1} a_2^{C_2} \ldots a_n^{C_n} \tag{A.10a}$$

Hence, the result of interest is:

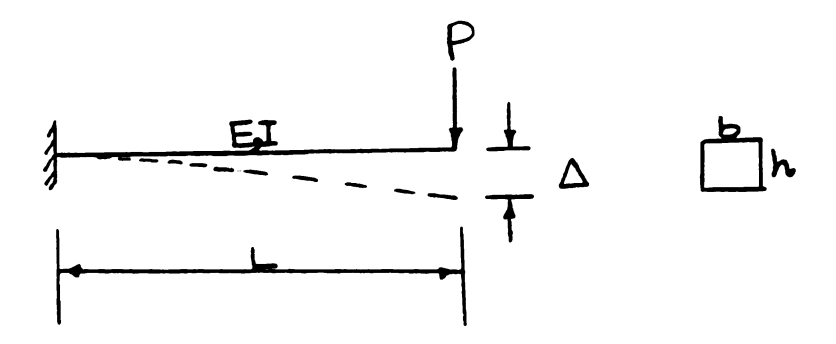
$$f(a_1, a_2, ..., a_n) = C_{\alpha} a_1^{C_1} a_2^{C_2} ..., a_n^{C_n}$$
 (A.10b)

That is, any measurable phenomenon may be evaluated in terms of the factors causing it. The application of Dimensional Analysis therefore reduces to the problem of trying to identify all the primary quantities and then finding the dimensionless exponents. To facilitate this, the Buckingham Π - theorem is often quite useful.

THEOREM 2: BUCKINGHAM II - THEOREM

The number of dimensionless products S in a complete set is equal to the total number of variables n minus the rank r, of their dimensional matrix. [The rank of the dimensional matrix is also equal to the number of the basic dimensions involved, and the two are often used interchangeably.]

The theorem is best illustrated with an example. Consider the case of a cantilever beam loaded by P located at the end of the beam as shown.



Suppose we wish to find the deflection Δ at the end of the beam. We begin by identifying the primary quantities. Thus we write:

$$\Delta = f(p, L, b, h, E)$$

where:		Dimension
	Δ = required deflection	L
	P = applied force	F
	L = length of beam	L
	b = width of beam	L
	h = height of beam	L

E = modulus of elasticity of beam material

There are six variables (Δ , P, L, b, h, E) and with only two fundamental dimensions (F, L) Buckingham's theory yields four independent terms (also called Π - terms).

By theorem (1) we write:

and in terms of their dimensions

These may be arranged in a matrix form:

			C			
F	0	1	0	0	0	1
L	1	1 0	1	1	1	-2

Such a matrix is called the "dimensional matrix". It can be easily verified that the rank of the matrix equals the number of fundamental dimensions used (in this case r=2). Thus we can choose to solve for any r (=2) independent (Π) terms in terms of the rest. Suppose we choose to solve for c_2 , and c_3 in terms of c_4 , c_5 , and c_6 .

From equation (A.llb), by equating identical exponents, we arrive at a system of simultaneous equations in the exponents c_i:

F:
$$c_2 + c_5 = 0$$
 (A.12)

L:
$$c + c + c + c - 2c = 0$$
 (A.13)

We then set c = 1, c = c = c = 0 and solve for c and c. Hence, from (A.12),

$$c_2 + 0 = 0$$
, or $c_2 = 0$

and from (A.13),

$$1 + c_3 = 0$$
, or $c_3 = -1$

Thus,

$$\Pi_{1} = \Delta^{c_{1}} P^{c_{2}} L^{c_{3}} b^{c_{4}} h^{c_{5}} E^{c_{6}} = \Delta^{1} P^{0} L^{-1} b^{0} h^{0} E^{0} = \frac{\Delta}{r}$$

Proceeding in the same manner, that is setting c = 1, c = c = c = 0, etc., we get:

$$II_2 = \frac{b}{L}$$

$$\Pi_3 = \frac{h}{L}$$

$$\Pi_{L} = \frac{EL^{4}}{P}$$

The various Π - terms may now be combined, by theorem 1, into a functional relationship.

Hence,

$$\Pi_{1} = f(\Pi_{2}, \Pi_{3}, \Pi_{4})$$

or,

$$\frac{\Delta}{L} = f \left(\frac{b}{L}, \frac{h}{L}, \frac{EL^2}{P} \right) \tag{A.14}$$

Any number of Π - terms may be transformed by means of multiplication and/or division only, provided their dimensionless character is unaltered. Performing this operation in equation (A.14) we finally get:

$$\frac{\Delta}{L} = f\left(\frac{b}{L}, \frac{h}{b}, \frac{P}{EL^2}\right) \tag{A.15}$$

The exact nature of the relationship among the various Π - terms (equation (A.15)can only be established by means of a well-controlled experiment and/or some suitable analytical procedure. However, it is obvious that the number of independent quantities to be varied in an experiment has now been reduced from the original six to just

three. Further, any Π - term is considered varied if at least one of the parameters comprising the term is varied. Therefore the choice of which parameter to vary may be dictated by convenience, economy, and feasibility.

The appeal of the theory of dimensional analysis is that a thorough prior knowledge of the physics of the problem is, strictly speaking, not mandatory. Such knowledge, however, is quite useful. For example, if in the present beam-deflection problem, it is known apriori that the variables b and h may be combined into the moment of inertia I, $(I = \frac{1}{12} \text{ bh}^3 = L^4)$, the amount of rigor will be even much more reduced. A well-controlled experiment should then yield $\Delta = \frac{PL^3}{3EI}$, or something reasonably close, within the limits of experimental error.

DEVELOPMENT OF THE PREDICTION EQUATION

In Chapter III, the non-dimensional parameters were shown to be related by the equation:

$$\pi = f(\pi, \pi) \tag{A.16}$$

where:

$$\pi_1 = \frac{K}{\gamma}$$

$$\pi_2 = H/D$$

$$\pi_3 = \theta$$

Selected values of these are shown in Tables (A-1) and (A-2). If π is kept constant, π and π are seen to fit the equation

$$\pi_1 = C_d \pi_2^{\alpha^*} \tag{A.17}$$

where C_d and α^* may be functions of other salient parameters of the soil-steel structure (for example, the span).

Equation (A.17) is transformed to a logarithmic scale to give:

$$\log \pi_{1} = \log C_{d} + \alpha^{*} \log \pi_{2}$$
 (A.18)

This is easily recognized as the equation of a straight line with slope α^{\star} , and intercept $C_{\rm d}$ on the π_1 - axis.

Figure (A-1) is a plot of Log π versus π for diameters of 300 and 200 inches, and π held constant at 1.0 Π and 0.55 Π . Using the method of least squares, the following results are deduced for C_d and α^* :

Diameters (inches)	<u>c</u> a	<u>α*</u>
100	3.5	0.501
200	2.8	0.485
300	1.95	0.493

Hence, it is concluded that:

$$\pi_1 \approx C_d \sqrt{\frac{H}{D}}$$
 (A.19)

The same procedure is repeated for π with π held constant at 1.0 to give (Figure A-2):

$$\pi_1 \approx 0.5 \ (1+5.4 \ \frac{\theta}{\pi})$$
 (A.20)

Next C_{d} is plotted as a function of the span Figure (A-3) to give:

$$C_{d} = 4.25 - \frac{0.75D}{100}$$
 (A.21)

Finally, using the method described in (28) the above equations are combined to give the prediction equation:

$$\pi_{1} (\pi_{2}, \pi_{3}) \simeq \left[C_{d} \sqrt{\frac{H}{D}}\right] *0.5* \left[1+5.4 \frac{\theta}{\pi}\right]$$

$$0.5 \left[1+5.4 \frac{\theta}{\pi}\right]_{\theta=0.55_{\pi}}^{3-2}$$
(A.22)

That is,

$$\pi_{1} = \left[\frac{C_{d} \sqrt{\frac{H}{D}}}{4} \right] \left[\frac{1+5.4 \frac{\theta}{\pi}}{\pi} \right]$$
(A.23)

APPENDIX B

FLOW CHARTS FOR COMPUTER PROGRAMS

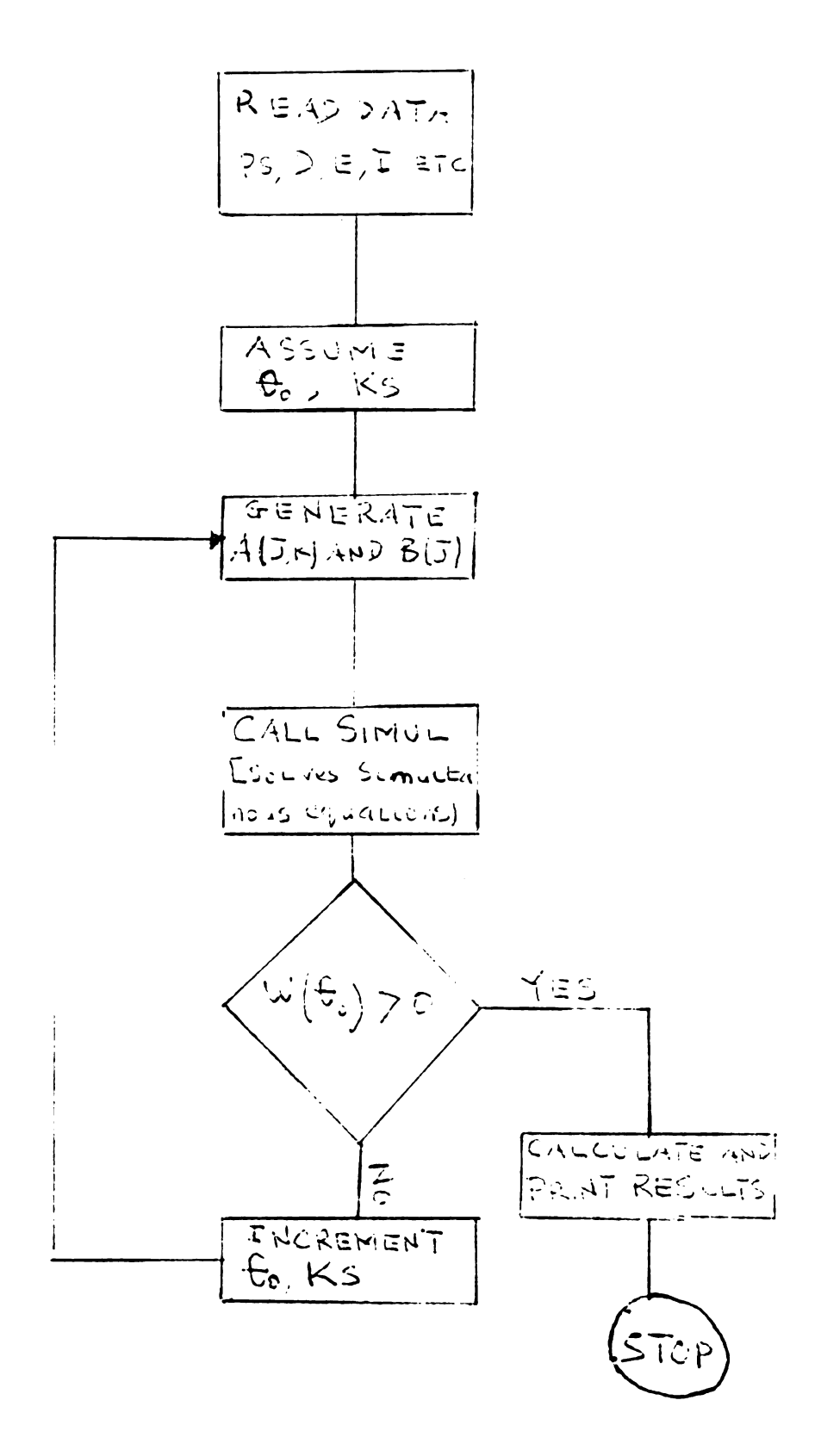


FIGURE B-1: FLOW CHART FOR PREBUCKLING ANALYSIS.

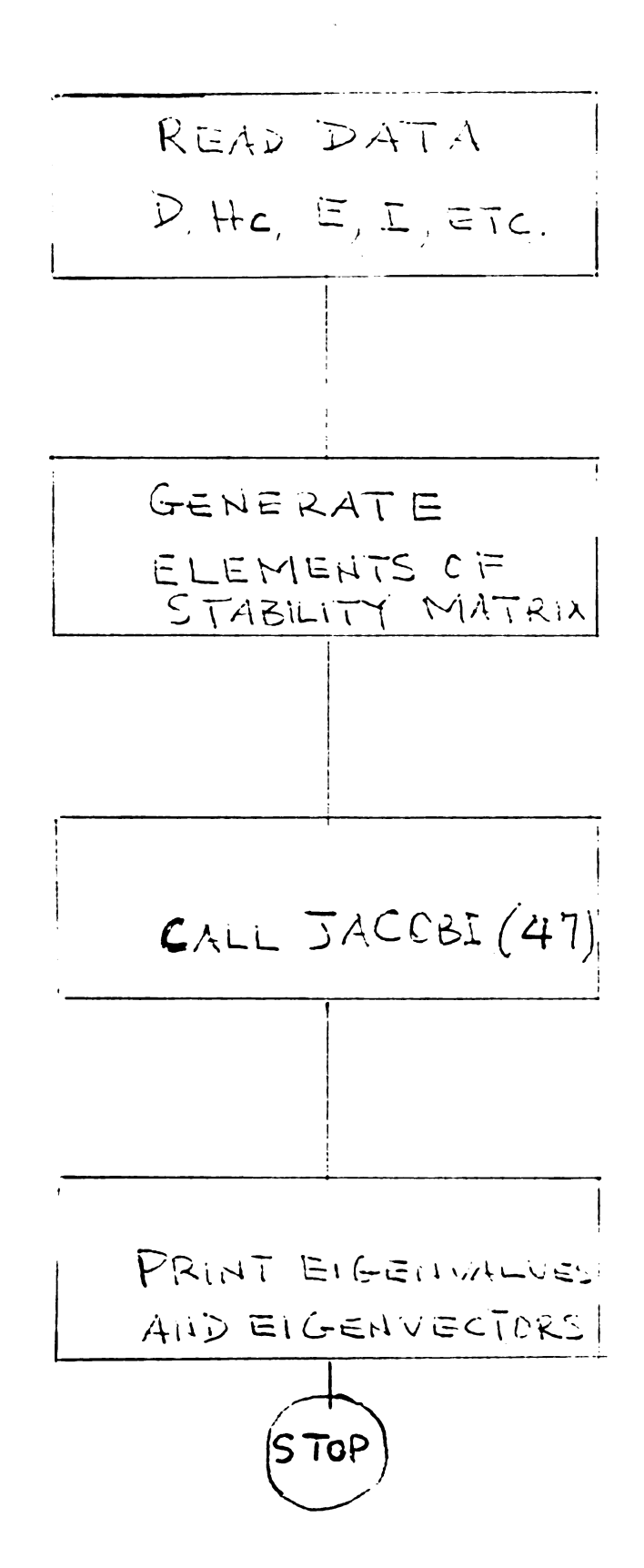
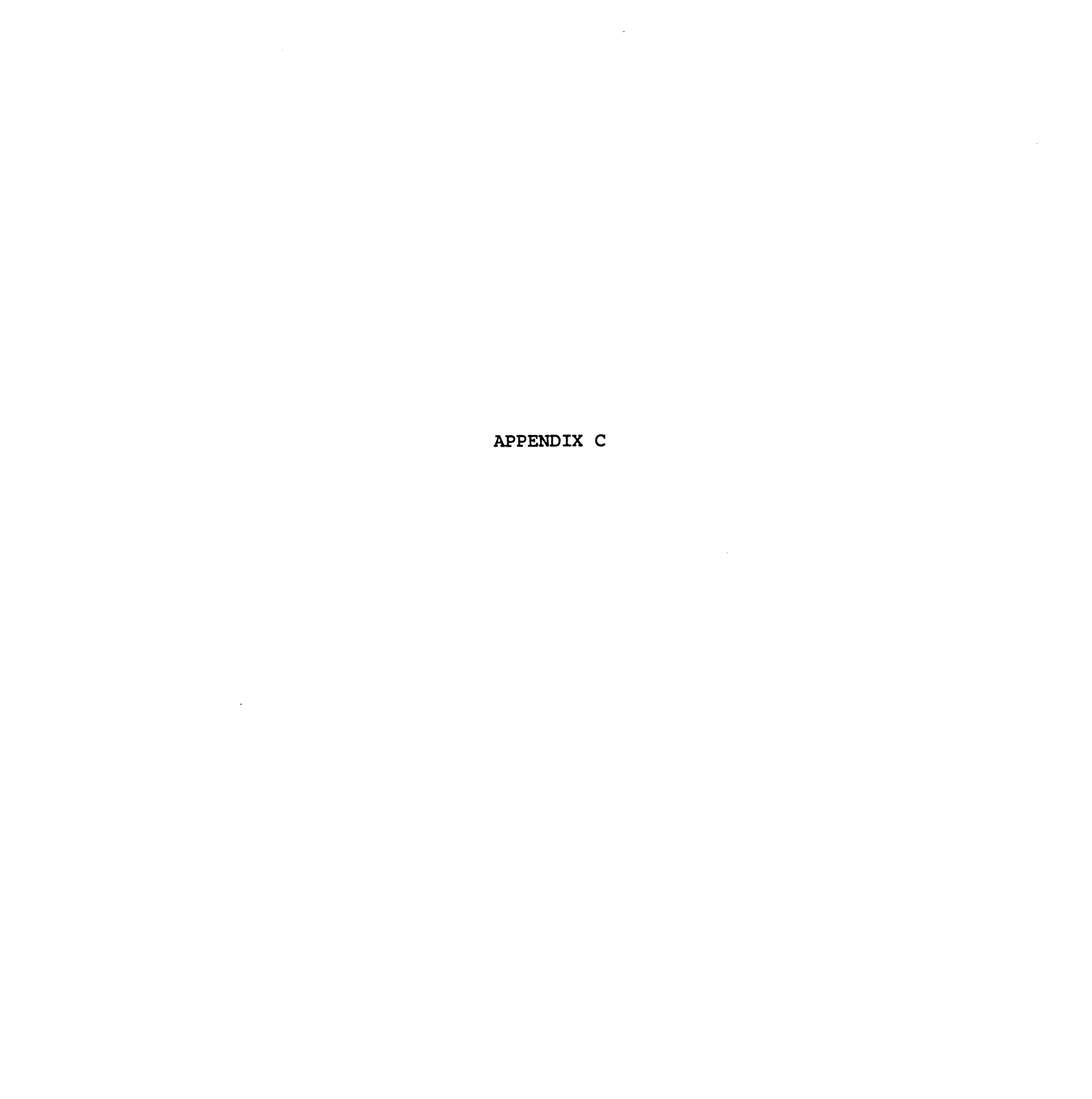


FIGURE B-2: FLOW CHART FOR BUCKLING ANALYSIS.



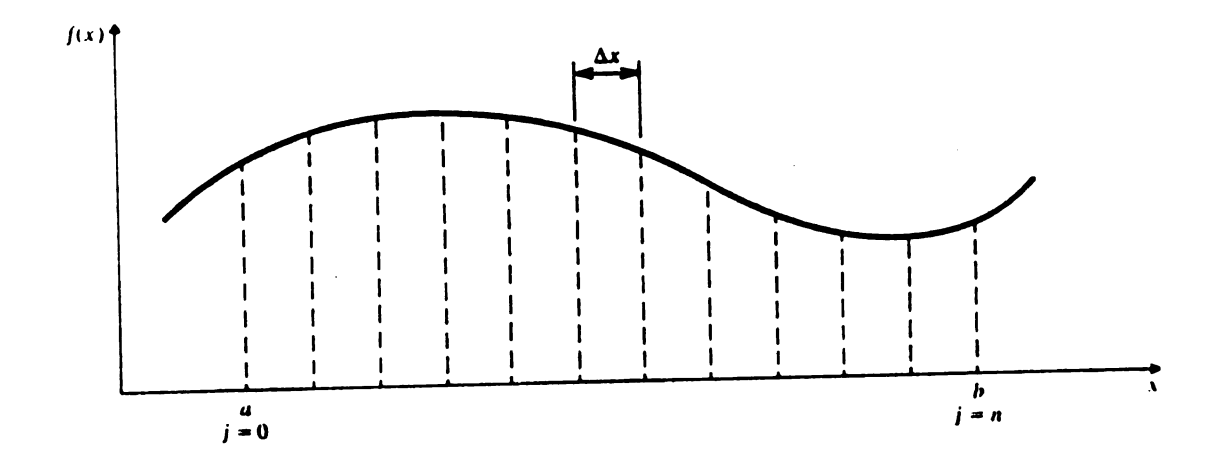
APPENDIX C

NUMERICAL METHODS IN ENGINEERING APPLICATIONS

This brief discussion of numerical methods is limited to those mentioned in this study, namely trapezoid rule of numerical integration, the solution of matrix eigenvalue problems, and the least-squares method of curve fitting.

C.1 NUMERICAL INTEGRATION (TRAPEZOID RULE)

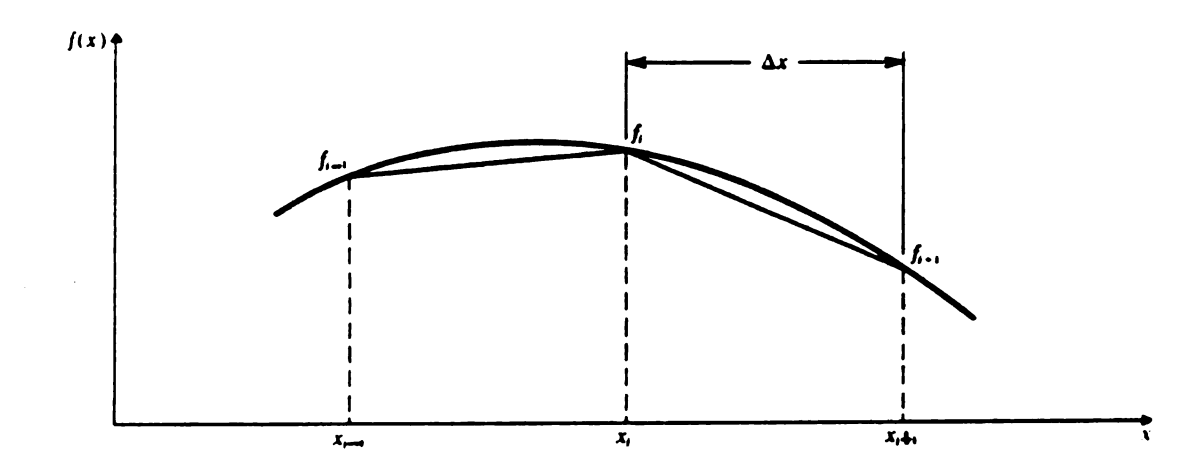
Consider an integrable function f(x) on the interval $a \le x \le b$ (Figure C-1)



We divide the interval $a \le x \le b$ into n equal subintervals (also called panels) of width Δx , such that

$$\Delta x = \frac{b-a}{n} \tag{C.1}$$

From an enlarged view of two such adjacent panels (Figure C-2) the area of each panel is given approximately by



$$\int_{x_{j-1}}^{x_j} f(x) dx = \frac{f_{j-1} + f_i}{2} (\Delta x)$$
 (C.2)

$$\int_{x_{j}}^{x_{j+1}} f(x) dx = \frac{f_{j} + f_{j+1}}{2} (\Delta x)$$
 (C.3)

The integral of the function f(x) over the two panels is given by

$$\int_{x_{j-1}}^{x_{j+1}} f(x) dx = \int_{x_{j-1}}^{x_{j}} f(x) dx + \int_{x_{j}}^{x_{j+1}} f(x) dx$$

which, upon introducing Equations (C.2) and (C.3) is given approximately by

$$\int_{x_{j-1}}^{x_{j+1}} f(x) dx \approx \frac{\Delta x}{2} (f_{j-1} + 2f_{j} + f_{j+1})$$
 (C.4)

This is easily recognized as the area of the two trapezia which approximate the original function f(x) in the interval x_{i-1} to x_{i+1} .

By extending Equation (C.4) over the entire region, the complete integral becomes

$$\int_{a}^{b} f(x) dx = \frac{\Delta x}{2} (f_{0} + 2f_{1} + 2f_{2} + \dots + 2f_{n-2} + 2f_{n-1} + f_{n})$$
(C.5)

or

$$\int_{a}^{b} f(x) dx = \frac{\Delta x}{2} (f_{0} + f_{n} + 2 \sum_{j=1}^{n-1} f_{j})$$
 (C.6)

where, $f_0 = f(a)$ and $f_n = f(b)$.

It is apparent that reducing Δx will generally give a better approximation to the original integral.

This geometric interpretation of the trapezoid rule provides no information about the error terms. A more elaborate derivation (38) utilizing Taylor series expansion gives the "trapezoidal rule with end correction", so-called because f' is needed only at the ends of the interval:

$$\int_{a}^{b} f(x) dx = \frac{\Delta x}{2} (f_{o} + f_{n} + 2 \sum_{j=1}^{n-1} f_{j}) - \frac{(\Delta x)^{2}}{12} [f'(b) - f'(a)]$$
(C.7)

C.2 THE METHOD OF LEAST SQUARES

The method of least squares is based on the premise that a measure of the accuracy of a function g(x) used as an approximation to some observed data f(x), is the magnitude d(x) of the local distance between the two functions.

That is,

$$d(x) = |f(x) - g(x)| \qquad (C.8)$$

The objective in the least squares method is to minimize d(x) over the region of x where the approximation g(x) is applied. Let E denote the sume of the squares of d(x) taken at each of n points x in the region of interest.

That is,

$$E = \sum_{i=1}^{n} d^{2}(x_{i})$$
 (C.9)

Obviously if d(x) is a minimum, so also is E. (It is such reasoning that forms the basis for calling this the method of "Least Squares".) In general we make a rational assumption for the approximating function g(x). Suppose g(x) is a polynomial of degree L.

That is,

$$g(x) = a_0 + a_1 x + a_2 x^2 + ... + a_L x^L$$
 (C.10)

Then,

$$E = \sum_{i=1}^{n} |f(x_i) - g(x_i)|^2 = \sum_{i=1}^{n} |g(x_i) - f(x_i)|^2 =$$

$$\sum_{i=1}^{n} [g(x_i) - f(x_i)]^2$$
 (C.11)

Introducing Equation (C.10) we get, for some point i:

$$E = \sum_{i=1}^{n} [a_0 + a_1 x_i + a_2 x_i^2 + ... + a_L x_i^L - f(x_i)]^2 \qquad (C.12)$$

E is minimized by equating to zero the partial derivatives of E with respect to each of the (L+1) coefficients in Equation (C.12).

Hence,

$$\frac{\partial \mathbf{a}}{\partial \mathbf{e}} = 0$$

$$\frac{\partial \mathbf{E}}{\partial \mathbf{a}} = 0$$

(C.13)

$$\frac{\partial E}{\partial a_2} = 0$$

•

٠

$$\frac{\partial \mathbf{E}}{\partial \mathbf{a}_{\mathbf{r}}} = \mathbf{C}$$

For example,

$$\frac{\partial E}{\partial a_{0}} = \frac{\partial}{a_{0}} \begin{bmatrix} \sum_{i=1}^{n} [a_{0} + a_{1}x_{i} + a_{2}x_{i}^{2} + \dots + a_{L}x_{i}^{L} - f(x_{i})]^{2}$$

$$= \sum_{i=1}^{n} \frac{\partial}{\partial a_{0}} [a_{0} + a_{1}x_{i} + a_{2}x_{i}^{2} + \dots + a_{L}x_{i}^{L} - f(x_{i})]^{2}$$

$$= \sum_{i=1}^{n} 2[a_{0} + a_{1}x_{1} + a_{2}x_{i}^{2} + \dots + a_{L}x_{i}^{L} - f(x_{i})]$$

$$\left\{ \frac{\partial}{\partial a_{0}} [a_{0} + a_{1}x_{i} + a_{2}x_{i}^{2} + \dots + a_{L}x_{i}^{L} - f(x_{i})] \right\}$$

$$= \sum_{i=1}^{n} 2[a_{0} + a_{1}x_{i} + a_{2}x_{i}^{2} + \dots + a_{L}x_{i}^{L} - f(x_{i})]$$

$$= \sum_{i=1}^{n} 2[a_{0} + a_{1}x_{i} + a_{2}x_{i}^{2} + \dots + a_{L}x_{i}^{L} - f(x_{i})]$$

$$= \sum_{i=1}^{n} 2[a_{0} + a_{1}x_{i} + a_{2}x_{i}^{2} + \dots + a_{L}x_{i}^{L} - f(x_{i})]$$

$$= (C.14)$$

The rest of Equations (C.13) can be evaluated similarly to give a set of (L+1) equations in (L+1) unknowns. (The proof that these equations do in fact yield a minimum for E is found in several standard references on numerical methods).

The complete set of the simultaneous linear equations in the coefficients of the polynomial is readily seen to be:

$$\begin{bmatrix}
\mathbf{n} & \Sigma \mathbf{x}_{\mathbf{i}} & \Sigma \mathbf{x}_{\mathbf{i}}^{2} & \dots & \Sigma \mathbf{x}_{\mathbf{i}}^{L} & \mathbf{a}_{\mathbf{0}} \\
\Sigma \mathbf{x}_{\mathbf{i}} & \Sigma \mathbf{x}_{\mathbf{L}}^{2} & \Sigma \mathbf{x}_{\mathbf{i}}^{3} & \dots & \Sigma \mathbf{x}_{\mathbf{i}}^{L+1} & \mathbf{a}_{\mathbf{1}} \\
\Sigma \mathbf{x}_{\mathbf{i}}^{2} & \Sigma \mathbf{x}_{\mathbf{i}}^{3} & \Sigma \mathbf{x}_{\mathbf{i}}^{4} & \dots & \Sigma \mathbf{x}_{\mathbf{i}}^{L+2} & \mathbf{a}_{\mathbf{2}} \\
\dots & \dots & \dots & \dots & \dots & \dots & \dots \\
\Sigma \mathbf{x}_{\mathbf{i}}^{L} & \Sigma \mathbf{x}_{\mathbf{i}}^{L+1} & \Sigma \mathbf{x}_{\mathbf{i}}^{L+2} & \Sigma \mathbf{x}_{\mathbf{i}}^{2L} & \mathbf{a}_{\mathbf{L}}
\end{bmatrix} = \begin{bmatrix} \Sigma \mathbf{f}(\mathbf{x}_{\mathbf{i}}) \\ \Sigma \mathbf{x}_{\mathbf{i}} \mathbf{f}(\mathbf{x}_{\mathbf{i}}) \\ \vdots \\ \Sigma \mathbf{x}_{\mathbf{i}}^{L} \mathbf{f}(\mathbf{x}_{\mathbf{i}}) \end{bmatrix}$$

$$(C.15)$$

C.3 SOLUTION OF MATRIX EIGENVALUE PROBLEMS

The fundamental eigenvalue problem is of the form:

$$(H - \lambda I) X = 0$$
 (C.16)

where H is a known square matrix, X is an unknown column vector with the same row dimension as H, λ is an unknown constant (the eigenvalue), and I the identity matrix of the same size as H.

Since Equation (C.16) represents a set of homogenous linear equations, a non-trivial solution exists only if:

$$\det (H - \lambda I) = 0 \tag{C.17}$$

Expansion of Equation (C.17) yields a polynomial of some degree n in λ , solution of which gives the desired eigenvalues $\lambda_{\bf i}$, i = 1, n. In general, the smallest (or fundamental) eigenvalue is of more significance, representing a variety of physical quantities depending

upon the class of problems being solved. (In the present case, λ_{\min} is the buckling load.)

In many instances, the eigenvalue problem is not of the form of equation (C.16) but rather of the form:

$$A X = \lambda B X \tag{C.18}$$

where B is not an identity matrix.

The solution technique still involves transforming A X = λ B X into the form H X = λ X. If B is positive-definite², then it can be written as the product of a lower triangular matrix and its transpose. That is,

$$B = L L^{T}$$
 (C.19)

Premultiplying (C.18) by L⁻¹ gives:

$$L^{-1} A X = \lambda L^{-1} B X = \lambda L^{-1} (L L^{T}) X = \lambda L^{T} X$$
 (C.20)

Now,

$$(L^{-1})^{T} = (L^{T})^{-1}$$

$$(L^{-1})^{T} L^{T} = I$$

$$(C.21)$$

$$A (L^{-1})^{T} L^{T} = A I = A$$

Hence the left hand side of equation (C.20) becomes:

$$L^{-1} A X = L^{-1} A (L^{-1})^{T} L^{T} X$$
 (C.22)

² A matrix is positive-definite for our purposes if all the eigenvalues are positive.

Using (C.22) in (C.20) we get:

$$(L^{-1} A (L^{-1})^{T}) (L^{T} X) = \lambda L^{T} X$$
 (C.23)

which can finally be written as:

$$H Z = \lambda Z \tag{C.24}$$

where H is a symmetric matrix, and $Z = L^{T} X$.

The eigenvalues of the new matrix are still the same as the original problem and the eigenvectors Z are related to those of the original problem by:

$$X = (L^{-1})^{T} Z$$
 (C.25)

It only remains to obtain the decomposition of B into LL^T (Equation (C.19)). This is readily accomplished by means of the choleski decomposition (46). Hence, if the elements of B are b_{ij} and of L are l_{ij} , the desired decomposition is given in (46) as:

$$1_{11} = (b_{11})^{\frac{1}{2}}$$

$$1_{ij} = (b_{ij} - \sum_{k=1}^{j-1} 1_{ik} 1_{jk}) / 1_{ij}, j=2, 2, ..., i-1$$

$$1_{ii} = b_{ii} - \sum_{k=1}^{i-1} 1_{ik}^{2}$$

$$...,n$$

$$1_{i-1, j} = 0, j=1, i+1, ..., n$$
 (C.26)

Similarly, the inversion L^{-1} of L is given as:

$$\frac{1}{1_{11}} = 1/1_{1i}$$

$$\frac{-1}{1_{11}} = 1/1_{1i}$$

$$\frac{1}{1_{11}} = 1/1_{1i}$$

$$\frac{-1}{1_{1j}} = -\sum_{k=j+1}^{i} \frac{-1}{ik} \frac{1}{kj}$$

$$\frac{-1}{k=j+1}, j=i-1, i-2, ..., 1$$
(C.27)

For a large system, the polynomial method is clearly inefficient for the obvious reason that solving for the roots of the resulting polynomial equations can present difficulties. A number of efficient solution techniques are available and only the JACOBI method is briefly outlined here.

The Jacobi method attempts, through a series of orthogonal transformations, to convert the matrix H to a diagonal form. That is, if U denotes the orthogonal matrix at a praticular step, then \textbf{U}^T H U reduces the element in the \textbf{p}^{th} row and \textbf{q}^{th} column of H to zero. This can be accomplished if U is of the form:

where C and S are constants which depend on the elements of H and all the off-diagonal elements of U are zero except for u_{pq} and u_{qp} which are S and -S respectively. All diagonal elements of U are 1 except for u_{pp} and u_{qq} which are C. Premultiplying H by u^T and post-multiplying by U gives:

$$h_{pp} = C^{2}h_{pp} + S^{2}h_{qq} - 2CSh_{pq}$$

$$h_{qq} = C^{2}h_{qq} + S^{2}h_{pp} + 2CSh_{pq}$$

$$C.29 - C.31$$

$$h_{pq} = h_{qp} = (C^{2}-S^{2})h_{pq} + CS(h_{pp}-h_{qq})$$

A detailed procedure for selecting C and S are given in (37) where it is shown that:

$$C = \frac{1}{2} + \frac{|\alpha|}{2\beta}$$
 (C.32)

and

$$S = \frac{\alpha \ (-h_{pq})}{2 \beta |\alpha| C}$$
 (C.33)

where
$$\alpha = \frac{1}{2} (h_{pp} - h_{qq})$$
 and $\beta = (h_{pq}^2 + \alpha^2)^{\frac{1}{2}}$

The effects of the orthogonal transformations on all other elements in the p^{th} and q^{th} rows and columns of H are as follows:

pth row and qth row (j # p or q)

p^{th} column and q^{th} column ($i \neq p$ or q)

All other elements of H remain unchanged.

Hence, the solution technique is to select the element h_{pq} of the matrix H, which we desire to destroy, then calculate c and s 1 1 from (C.32) and (C.33) and the new values h_{pp} and h_{qq} from (C.29 - C.31) (with h_{pq} and h_{qp} set to zero). Finally the rest of the new elements of H are obtained from (C.34) and (C.35). The procedure is then repeated with a new choice of p and q until the off-diagonal elements become sufficiently small. (Since this is an iterative method, the off-diagonal elements will not in general be exactly zero.)

An efficient procedure for choosing which elements h_{pq} to destroy, as well as deciding when the solution has converged is the so-called threshold method. Briefly, the method involves the following steps:

(i) Define V, the sum of the off-diagonal elements:

$$v = \sum_{i=1}^{n} \sum_{j=1}^{n} (h_{ij})^{2}$$

$$i \neq j$$
(C.36)

- (ii) Compute V for the original untransformed matrix H and then compute a "threshold" value $\mu_1 = \sqrt{\frac{v_o}{n}}$
- (iii) In one sweep through the matrix, annihilate any off-diagonal element greater than or equal to μ_{1} .
- (iv) Calculate a new threshold $\mu_2 = \frac{\mu_1}{n}$ and repeat the sweep through the matrix, annihilating any off-diagonal element greater than or equal to μ_2 .
- (v) Repeat the procedure as often as necessary till $\mu_{i} \leq \epsilon \mu_{l}$, where ϵ is a prescribed convergence limit (typically \leq 10⁻⁶).

The eigenvectors are contained in another set of matrices R whose elements can be modified along with H. The elements of R during the transformations are:

$$r_{ip} = cr_{ip} - sr_{iq}$$
 (C.37)

qth column

$$r_{iq} = sr_{ip} + cr_{iq}$$
 (C.38)

All other elements remain unchanged. Upon eventual convergence, the columns of R become the eigenvectors of the original matrix.

APPENDIX D

APPENDIX D

ELEMENTS OF VARIATIONAL CALCULUS*

A) FIRST AND SECOND VARIATIONS OF POTENTIAL ENERGY

Consider a continuous system whose potential energy V is a function of a displacement variable w(x).

Then,

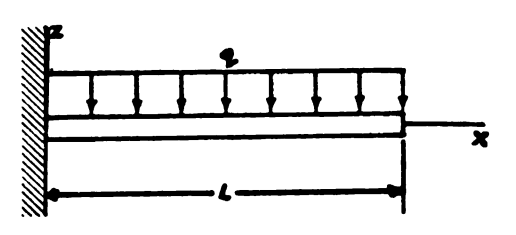
$$V = \int_{x}^{x} F [w(x)] dx$$
 (D.1)

where F is a known function of w, and w an unknown function of x.

Such a quantity as V whose values depend on one or more continuous variables rather than on a number of discreet variables is called a FUNCTIONAL.

Suppose for example that our continuous system is a cantilever beam subjected to a uniformly distributed load. Then the total potential energy may be written

FIGURE D-1: Cantilever beam subjected to uniformly distributed load.



as the sum of the strain energy and the potential energy of applied loads.

^{*}The following material is taken from Reference (33) and much of the original notation has been retained.

Hence,

$$V = \int_{0}^{L} \left[\frac{EI}{2} (w'')^{2} + qw \right] dx$$
where
$$w'' = \frac{d^{2}w}{dx^{2}}$$

For the cantilever beam, the boundary conditions are of two kinds:

- (I) Boundary conditions of physical restraint, also called forced or geometric boundary conditions -- i.e. w = w' = 0 at x = 0.
- (II) Boundary conditions of shear (Q) and moments (M) at x = L -i.e. Q = M = 0 at x = L.

Suppose the beam is in equilibrium in some configuration $w = w_0$. Suppose further that we permit an infinitesimal increment w_1 from equilibrium such that,

$$w \rightarrow w_0 + w_1$$

where the arrow means "replaced by". (Both w_0 and w_1 must be continuous and twice differentiable in the interval $0 \le X \le L$).

For convenience, let $w_1(x) \equiv \varepsilon \zeta(x)$ where ε is an arbitrary small constant and $\zeta(x)$ is an admissible but arbitrary function (i.e. $\zeta(x)$ satisfies the necessary geometric boundary conditions).

Then,

$$V + \Delta V = \int_{0}^{L} \left[\frac{EI}{2} \left(w_{0}^{"} + \varepsilon \zeta^{"} \right)^{2} + q \left(w_{0}^{"} + \varepsilon \zeta \right) \right] dx \qquad (D.3)$$

where ΔV is the change in potential energy resulting from a variation in w.

By expanding Equation (D.3) and subtracting Equation (D.2) from the result, the change in potential energy ΔV can be written as,

$$\Delta V = \varepsilon \int_{0}^{L} (EI w \zeta'' + q\zeta) dx + \varepsilon^{2} \frac{EI}{2} \int_{0}^{L} (\zeta'')^{2} dx \qquad (D.4)$$

The sum of the first-order terms in the expression for ΔV is called the "first variation" of V and denoted by the symbol δV . The sum of the second-order terms is called the "second variation" of V and denoted by the symbol $\frac{1}{2}$ $\delta^2 V$. For our example,

$$\delta V = \epsilon \int_{0}^{L} (EIw_{0}"\zeta" + q\zeta) dx$$
(D.5 a-b)

$$\frac{1}{2} \delta^2 V = \varepsilon^2 \frac{EI}{2} \int_0^L (\zeta'')^2 dx$$

B) THE EULER EQUATIONS

Consider a structure for which the integrand F is a function of one independent variable x, and one dependent variable w and its derivatives such that:

$$V = \int_{x}^{x_{1}} F(x, w, w', w'') dx$$
 (D.6)

Suppose as before, we permit an infinitesimal variation in w such that $w \longrightarrow w_0 + w_1$, with w_0 being an equilibrium position. If $w_1(x) = {}^{\xi}\zeta(x)$, ${}^{\xi}$ being an arbitrary small constant and $\zeta(x)$ any arbitrary admissible function, then:

$$\Delta V = \int_{\mathbf{x}}^{\mathbf{x}} [F(\mathbf{x}, \mathbf{w}_{o} + \varepsilon \zeta, \mathbf{w}_{o}' + \varepsilon \zeta', \mathbf{w}_{o}'' + \varepsilon \zeta'')$$

$$- F(\mathbf{x}_{o}, \mathbf{w}_{o}, \mathbf{w}_{o}'', \mathbf{w}_{o}''') d\mathbf{x}$$
(D.7)

Expansion of Equation (D.7) in Taylor's series gives, for the first variation:

$$\delta V = \varepsilon \int_{x_0}^{x_1} \left(\frac{\partial F}{\partial w_0} \zeta + \frac{\partial F}{\partial w_0} \zeta' + \frac{\partial F}{\partial w_0''} \zeta'' \right) dx \qquad (D.8 a)$$

The criterion for equilibrium is that the first variation of V be equal to zero, and because ε is arbitrary we then have:

$$\int_{\mathbf{x}_0}^{\mathbf{x}_1} \left(\frac{\partial \mathbf{F}}{\partial \mathbf{w}} \zeta + \frac{\partial \mathbf{F}}{\partial \mathbf{w}} \zeta' + \frac{\partial \mathbf{F}}{\partial \mathbf{w}} \zeta'' \right) d\mathbf{x} = 0$$
 (D.8 b)

Repeated integration by parts yields:

$$\int_{x}^{x} \left(\frac{\partial F}{\partial w} = \frac{d}{dx} \frac{\partial F}{\partial w} + \frac{d^{2}}{dx^{2}} \frac{\partial F}{\partial w} \right) \zeta dx = 0$$
 (D.9 a)

which ultimately simplifies to:

$$\frac{\partial F}{\partial w} - \frac{d}{dx} \frac{\partial F}{\partial w_o^2} + \frac{d^2}{dx^2} \frac{\partial F}{\partial w_o^{"}} = 0, \quad x_o \le x \le x_1$$
 (D.9b)

Equation (D.9 b) is known as the EULER EQUATION of the calculus of variations. It is easily extended to a multiple degree-of-freedom system. For example, if there are two dependent variables u(x) and w(x), with the highest order of the derivatives in u and w being the first and second order respectively, the Euler equations are:

$$\frac{\partial \mathbf{F}}{\partial \mathbf{u}} - \frac{\mathbf{d}}{\mathbf{dx}} \frac{\partial \mathbf{F}}{\partial \mathbf{u}} = 0$$

$$\frac{\partial \mathbf{F}}{\partial \mathbf{w}} - \frac{\mathbf{d}}{\mathbf{dx}} \frac{\partial \mathbf{F}}{\partial \mathbf{w}} + \frac{\mathbf{d}^2}{\mathbf{dx}^2} \frac{\partial \mathbf{F}}{\partial \mathbf{w}} = 0$$
(D.10 a-b)

Finally, if there are three dependent variables u, v, w and two independent variables x, y, and if the highest order of the derivatives are first order in u and v and second order in w, the Euler equations are found to be of the form:

$$\frac{\partial \mathbf{F}}{\partial \mathbf{u}} - \frac{\partial}{\partial \mathbf{x}} \frac{\partial \mathbf{F}}{\partial \mathbf{u}_{,\mathbf{x}}} - \frac{\partial}{\partial \mathbf{y}} \frac{\partial \mathbf{F}}{\partial \mathbf{u}_{,\mathbf{y}}} = 0$$

$$\frac{\partial \mathbf{F}}{\partial \mathbf{v}} - \frac{\partial}{\partial \mathbf{x}} \frac{\partial \mathbf{F}}{\partial \mathbf{v}_{,\mathbf{y}}} + \frac{\partial}{\partial \mathbf{y}} \frac{\partial \mathbf{F}}{\partial \mathbf{v}_{,\mathbf{y}}} = 0$$
(D.11)

$$\frac{\partial \mathbf{F}}{\partial \mathbf{w}} - \frac{\partial}{\partial \mathbf{x}} \frac{\partial}{\partial \mathbf{w_{x}}} - \frac{\partial}{\partial \mathbf{y}} \frac{\partial \mathbf{F}}{\partial \mathbf{w_{y}}} + \frac{\partial^{2}}{\partial \mathbf{x}^{2}} \frac{\partial \mathbf{F}}{\partial \mathbf{w_{xx}}} + \frac{\partial^{2}}{\partial \mathbf{x} \partial \mathbf{y}} \frac{\partial \mathbf{F}}{\partial \mathbf{w_{xy}}}$$

$$+ \frac{\partial^2}{\partial y^2} \frac{\partial F}{\partial w_{,yy}} = 0$$

